THE UNIVERSITY OF EDINBURGH
INSTITUTE OF ECOLOGY AND RESOURCE MANAGEMENT

# REMOTE SENSING OF PHOTOSYNTHETIC-LIGHT-USE EFFICIENCY

Caroline Jane Nichol
B. Sc. (Hons) Ecological Science, University of Edinburgh

A thesis submitted for the Degree of Doctor of Philosophy

October 2000.

## DECLARATION

This thesis has been composed by myself from the results of my own work, except where stated otherwise, and has not been submitted in any other application for a degree.

Caroline J Nichol
October, 2000

***I dedicate this Thesis to my parents***
***with much love.***

*Seididh gaoth is dearrsaidh grian*
*Ach thig an la is thig an t-am*
*Airson an ubhal as airde*
*Air a'chraobh a bhuin*

*from "An Ubhal as Airde"*
*C.MacDonald/R.MacDonald, 1987*

## ABSTRACT

This study investigated the use of the Photochemical Reflectance Index (PRI) for estimating the light use efficiency of photosynthesis (LUE) of individual leaves and forest canopies.

Narrow waveband spectral reflectance, chlorophyll fluorescence and gas exchange measurements were made sequentially on individual leaves of *Vicia faba* at three light levels of 500, 1000 and 1500 μmol $m^{-2}$ $s^{-1}$. PRI was calculated from the reflectance data and correlated with LUE calculated from gas exchange and photosystem II (PS II) efficiency measured from chlorophyll fluorescence. PRI was linearly related to photosynthetic LUE and PS II efficiency over the range of light levels and followed the diurnal light response of photosynthetic light-use-efficiency.

The relationship between PRI and LUE was then investigated over boreal forests in Canada. Reflectance measurements of four stands were made from a helicopter-mounted spectroradiometer during the 1994 growing season. Eddy covariance towers were measuring $CO_2$ fluxes during this time and LUE was calculated from these data. A strong linear relationship was found between PRI and LUE for the four sites, and when expressed on a functional type basis of conifer and deciduous, the relationships were stronger still.

The relationship between PRI and LUE at the canopy scale was further investigated in boreal forest in Siberia during the "green-up" period from winter into spring in 2000. During this time the photosystems were under stress as a result of extremes of temperature (from -20° C to +35° C) coupled with a high radiation load. Reflectance measurements of four stands were made from a helicopter-mounted spectroradiometer and PRI was calculated from these data. Eddy covariance towers were operating at each site and offered a means to calculate LUE. A significant linear relationship was apparent between PRI and LUE although the relationship was weaker than that found between PRI and LUE in the Canadian boreal forest. Collating the data for all the boreal forests highlighted a difference between the slopes of the PRI:LUE relationship. Reflectance measurements were also made from the eddy covariance tower of the Scots pine canopy and needles were sampled simultaneously for xanthophyll pigment determination. Strong linear relationships were observed between PRI, the epoxidation state of the xanthophyll cycle and LUE over the seasonal change and the diurnal cycle.

The sensitivity of PRI to a number of extraneous variables was investigated using the SAIL model. Needle reflectance and transmittance data were input into the SAIL model to simulate the reflectance of a homogeneous canopy. Realistic variations were introduced into the observations for a varying canopy structure whilst keeping the needle and background optics constant. PRI was found to be most sensitive to background reflectance, solar zenith angle and leaf angle distribution (LAD) particularly when leaf are index was low (0.25-3).

## *Acknowledgements*

First and foremost I would like to thank my supervisor, John Grace, for his guidance and continuous support throughout this project. My thanks also go to my second supervisor, John Moncrieff, for valuable assistance and advice at various intervals. Financial assistance was provided through a NERC Ph.D. studentship. Its receipt is gratefully acknowledged.

The organisations that facilitated my work included NASAs Goddard Space Flight Center, Greenbelt MD, USA, the Max-Planck Institute for Biogeochemistry, Jena, Germany and the Institute of Forest, Siberian Branch of the Russian Academy of Sciences, Krasnoyarsk, Russia.

At NASA, my work was sponsored by the Planetary Biology Internship programme. I thank Forrest Hall for supervising my work and time at Goddard and Fred Huemmrich for invaluable discussion about data and science in general. Technical support from Dave Landis and Anthony Young is also gratefully acknowledged. I also thank Carla and Rok for their generosity and providing me with accommodation during my stay in Maryland.

Special thanks go to Jon Lloyd at the Max-Planck Institute for giving me the opportunity to work in Siberia. The smooth running of my work would not have been possible without the tireless commitment of Olga Shibistova who I thank for organising the flying, translation services, friendship and for generally taking excellent care of everything. I thank Almut Arneth, Olaf Kolle, Carola Roser, Alexander Knoll, Waldemar Ziegler and Daniil for supplying me with the corrected flux data and stand information for the east and west camps. I also thank our camp guard Sascha for religiously accompanying me to the tower and encouraging my use of the Russian language, albeit limited. Analysis of the needle samples for pigment content was carried out by Shizue Matsubara at the Research School of Biological Sciences, Australian National University, Canberra. The Barnson Fund also provided additional funding for personal field equipment. Its receipt is gratefully acknowledged.

In Edinburgh special thanks go to Fiona Carswell, Yadvinder Malhi, Patrick Meir and Emiliano Pegoraro for their continuous support, good humour, musical appreciation and large appetites. I also thank Shiela Wilson for helping out with many things over the past three years.

Thanks to everyone at Lothian Branch of the British Red Cross for the nights out and great company on many memorable First Aid duties. To Mairi and Kirsty from An Comman Ceilteach for excellent craic and putting up with my bad Gaelic.

Special thanks to flatmates past and present for making life at home so entertaining – Trevor Blackall, Jayne Brian, Beverley Burnside, Tracey Clapperton, Sarah McConnell and Julie McKinney. A special thank you also to my sister Mairi and friends who helped me along the way, Lesley, Shona, Ceri, Sian, Alistair, Stewart, Ana, Sandra, and Johanna. An extra special thank you to Jens for being so supportive and helping out wherever possible.

## TABLE OF CONTENTS

## LIST OF FIGURES

## LIST OF TABLES

## LIST OF SYMBOLS AND ABBREVIATIONS

### ABBREVIATIONS

| | |
|---|---|
| A | Antheraxanthin |
| *A* | Assimilation (photosynthetic) |
| ABRACOS | Anglo-Brazilian Amazonian Climate Observation Study |
| APAR | Absorbed Photosynthetically Active Radiation |
| ADP | Adenosine diphosphate (Inorganic phosphate) |
| ASTER | Advanced Spaceborne Thermal Emission and Reflection Radiometer |
| ATP | Adenosine triphosphate (high energy product of photosynthesis) |
| AVIRIS | Airborne Visible Infrared Imaging Spectrometer |
| BOREAS | Boreal Ecosystem Atmosphere Study |
| CAM | Crassulacean Acid Metabolism |
| $^1$Chl* | Excited state chlorophyll |
| D1 | Photosystem II protein |
| ER – 2 | Earth Resolution NASA Aircraft |
| EOS | Earth Observing System |
| EPS | Epoxidation state |
| $f_{APAR}$ | Fraction of absorbed photosynthetically active radiation |
| FIFE | First International Satellite Land Surface Climatology Project Field Experiment |
| $\Delta F/Fm$ | The ratio of variable to maximum chlorophyll fluorescence |
| GCM | Global Circulation Model |
| GSFC | Goddard Space Flight Center |
| HAPEX-SAHEL | Hydrological and Atmospheric Pilot Experiment in the Sahel |
| HPLC | High Phase Liquid Chromatography |
| IFOV | Instantaneous field of view |

| | |
|---|---|
| IPAR | Intercepted photosynthetically active radiation |
| NASA – JPL | NASA Jet Propulsion Laboratory |
| LAD | Leaf angle distribution |
| LAI | Leaf area index |
| LBA | Large Scale Biosphere-Atmosphere Experiment in Amazonia |
| LUE | Light use efficiency |
| $NADP^+$ | Electron acceptor molecule |
| NADPH | High energy product of photosynthesis |
| NASA | National Aeronautics and Space Administration |
| NDVI | Normalised Difference Vegetation Index |
| NOAA-AVHRR | National Oceanic and Atmospheric Administration - Advanced Very High Resolution Radiometer |
| NSA | Northern Study Area |
| $^1O_2$* | Excited state oxygen |
| MODIS | Moderate Resolution Imaging Spectroradiometer |
| NIR | Near infrared |
| PPFD | Photosynthetic photon flux density |
| PRI | Photochemical reflectance index |
| $PS_{max}$ | Maximum photosynthesis rate |
| $q_E$ | Energy dependent quenching of chlorophyll fluorescence |
| $q_I$ | Photoinhibitory quenching of chlorophyll fluorescence |
| $q_N$ | Non photochemical quenching of chlorophyll fluorescence |
| $q_P$ | Photochemical quenching of chlorophyll fluorescence |
| PS II | Photosystem II |
| $R$ | Reflectance (when followed by a wavelength in superscript) |
| RSS | Remote sensing science |
| SAIL | Scattering from Arbitrarily Inclined Leaves |
| SE-590 | Spectron Engineering 590 |
| SiB2 | Simple Biosphere Model 2 |
| SSA | Southern Study Area |

| | |
|---|---|
| SVI | Spectral Vegetation Index |
| SZA | Solar Zenith Angle |
| TE | Terrestrial Ecology |
| $T_s$ | Soil temperature |
| V | Violaxanthin |
| $u^*$ | Friction velocity |
| VIS | Visible reflectance |
| WFF | Wallops Flight Facility |
| Z | Zeaxanthin |

**GREEK ALPHABET**

| | |
|---|---|
| ε | Radiation use efficiency |

# 1. INTRODUCTION

## GLOBAL BIOSPHERIC RESEARCH

The dynamics of the terrestrial biosphere are a key feature in current global change research. The Kyoto protocol of 1997 signalled that dramatic decisions may need to be made to reduce emissions of $CO_2$ and hence reduce the rate of warming. Such decisions will thus rely heavily on improved measurement of global biospheric processes such as photosynthesis and respiration (Schimel, 1998).

A broad spectrum of national and international programmes spanning the world's major biomes of continental temperate grassland (FIFE), desert savanna (HAPEX-SAHEL) temperate forest, boreal forest (BOREAS), tropical rain forest (ABRACOS and LBA) have been undertaken in the past 10 years incorporating global satellite sensor observations, performing field measurements of $CO_2$ and $H_2O$ fluxes and stimulating global model development. Such research will enable longer term trends to be evaluated and thus allow for an early indication of biospheric changes which would otherwise go undetected.

Much of what has been learned about the global carbon budget has arisen from observations of atmospheric $CO_2$ trends and $^{13}C/^{12}C$ isotope ratios. From these studies we have learned that half of the annual anthropogenic $CO_2$ emission into the atmosphere has been taken up by the oceans and terrestrial biosphere (Keeling *et al.*, 1989), and that a significant uptake of atmospheric $CO_2$ is occurring at the mid-latitudes of the Northern Hemisphere (Tans *et al.*, 1990, Ciais *et al.*, 1995). It is also clear that there is large year to year variation in uptake of $CO_2$ by the terrestrial biosphere with the seasonality of biosphere carbon flux changing with the timing and amplitude of seasonal cycles (Field *et al.*, 1998).

Such changes in the biosphere point to a pressing need to improve understanding of the processes that regulate the uptake and release of $CO_2$. Process studies are

generally conducted at tower sites, and frequently employ eddy covariance and chamber measurements of $CO_2$ and $H_20$ fluxes. However, tower sites define fluxes over spatial areas of around 1 $km^2$, so towers could never be sufficiently numerous to cover whole regions. Much effort has been put into developing new techniques for large area observation. This thesis is thus a contribution to that effort.

## SATELLITE REMOTE SENSING

One method by which we can increase our understanding of regional and global vegetation processes such as photosynthesis is through the analysis of remotely sensed observations. Over the past 40 years, satellite sensors have provided consistent and repeatable global observations required to analyse the regional activity and seasonal dynamics of the biosphere. Whilst such observations could never represent (as yet) the fine detail observed at field sites, they do nonetheless provide consistent discrete observations repeated systematically over a number of temporal scales (Goward and Dye,1996). Observatories, such as the National Oceanic and Atmospheric Administration (NOAA) Advanced Very High Resolution Radiometer (AVHRR) are able to collect daily data of the entire planetary surface at a spatial resolution of 1.1 km (Townsend and Tucker, 1981). Sensors carried on other satellites can however sample at finer spatial (15 - 250 m) and spectral resolutions The Moderate Resolution Imaging Spectroradiometer, MODIS, samples the spectrum at a resolution of 10 nm; the MEdium Resolution Imaging Spectrometer, MERIS samples at 1.8 nm and the Hyperion Hyperspectral Imager samples at approximately 9.5 nm. Sensors carried on aircraft, for example, the Airborne Visible and Infrared Imaging Spectrometer AVIRIS, Compact Airborne Spectrographic Imager, CASI) can sample an even finer spatial (~ 20 m and 1-10 m respectively) and spectral resolution 10 nm and 1.8 nm respectively.

Thus remote sensing both from spaceborne and airborne systems offers a means with which to examine the physical and biological processes occurring on the Earth.

Remote sensing studies focus on the use of reflected and emitted electromagnetic radiation to extract information about the type and condition of components at the earths surface. Green vegetation can be clearly distinguished from other components of the landscape by the differences in their optical properties in visible (VIS) and near-infrared (NIR) spectral regions. The spectral reflectance of green foliage differs between these two spectral regions, with the NIR reflectance being much greater than the VIS, whilst soils have similar reflectance over these two bands (Williams *et al.*, 1989). By comparing the visible and NIR reflectances the relative amounts of soil and green vegetation may be determined (Jensen, 1983). A number of methods of making spectral comparisons between the VIS and NIR reflectances have been developed. One method is through the use of spectral vegetation indices (SVIs). These SVIs are generally algebraic combinations of reflectance values.

An ideal SVI should maximise its sensitivity to the biophysical variable of interest and minimise variation due to other characteristics, such as background reflectance. The SVI should also be linearly related to the biophysical variable. The most widely used SVI is the Normalised Difference Vegetation Index (NDVI), which is the difference between the NIR and VIS reflectance divided by their sum. The normalisation is used to partially account for changes in illumination (Jackson *et al.*, 1983).

## REMOTE SENSING OF BIOPHYSICAL AND PHYSIOLOGICAL PROPERTIES OF FORESTS IN OPTICAL WAVELENGTHS

### FOREST BIOPHYSICAL PROPERTIES

The biophysical properties of forests can be estimated using two approaches (Hall *et al.*, 1995). Regression analysis or conditional simulation (Dungan, 1998) can be used to relate various measurements of radiative flux (radiance, reflectance, ratios of radiance or reflectance, e.g. NDVI, and changes in radiance or reflectance) to measurements made on the ground of biophysical properties. The second approach

utilises "canopy reflectance models", and is discussed later in this chapter in greater detail.

Using the first of these methods, one relevant biophysical variable that can be estimated with reliability is leaf area index (LAI) (Curran *et al.*, 1992, Spanner *et al.*, 1994, Fassnacht *et al.*, 1997) which is a required input into ecosystem simulation models. The LAI of a forest canopy defines the one sided area of leaves per unit area of ground (Curran, 1983). LAI is important in ecosystem modelling because it can be used to (1) calculated the minimum light levels needed to control stomatal opening; and (2) regulate both the interception of precipitation and absorption of photosynthetically active radiation (APAR)(Bonan, 1993).

**FOERST PHYSIOLOGICAL PROPERTIES**

In addition to biophysical variables, the physiological property of absorbed PAR, of the fraction of absorbed PAR ($f_{APAR}$) can also be estimated using remote sensing.

Much remote sensing of vegetation processes in recent years has focused on the link between NDVI and the fraction of photosynthetically active radiation absorbed by a plant canopy ($f_{APAR}$). For most vegetation, this is approximately linear (Baret and Guyot, 1991, Goward and Huemmrich, 1992, Gamon *et al.*, 1995) meaning that NDVI should provide a useful estimate of the *potential* photosynthetic capacity (Myneni *et al.*, 1995). A simple model can link $f_{APAR}$ (which is estimated from NDVI) to ecosystem production through the use of a light use efficiency parameter ($\varepsilon$) that describes the ability of the plant to convert the absorbed energy into biomass. However the use of such models requires an accurate estimate of $\varepsilon$. Many authors have assumed this to be uniform across ecosystems and as such have treated this value as a constant in the model. A number of studies have demonstrated that this is not the case (Runyon *et al.*, 1994, Gamon *et al.*, 1995, Joel *et al.*, 1997). Stress factors, such as temperature and water availability, can severely reduce the efficiency of photosystem II (Prince, 1991), which manifests itself through reductions in the

rates of carboxylation and PS II activity. In many ecosystems this reduction in efficiency is evident as photosynthetic down-regulation (i.e. short term reversible reduction in photosynthetic activity) detectable by changes in stomatal aperture, carboxylation and photosystem II activity (Sellers *et al.*, 1996, Gamon *et al.*, 1997). Reduced efficiency caused by stress can result in a *five fold* variation in photosynthesis rates without a detectable change in NDVI or canopy structure (Gamon *et al.*, 1997). Modelling studies linking global circulation models (GCM) to atmospheric transport and physiological models (SiB2) have shown that downregulation can impact climate predictions to the extent that overlooking downregulation may lead to incorrect conclusions regarding the global carbon balance (Sellers *et al.*, 1996).

Thus, a direct measure of photosynthetic efficiency from remote sensing of spatial or temporal variation, would be highly desirable.

The impetus for developing remote sensing approaches to large-area photosynthetic determination stems from four important considerations. (I) Remote sensing offers approaches which are non-invasive. (II) Remote sensing of photosynthesis provides an opportunity to test our capacity for the up-scaling of physiological measurements made at smaller areas. Just as the controls on photosynthesis differ at the leaf and chloroplast level (Woodrow, 1990), they also may differ between the leaf and higher levels of organisation. (III) A clearer picture of spatial patterns of photosynthesis could suggest new hypotheses that will lead to an increased understanding of the ecological and physiological controls of $CO_2$ exchange at the leaf and plant level. (IV) Finally, related to the previous considerations, the increasing evidence that human activity is influencing the Earth's vegetation places a high priority on developing more extensive approaches to ecophysiology. Global estimations of photosynthesis are pivotal for assessing a key quantity in the global carbon budget. The role of $CO_2$ as a greenhouse gas and climate forcer along with the uncertainty of the flux coming from and going into the terrestrial biosphere (Tans *et al.*, 1990),

combines to make terrestrial photosynthesis and its remote determination an important research issue.

There exists a range of remote sensing methods potentially useful for assessing photosynthesis. These fall into three categories. One class of methods is related to photosynthetic capacity or the potential for uptake of $CO_2$. Examples of this include the estimation of leaf area index (LAI), total canopy nitrogen, and the fraction of absorbed photosynthetically active radiation ($f_{APAR}$), as previously mentioned. A second class of methods provides environmental variables that are required by photosynthesis models. These include estimates of surface temperature, incoming solar radiation and soil moisture. A third class of methods is related to instantaneous $CO_2$ exchange. Examples of this class include the use of canopy temperature as a means to calculate stomatal conductance, or others that probe chlorophyll fluorescence and the status of xanthophyll cycle pigments.

This thesis focuses on the xanthophyll cycle, its function, its role in photosynthesis and its estimation by remote sensing.

## GENERAL AIMS OF THIS THESIS

The general aim of this thesis is to explore the relationship between the light-use-efficiency of photosynthesis and the status of the xanthophyll cycle using remote sensing. There follows a review of the linkage between the processes of photosynthesis and the activity of the xanthophyll cycle. After that, a statement of specific objectives are made.

## PHOTOSYNTHESIS, NONPHOTOCHEMICAL QUENCHING AND THE XANTHOPHYLL CYCLE

Photosynthesis involves the co-ordination of a number of reactions which are separated both spatially and temporally. These reactions begin in the thylakoid membrane where light is absorbed by antenna pigments. Primary photochemistry by reaction centre pigments follows, and terminates with the partitioning of photosynthate with the distribution of fixed carbon to the metabolic sinks of the organism.

The absorption of light by chlorophyll and the conversion of this energy in the form of chlorophyll excited states represents the starting point for the photosynthetic reactions. The conversion of this excited state energy into chemical energy is carried out by the reaction centres and is the driving force behind photosynthetic electron transport, the production of the high energy compounds ATP and NADPH, and the utilisation of these products in carbon fixation.

Whilst the utilisation of excited state chlorophyll by electron transport is the dominant pathway for energy dissipation, the de-excitation of chlorophyll occurs as one of a number of competing processes. Figure 1.1 outlines these competing processes.

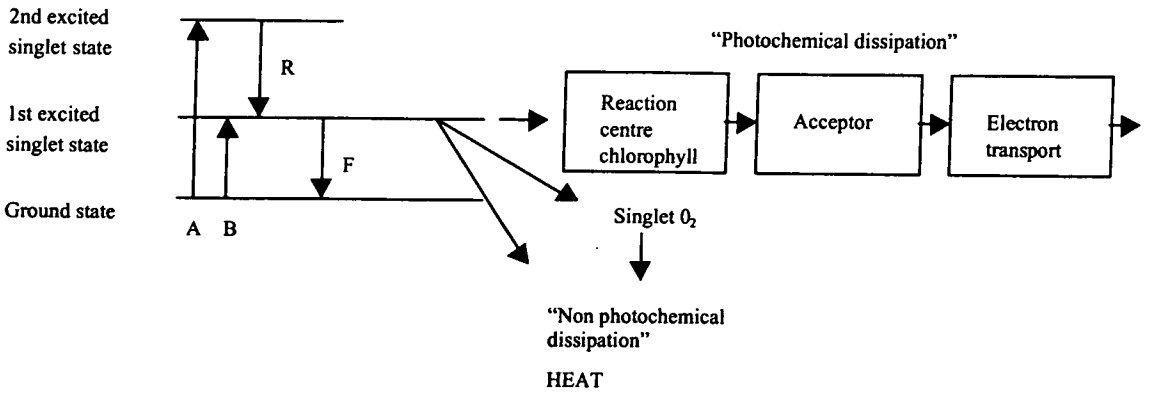


**Figure 1.1**. Simplified representation of the processes that compete for chlorophyll excited states in the antenna. Absorption of a photon raises the electron to either the first or second excited states depending on the absorption of a blue or red photon (A and B respectively). Dissipation of excitation energy from the $2^{nd}$ excited state occurs by radiationless transition (R) and decay from the $1^{st}$ excited state occurs through chlorophyll fluorescence (F) and heat (non photochemical quenching). Photochemical utilisation (photochemical quenching) of absorbed photons is through transfer to reaction centre chlorophyll, and subsequent electron transport chains, driving photosynthesis.

Light absorption also represents one of the pathways in which environmentally induced damage occurs in plants (Krause, 1988, Long *et al.*, 1994). When the photosynthetic apparatus absorbs more energy than it can utilise in photochemistry, the potential for formation of reactive oxygen species (singlet $O_2$, superoxide and associated free radicals) increases and can result in considerable damage to the PS II reaction centre complex.

When is light/PPFD in excess? Up to a certain level of PPFD, an increase in PPFD absorption results in an increase in photosynthetic $CO_2$ fixation. However, the increases in PPFD a plant experiences throughout the day result in a decrease in the ability to process this excitation through photochemistry, and thus decrease photosystem efficiency, and overall photosynthetic efficiency. This is highlighted by the predicted absorption and utilisation of PPFD of a $C_3$ plant in Figure 1.2. The utilisation of quanta absorbed with respect to photon flux density is described by the typical non-rectangular hyperbolic response of photosynthesis to PPFD. At low photon fluxes (~ 100 μmol $m^{-2}$ $s^{-1}$) more than 80 % of the absorbed quanta are utilised in photosynthesis, in accordance with the maximum quantum yield of oxygen evolution (i.e. 8-10 photons are needed to fix one $CO_2$ giving a maximum efficiency of 0.1 mol $CO_2$ per mol photons, Bjorkman and Demmig, 1987). When the photon flux density approaches half that of full sunlight (~1000 μmol $m^{-2}$ $s^{-1}$) as little as 25 % of the absorbed PPFD is utilised, and in full PPFD (~ 2000 μmol $m^{-2}$ $s^{-1}$), only around 10 % is utilised. Under otherwise optimal conditions the greater the gap between absorption and utilisation the greater the over-excitation of the photosynthetic apparatus and greater need for energy dissipation mechanisms.

It is critical to realise that any increase in light intensity is not the only environmental change that can lead to excess light absorption. Any stress factor that brings about a decrease in the rate of photosynthesis, for a constant PPFD, will result in excess light absorption. For example, plants that experience water stress will close their stomata and experience a reduction in leaf internal $CO_2$ concentration and rates of

photosynthesis. This topic still requires considerable investigation but the variability that exists in light, water and temperature in the natural environment suggests that excess light absorption, and its dissipation, is a problem that has long been encountered by plants in the field (Long *et al.*, 1994, Owens, 1996).

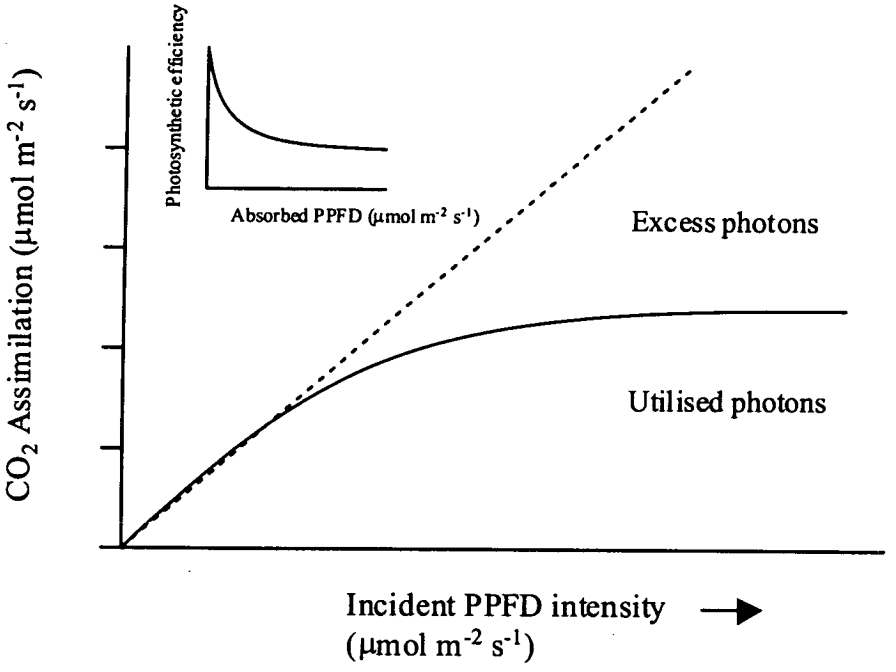


**Figure 1.2** An idealised photosynthesis-irradiance curve showing the relationship between the rate of photosynthesis and incident PPFD

An understanding of the consequences of excess light absorption requires consideration of the coupled light and dark reactions of photosynthesis. For any environmental factor (e.g. temperature) which results in a limitation of photosynthesis in the dark reaction, there is an inhibition of electron transport due to a slower regeneration of $NADP^+$ and ADP or inorganic phosphate. This leads to a closing of the reaction centres in PS II to incoming energy and an increased acidification of the thylakoid lumen. This decrease in PS II photochemistry results in a higher yield of chlorophyll fluorescence. If the rate of triplet formation exceeds the capacity of the plant's ability to dissipate this energy safely, damage to the photosystems will result.

The chloroplasts however contain the necessary metabolic machinery to deal with the consequences of such excess light absorption both directly and indirectly. Indirect examples include the removal of superoxide and resulting free radicals (Pell and Steffen, 1991) and repair of damaged PS II reaction centres through synthesis and insertion of new polypeptides (Melis, 1991). Recently, a regulatory process has been described where excess light absorption is dissipated as heat in competition with processes that cause light induced damage.

## REGULATING LIGHT ENERGY UTILISATION : NON PHOTOCHEMICAL QUENCHING ($q_N$)

The regulation of energy utilisation in photosynthesis is controlled by a group of reactions called non-photochemical quenching, or $q_N$. The process of non-photochemical quenching of chlorophyll excited states competes with photochemical quenching ($q_p$, i.e the processes that lead to photosynthesis) in the reaction centres, by creating a pathway for the decay of excited states in the antenna. For a plant to maintain optimal efficiency under a variety of growth conditions, the process of non-photochemical quenching must allow for maximal light utilisation under light limiting conditions and regulate quenching. That is, the processes that regulate $q_N$

must sense the imbalance between the rate of light absorption and the capacity for light utilisation in photosynthesis and adjust $q_N$ accordingly to only dissipate the excess fraction of light.

The measurement of quenching mechanisms is closely tied to the measurement of chlorophyll fluorescence because the reactions of $q_N$ and $q_P$ compete with the other decay processes of fluorescence, thermal emission and triplet formation, as outlined earlier. As such, $q_N$ is commonly referred to as "non-photochemical quenching of chlorophyll fluorescence". It should be noted that this process is not regulating fluorescence but rather regulating the fate of chlorophyll excited states by competing with other processes of de-excitation.

The physiological processes that contribute to total non-photochemical quenching are both complex and heterogeneous. These processes fall into three categories (i) *energy dependent quenching* ($q_E$) which is regulated by the pH of the thylakoid lumen (Demmig-Adams, 1990, Horton *et al.*, 1994), (ii) *photoinhibitory quenching* ($q_I$) which is related to the slowly reversible, light dependent decrease in light saturated rate of photosynthesis (Ruben and Horton, 1995) and (iii) *light state transitions* which quench PS II fluorescence by physically altering the antenna size of PS II units. Whilst each of these processes contributes to total $q_N$, under normal physiological growth conditions, $q_E$ is the major component of $q_N$.

**PROPOSED MECHANISM FOR $q_E$**

There is wide agreement that the principle role of $q_N$ is in the dissipation of excess light absorption in competition with photochemistry, chlorophyll fluorescence and other decay processes. Because the energy storage in the reaction centres, and fluorescence emission, were found to be decreasing as $q_N$ increased, a new process that dissipates excess energy as heat was proposed.

The key process *controlling* this dissipation of excess energy through non-photochemical quenching involves a group of carotenoids called the xanthophylls. A change in the relative concentration of xanthophyll cycle pigments is induced by a change (decrease) in the pH within the thylakoid membrane, a response induced by excess light absorption. Demmig-Adams and Adams (1990) were the first to demonstrate a correlation between $q_N$ and the accumulation of the carotenoid zeaxanthin in the thylakoid membranes. The mechanism is described as follows.

Under conditions of excess absorption of PPFD, the pigment violaxanthin is converted to zeaxanthin via an intermediate antheraxanthin (see Figure 1.3). This reaction is reversible under low PPFD levels (for a review see Demmig-Adams and dams, 1992, Long *et al.*, 1994, Osmond *et al.*, 1999). This sequence of two independent reactions, is termed the xanthophyll cycle, and is present throughout the plant kingdom (Demmig-Adams and Adams, 1993). The carotenoids that participate in this cycle are the only carotenoids in the photosynthetic membrane that are capable of rapid PPFD induced concentration changes. Until recently the functional role of this cycle has remained elusive.

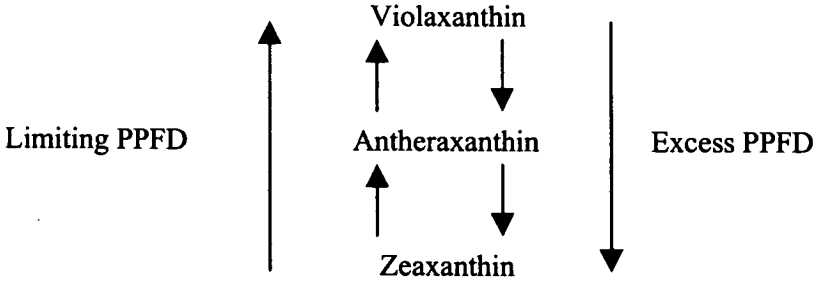


**Figure 1.3** Schematic representation of the Xanthophyll cycle.

Numerous studies have documented relationships between increased levels of zeaxanthin and increases in energy dissipation, as estimated from measurements of

$q_N$ (Demmig-Adams, 1990, Gilmore and Yamamoto, 1993, Demmig-Adams and Adams, 1994, Demmig-Adams *et al.*, 1995, 1998, Demmig-Adams and Adams, 1996, Demmig-Adams, 1998,) leading to the proposal that zeaxanthin mediates the harmless dissipation of excess PPFD in the form of heat. It has been proposed that zeaxanthin catalyses the removal of the same energised form of chlorophyll (excited singlet chlorophyll, or $^1$Chl*) that gives rise to chlorophyll fluorescence, and is the same chlorophyll that is used for photosynthesis. The xanthophyll cycle seemed to be particularly suited to interfere at this sensitive step, allowing the efficient use of energy under low PPFD, switching to rapid dissipation of the excess energy under high PPFD.

Initially there was resistance to the causal link between zeaxanthin and its role in energy dissipation. It was thought that there lacked a mechanism by which the energy could be directly transferred from the light harvesting chlorophyll to zeaxanthin. Contemporary theory suggested that it was thermodynamically impossible for energy to be transferred from $^1$Chl* to zeaxanthin (Siefermann, 1987, Demmig-Adams and Adams, 1996). Subsequently, this question concerning the involvement of the xanthophyll cycle in energy dissipation has received intense interest, resulting in new insights into the mechanism, regulation, ubiquity and environmental responses of this energy dissipation mechanism.

However, advances over the past eight years have confirmed a causal link between the combined presence of zeaxanthin (and antheraxanthin) and a low pH within the thylakoid lumen on the one hand, and energy dissipation on the other (Bjorkman and Demmig, 1987, Horton and Ruben, 1992, Demmig-Adams and Adams, 1992, Demmig-Adams and Adams 1993, Frank *et al.*, 1994, Pfundel and Bilger, 1994, Long *et al.*, 1994, Demmig-Adams and Adams, 1996, Demmig-Adams *et al.*, 1995, Osmond and Grace, 1995, Owens, 1996, Demmig-Adams, 1998, Osmond, 1999). These findings demonstrated that high energy/pH dependent and xanthophyll cycle dependent energy dissipation were in fact one and the same mechanism. Studies of

the photophysics of the xanthophyll cycle have demonstrated that a simple and direct downhill reverse transfer of energy from excited states of chlorophyll ($^1$Chl*) to zeaxanthin is thermodynamically possible (Gilmore, 1997). In essence, zeaxanthin acts like a lightening rod, receiving the excess energy and dissipating it harmlessly as heat, thus reducing the likelihood of $^1$Chl* passing energy onto oxygen creating the excited form of oxygen ($^1O_2$*) which is highly reactive and leads to the potential for photo-oxidative damage.

Considerable debate centred on whether energy dissipation could be induced by low pH alone, or whether the presence of zeaxanthin (with antheraxanthin) was necessary for energy dissipation to occur (Gilmore and Yamamoto, 1993, Pfundel and Bilger, 1994, Horton *et al.*, 1994, Owens, 1996). A series of experiments showed that the key energy dissipation process is obligatorily and stochiometrically dependent on the presence of both antheraxanthin and zeaxanthin (Gilmore and Yamamoto, 1992, Gilmore and Yamamoto, 1993, Gilmore *et al.*, 1994, Gilmore *et al.*, 1995). In addition to this, an elegant experiment where zeaxanthin was allowed to convert back to violaxanthin under excess light led to a loss of energy dissipation activity despite the presence of a low luminal pH (Gilmore *et al.*, 1994). Despite the recent breakthroughs on the function of the xanthophyll cycle, the exact of this thermal energy dissipation within the photosynthetic apparatus is unknown. A breakthrough study by Li *et al.*, (2000) found that the presence of one specific protein (CP22 or PsbS) was essential for the thermal energy dissipation to occur. The authors isolated a mutant from *Arabidopsis thaliana* that contained normal levels of zeaxanthin but was deficient in energy dissipation (i.e. $q_N$). It was shown that this mutant lacked the PsbS protein. They thus reintroduced the protein into the mutant plant which regained the ability to dissipate the energy thermally. Questions that still remain however are the exact location of this protein. Knowing this means the actual site of energy dissipation (and the structural change that accompanies it) may be identified. Before the function of PsbS was known however, increased levels were observed in needles of Scots pine (*Pinus sylvestris*) in winter.

In nature, a fluctuating PPFD environment and changes in the levels of zeaxanthin occur in parallel.

A number of laboratory and field studies have focused on the light dependent responses of xanthophyll cycle pigments. Adams and Demmig-Adams (1992) examined the changes in the xanthophyll pigment compositions of a number of crop species in response to diurnal changes in sunlight. It was found in all cases that large amounts of zeaxanthin were formed at peak irradiance (full PPFD) together with depressed rates of photosynthesis. Over the diurnal cycle, changes in zeaxanthin content closely tracked changes in PPFD for all the species sampled.

In a similar study, the xanthophyll cycle pigments and photosynthesis capacity ($PS_{max}$) in 25 species in different light environments (canopy, gap and understorey) within a Panamanian tropical forest were examined (Koniger *et al.*, 1995). Sun exposed leaves of canopy tree species exhibited the highest photosynthesis capacities and largest xanthophyll cycle pool sizes. Under high PPFD, canopy leaves converted 96% of the xanthophyll cycle pool into zeaxanthin. At the end of the diurnal cycle, the zeaxanthin still accounted for 14 % of the total pool of xanthophyll cycle pigments. Leaves sampled in the gap displayed intermediate levels of $PS_{max}$ and a 43% lower carotenoid content than the canopy leaves, but under high light the gap species converted 86% of their pool to zeaxanthin. The understorey species had the lowest values of $PS_{max}$ and the smallest xanthophyll cycle pool. During periods of sunflecks, of 1-2 minutes duration, the conversion to zeaxanthin was negligible. Watling *et al.*, (1997) also examined the responses of rain forest understorey plants to excess PPFD during sunflecks. This study also found high concentrations of zeaxanthin in leaves subject to excess PPFD, but this was for periods of around 100 minutes, not the 1-2 minutes experienced by the leaves examined in the work of Koniger *et al.*, (1995).

Demmig-Adams and Adams (1996) analysed the efficiency of photosystem II, NPQ and xanthophyll cycle composition, *in situ*, in plants in their natural environment. Different degrees of light stress were experienced by a range of plant types, including trees, shrubs and herbs. All plants however displayed the same close relationship for changes in intrinsic PS II efficiency, $q_N$, and levels of zeaxanthin and antheraxanthin, as a function of the light stress. Thus, the same conversion state of the xanthophyll cycle and the same level of dissipation were observed for a given level of light stress and independent of species. Since all increases in thermal energy dissipation were associated with increases in the levels of zeaxanthin, there was no indication of any form of xanthophyll cycle independent energy dissipation. Thus, the diurnal changes in intrinsic PS II efficiency in nature are caused by changes in which the efficiency with which excitation is passed from the antennae to the reaction centres, and are likely to be purely photoprotective.

Schindler and Lichtenthaler (1996) examined the changes in photosynthesis, chlorophyll fluorescence and xanthophyll cycle composition in leaves of field-grown maple trees on sunny and cloudy days. Over the diurnal course, as PPFD increased net photosynthesis rose with PPFD in the morning, as did the concentration of zeaxanthin. When the rate of $CO_2$ fixation began to decrease at saturating levels of PPFD, larger amounts of zeaxanthin were accumulated and corresponding decreases in photosynthesis rates and increases in non-photochemical quenching were noted. These results further support the role of zeaxanthin in energy dissipation and photoprotection of the photosynthetic apparatus against exposure to high PPFD.

The studies of diurnal responses of xanthophyll cycle pigments that have been performed in environments with predictable patterns of PPFD clearly demonstrate that changes in zeaxanthin closely follow the changes in incident PPFD. However, in tropical environments, the changes in PPFD experienced during sunflecks or those experienced by rapidly changing cloud cover may be highly variable. In these

instances, depending on the time scale of exposure, the dynamics of the xanthophyll cycle conversion can vary.

## RESPONSE OF THE XANTHOPHYLL CYCLE TO THE INTERACTION OF LIGHT AND ENVIRONMENTAL STRESS

Environmental stress factors can influence the operation of the xanthophyll cycle (Demmig-Adams and Adams, 1992). These influences are not direct but rather act through the effect on their capacity for photosynthetic electron transport. Any environmental stress that causes a decrease in the rate of photosynthesis will have the effect of increasing the ratio of PPFD/photosynthesis, even if PPFD doesn't change. Under these circumstances, the absorption of light by chlorophyll leads to an increased level of excess excitation energy, and a need to increase the amount of energy dissipated thermally, thus providing greater protection (Demmig-Adams & Adams, 1992).

Current evidence suggests that zeaxanthin is important in the dissipation of additional thermal energy when the plants are subject to environmental stresses (such as water stress, sailinity, nutrient stress high and low temperature stress) in the presence of light. However, stress does not necessarily cause a sustained effect on photochemical efficiency (Ludlow *et al.*, 1988, Long *et al.*, 1994).

For plants distributed in temperate and sub-arctic northern hemisphere, low temperatures present the most obvious stress when combined with high levels of light. Exposure to freezing (and chilling) temperatures decreases the rates of photosynthesis and thus a given light intensity becomes progressively more excessive as photosynthesis falls. The boreal forests are found at high latitudes (50 - 70° N) where a strong seasonal change in climate occurs. Summer growth phases alternate with periods of winter dormancy where growth comes to an abrupt halt with

the onset of subfreezing temperatures. Before full winter dormancy is achieved, winter hardiness must be developed for winter survival (Levit, 1980).

Evidence to date shows that winter stress inhibition of photosynthesis is relatively well established for spruces and pines (Martin *et al.*, 1979, Linder and Troeng, 1980, Oquist and Ogren, 1985, Leverenz and Oquist, 1987, Lundmark *et al.*, 1988, Ottander and Oquist, 1991, Adams and Demmig-Adams, 1994, Hansen *et al.*, 1996, Verhoeven *et al.*, 1999). Thus high levels of light in combination with extreme low temperatures results in a strong inhibition of photosynthetic efficiency of PS II in conifers (Martin *et al.*, 1978). Conifers must therefore adapt their photosynthetic apparatus during severe winters where temperatures can drop as low as –70° C (Beck *et al.*, 1995).

Well before the onset of freezing temperatures, many conifers lose their PS II reaction centres (but also retain some inactive reaction centres), chlorophyll (up to 60 %) and the LHC proteins (Ottander *et al.*, 1995). An analysis of Scots pine (*Pinus sylvestris*) needles by Ottander *et al.*, (1995) showed a pronounced increase in the pool size of xanthophyll cycle pigments during the winter when temperatures were below freezing and incident light was at saturating intensity. As only a small portion of the chlorophyll remains in the needles, the absorption of light cannot be used in photochemistry (i.e. no active PS II reaction centres) and must therefore be dissipated via an alternative pathway. As Ottander *et al.*, (1995) and others (Ottander and Oquist, 1991, Adams and Demmig-Adams, 1994, Verhoeven *et al.*, 1996, Vogg *et al.*, 1998, Verhoeven *et al.*, 1999) have shown, the xanthophyll cycle is working to its highest capacity during this time in conifers to ensure that all excess excitation is funnelled away via the xanthophyll cycle.

An interesting point further noted by Ottander *et al.*, (1995) was that photochemical efficiency, the chlorophyll content and the content of a specific protein called *D*1 (which is essential to the functionality of the reaction centres) started to decrease

*before* any increase in the carotenoids of the xanthophylls during the transition from autumn to winter. Also, the increase in the pool size of the xanthophylls did not reach its peak until January, whereas the winter minimum of photochemical efficiency was reached in February. These findings, whilst controversial, suggest that the protection of the photosynthetic apparatus cannot be fully explained by the xanthophyll cycle.

The role of the xanthophyll cycle in these extreme environments is an area requiring further attention. Emphasis in this thesis is therefore placed on the role of the xanthophyll cycle in a boreal forest canopy during the winter spring transition when the forest was being exposed to sub-freezing temperatures (i.e. from – 20° C and above) during winter, up to 35° C during the spring.

## REMOTE SENSING OF PHOTOSYNTHETIC EFFICIENCY VIA THE XANTHOPHYLL CYCLE

The status of the xanthophyll cycle can be studied with optical techniques. Bilger *et al.*, (1989) demonstrated that the conversion from violaxanthin to zeaxanthin can be monitored through changes in absorbance from 505 – 515 nm and decrease in the reflectance at slightly longer wavelengths of 525 – 534 nm (Gamon *et al.*, 1990). This slight spectral shift can be related to a number of factors. The spectral difference may be the result of differing pathlengths of reflected and transmitted light between species. Also, varying degrees of chloroplast movement, which was prevented in the study of Bilger *et al.*, (1989) study but not in the study of Gamon *et al.*,(1990), could give rise to slightly different spectral peaks.

Gamon and co-workers (1992) thus developed an index based on the reflectance in the 525 – 534 nm spectral regions. A normalised index called the Photochemical Reflectance Index, or PRI, was formulated

$$PRI = (R_{REF} - R_{530})/(R_{REF} + R_{530})$$

where $R_{530}$ denotes the reflectance at 530 nm and $R_{REF}$ denotes the reflectance in a reference waveband. The reference waveband is used to remove the effects of spectral features such as chloroplast movement which might overlap with the signal of the xanthophyll cycle (Brugnoli and Bjorkman, 1992). The denominator minimises the influence of irradiance conditions (review and evaluation of the mathematical formulation of VI's can be found in Chen, 1996).

Following the pioneering work of Gamon *et al.,* (1990), Gamon, (1992) was the first to demonstrate the correlation between LUE and the PRI using sunflower canopies. Measurements of reflectance and gas exchange were made over intact canopies of control, nitrogen and water stressed sunflowers with diurnal course of PPFD typically experienced during the day. The results showed strong correlations between PRI and LUE in all three groups of treatments, although the relationship was degraded somewhat in the water stressed plants. Similar measurements have been made on several species representing $C_3$ and CAM photosynthetic pathways, as well as under drought stress conditions. PRI and LUE were found to change in parallel in diurnally changing sunlight levels outdoors. PRI was linearly related to $\Delta F/Fm$ (a fluorescence based index of photosystem II photochemical efficiency) as well as the instantaneous photosynthetic efficiency (Penuelas *et al.*, 1995, 1997 and Fillela, 1996).

More recently, Gamon *et al.*, (1997) explored the utility of PRI as an indicator of LUE in 20 species spanning three functional types: annual, deciduous perennial and evergreen perennial. Across the species, top canopy leaves in full sun at midday exhibited strong correlations between PRI and $\Delta F/Fm$. PRI was also found to be significantly correlated with both net $CO_2$ uptake and LUE measured by gas exchange.

Following this work, the question of whether the PRI : LUE relationship could hold over heterogeneous forest canopies remained to be investigated. Such a study was

undertaken by Nichol *et al.*, (2000) and is presented as part of this thesis. PRI was calculated from canopy reflectances measured over boreal forest (from a helicopter platform) and related to canopy photosynthetic efficiency, calculated from eddy covariance data. Strong linear relationships were found between PRI and the LUE of four contrasting boreal forest canopies of spruce, jack pine, aspen and fen. These results provide the first application of PRI at the landscape scale. More studies are warranted to test the nature of the PRI : LUE relationship for landscape and larger areas. This question forms the core of this thesis.

## CANOPY REFLECTANCE MODELS

As increased value is being placed on the use of remote sensing in biospheric research, a concomitant increase in the understanding of factors that influence vegetation reflectance signals has only been partially realised (Asner, 1998). Based on experimental and modelling studies, vegetation reflectance has been found to be a complex function, depending on the optical properties of constituent tissues (leaf, woody and stem), canopy biophysical attributes (e.g. leaf and stem area, leaf and stem orientation and foliage clumping), soil reflectance, illumination conditions and viewing geometry (Myneni *et al.*, 1989, Jacquemond *et al.*, 1992, Goward and Huemmrich, 1992, Asner, 1998).

Non photosynthetic material in the canopy (e.g. woody stems and standing litter) exert their own influence on the radiation field through their reflectance and transmittance properties (Asner *et al.*, 1998b). Leaf optical properties are a function of leaf structure, water content and concentration of biochemicals (Curran *et al.*, 1992, Fourty *et al.*, 1996). The variation observed in canopy reflectance is driven by the plant structural variables orientating the scatterers in three dimensional space. This allows for multiple interaction between incoming photons and leaves, woody material and soils. Understanding variations in canopy reflectance is pivotal for developing remote sensing applications.

Studies using vegetation indices (predominantly NDVI and NDVI adjusted indices) have shown that variations in the linearity of their relationship with biophysical variables such as green leaf area, biomass and percentage of green foliage, have been apparent under different observing conditions (Gamon *et al.*, 1995, Turner *et al.*, 1999). Many of these studies have employed the use of numerical radiative transfer models to investigate the influence of such extraneous variables while keeping other factors constant. (Goward and Huemmrich, 1992, Barton and North, *in press*). Modelling has the great advantage of being able to simulate a wide range of observing conditions quickly. However, the drawback is that models can only approximate the reality of remote sensing measurements.

A range of canopy reflectance models exist and these can be divided into four categories; (1) Geometric Models, (2) Turbid-Medium Models (3) Hybrid Models and (4) Computer Simulation Models (Goel *et al.*, 1988). Their classification is based on how light interactions are abstracted in the model design. A brief outline of these is given.

(1) Geometrical model. Geometrical objects describe the canopy and are placed on a background surface. The shapes are made up of spheres, ellipsoids, cones, or cylinders (or combinations of these) with their dimensions, number and placement being defined in the model along with the optical properties. Light interception by the canopy shapes and shadowing (with background reflectance) determines the reflectance of the scene. These models are generally useful for sparse canopies such as orchards or open conifer forests where multiple scattering is minimal.

(2) Turbid medium models. The canopy is modelled as a series of horizontally homogeneous parallel layers. The vegetation is considered to be small randomly distributed particles within each layer with each layer being defined with absorption and scattering properties. The canopy is described in terms of leaf area index (LAI) and leaf angle distribution (LAD). As the layers are uniform in the x and y directions,

the radiation field is dependent on depth only. Leaf size, distance between leaves and non-random horizontal leaf distribution are not taken into account in this model. These models are generally suitable for dense uniform canopies

(3) Computer simulation models. In these models the distribution, orientation and optical properties are pre-programmed in the computer. A Monte Carlo procedure is used to determine if a beam of light will hit an area of canopy (Goel, 1988). Following the path of the photon and its interactions with the canopy elements determines the radiation regime. As these models actually track the individual photons, the distribution of intensities may be calculated rather than calculation of averages. These models are computationally expensive but produce realistic descriptions of canopy reflectance.

(4) Hybrid models. These are generally a combination of Geometrical and Turbid Medium models where the canopy is described by a distribution of geometrical shapes. Within these shapes are absorbing and scattering particles as in the turbid medium. These models are generally complex and can describe a wide variety of conditions.

One of the most commonly used canopy reflectance models is the turbid medium model developed by Suits (1972). This model assumes that the canopy has an infinite horizontal extent and may be divided into layers with uniform characteristics. All the leaf elements are replaced by their vertical and horizontal projections. The interception of the radiant flux by the leaves is approximated by interceptions with their projections, and all reflectances are diffuse. Suits' model finds the directional reflectance as a function of view angle in the principle plane by finding the illumination of each infinitesimal layer in the canopy that can be seen from that view angle. This produces a non-lambertian reflectance in the principle plane. The SAIL model was thus developed which is a simple extension of the Suits model. It builds on the Suits model by including a distribution of leaf angles rather than a single leaf

angle. As a result, the SAIL model produces more realistic patterns of canopy bidirectional reflectance than the Suits model (Verhoef, 1984, Goward and Huemmrich, 1992).

Although effective for homogeneous canopies, the SAIL model has limited capabilities for simulating the reflectance of heterogeneous canopies. Thus more complex models are being increasingly adopted. The use of models both at the leaf and canopy scales can improve our understanding of the absorption and scattering of solar radiation in vegetation canopies. The modelling of canopy reflectance can be done to a high degree of accuracy by using a series of coupled models (which include leaf and canopy models) or complex functions in which there are a large number of variables (Dawson *et al.*, 1998).

Leaf optical models include the PROSPECT (Jacquemond and Baret, 1990), and LIBERTY (Leaf Incorporating Biochemicals Exhibiting Reflectance and Transmittance Yields) (Dawson *et al.*, 1998) models which simulate broadleaf and conifer needle reflectances respectively. Both of these models calculate the reflectance and transmittance values using measured or estimated surface concentrations of chlorophyll, carotenoids, water and leaf structure as inputs. These models have been designed such that the simulated leaf and needle reflectances could then be input to various canopy models, such as FLIGHT (Forest Light)(North, 1996, Dawson *et al.*, 1999) and SAIL (Verhoef, 1984, Andrieu *et al.*, 1997) to simulate the canopy reflectance. Further details of leaf and canopy reflectance models can be found in (Jacquemoud and Baret, 1990, Strahler *et al.*, 1994, North, 1996, Dawson *et al.*, 1998, Dawson *et al.*, 1999).

The potential of spectral vegetation indices for interpreting any feature of vegetation relies heavily on the fact that it is exclusively sensitive to the variable of interest. Evidence suggests that vegetation indices can be sensitive to extraneous factors. The reflectance of a scene is an integration of all its components. For a forest ecosystem

this includes the green foliage as well as the background components which include soil, bark, understorey vegetation and depending on location and time of year, snow. Few studies have reported the utility of spectral indices for conifer forests (McDonald *et al.*, 1998). The studies that have been conducted have focused on NDVI, which has been found to be highly sensitive to background reflectance (Huete *et al.*, 1998) as well as sun-sensor geometry (Gemmel and McDonald, 2000).

Only one publication to date has investigated the sensitivity of PRI to changing background conditions. Barton and North (*in press*) developed a quantitative model relating canopy PRI to LUE, and determined how sensitive the (above canopy) PRI signal was to perturbing effects such as leaf angle distribution and optical geometry. These findings found that at low canopy cover (LAI < 3) PRI was most sensitive to changes in LAI and background reflectance. They also found that the index was useful in tracking diurnal changes introduced by a solar angle, but also found that the index provided greater variation of view angle than most other indices.

The use of remote sensing as a tool for detecting changes in the xanthophyll cycle at the scale of forest canopies is clearly in its infancy. The applicability of PRI to serve as an indicator of photosynthetic efficiency remains to be tested in a number of different situations and contrasting ecosystems, particularly at the canopy scale. The robust nature of the relationship between a canopy PRI and LUE also has to be investigated further, which can be made easier through the use of models.

## SPECIFIC OBJECTIVES OF THE THESIS

The objectives of this thesis are as follows:

1. To investigate the relationships between the PRI and LUE in individual leaves of one $C_3$ species in glasshouse conditions.

2. To extend the relationships between the PRI and LUE to the canopy scale in two boreal forest ecosystems. Investigating the influence of winter stress on the relationships between the PRI and LUE.

3. To investigate the role of background reflectance in the canopy spectral signal and its effects on the calculation of PRI.

## THESIS STRUCTURE

This thesis investigates the use of remote sensing for estimating the efficiency of photosynthesis at the leaf and canopy scale. There are six chapters. Chapter 1 provides a review of the current literature with regard to this field of research. The underlying theme of comparing the Photochemical Reflectance Index (PRI) with photosynthetic light use efficiency (LUE) is maintained throughout.

*Chapter 2:* Measurements of leaf gas exchange, chlorophyll fluorescence and reflectance were made on a $C_3$ species in controlled glasshouse conditions. The relationships between PRI and LUE, from gas exchange, and the fluorescence based indicator of photosynthetic efficiency, were explored.

*Chapter 3:* Using a helicopter mounted spectroradiometer, seasonal canopy spectral reflectance was measured from a helicopter over boreal forest in Canada. Photosynthetic efficiency was calculated from eddy covariance data and correlated with PRI.

*Chapter 4:* Using a helicopter mounted spectroradiometer, canopy spectral reflectance was measured over boreal forest in Siberia during the winter spring transition. Photosynthetic efficiency was calculated from eddy covariance data and correlated with PRI. Tower based measurements of reflectance were also made at one of the sites, and comparisons with eddy covariance LUE estimates and xanthophyll cycle pigments were made.

*Chapter 5:* Canopy PRI was simulated using the SAIL model with leaf reflectance data from the boreal forest. The variability in PRI was assessed as functions of changing canopy structure, illumination quality and geometry, and background materials.

*Chapter 6*: Concluding remarks

BIBLIOGRAPHY

# 2. PRI, CHLOROPHYLL FLUORESCENCE AND PHOTOSYNTHETIC-LIGHT-USE EFFICIENCY OF LEAVES OF A $C_3$ SPECIES.

## 2.1 INTRODUCTION

Several processes of dissipation of excess light absorbed by plants have been linked to a decline in spectral reflectance near the wavelength 531 nm. A measurement of reflectance in this spectral region should thus be able to provide an indirect estimation of photosynthetic performance. A number of studies on individual leaves have reported that this reflectance signal was present over a range of photon flux density levels in several species differing in leaf morphology, habit and photosynthetic pathway (Gamon *et al.*, 1990, 1992, 1993, 1997). The index PRI (Photochemical Reflectance Index), derived from the reflectance signal has been closely correlated with xanthophyll cycle interconversion and photosynthetic light use efficiency.

This chapter presents a study to investigate the utility of PRI as an indicator of photosynthetic light use efficiency (hereafter referred to as LUE) in leaves of a single $C_3$ species grown under glasshouse conditions.

The aim of this study was to compare the photochemical reflectance index, PRI, with chlorophyll fluorescence and gas exchange measurements under controlled conditions to test this reflectance index for estimating photosynthetic LUE.

## 2.2 METHODS

### PLANT MATERIALS AND GROWTH CONDITIONS

Seeds of bean (*Vicia faba*) were germinated in full sunlight in glasshouse conditions on the campus of Edinburgh University. The seeds were planted in a standard FII medium which is a mixture of peat and 30 % sand. The plants were irrigated daily throughout the entire study. During the measurement period the photosynthetic photon flux density (PPFD) in the glasshouse ranged from 500 - 1500 μmol of photons $m^{-2}$ $s^{-1}$ and temperatures inside the glasshouse ranged from 17 - 22 °C. Measurements were made over a two week period from the end of July to the beginning of August 1998, 4 weeks after potting, on fully expanded leaves near each plants apex. Measurements were made on single leaves of 14 individual plants.

### GAS EXCHANGE

The $CO_2$ uptake was measured with a portable photosynthesis system equipped with a 2 x 3 cm opaque topped leaf chamber (LI-6400, Li-Cor, Lincoln, NE, USA). Incident radiation was provided by a series of halogen lamps and controlled between 500 and 1500 mols $m^{-2}$ $s^{-1}$ using neutral density filters. A quantum sensor inside the leaf chamber measured incident radiation at the leaf surface. A water bath was placed below the lamps to absorb infra-red radiation and effectively kept leaf temperature constant. The configuration can be seen in Figure 2.1.

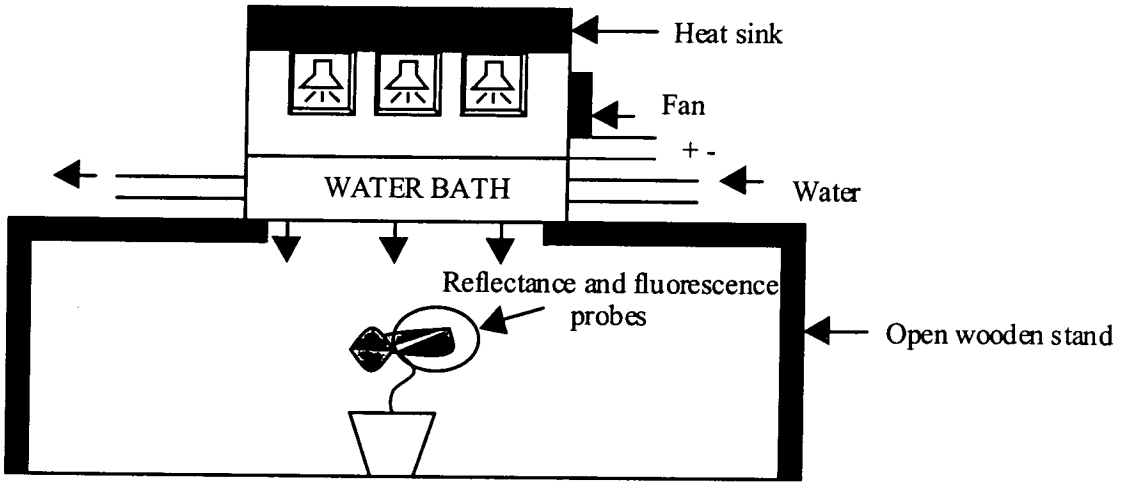


**Figure 2.1** Experimental set up for measurement of photosynthesis, reflectance and chlorophyll fluorescence.

A plant was selected at random and placed under the lamps, as shown in Figure 2.1. For each set of measurements, a single leaflet was placed in the LI-6400 chamber (with each leaf filling the chamber) at its natural angle of inclination. The incident light was set to either 500, 1000 or 1500 μmol $m^{-2}$ $s^{-1}$ (using the neutral density filters), in the morning, at midday and in the afternoon, at the times the times the plant would be experiencing such light levels. Carbon dioxide levels were provided by an external $CO_2$ source attached to the 6400. The air stream into the chamber head was maintained at 360 μmol $m^{-2}$ $s^{-1}$. The $CO_2$ levels were allowed to stabilise before collection and storage of photosynthesis data. Each gas exchange measurement took about six minutes.

Instantaneous photosynthetic LUE was calculated by dividing the $CO_2$ assimilation by the incident PPFD recorded by the quantum sensor inside the leaf chamber at the time of measurement.

**OPTICAL MEASUREMENTS (REFLECTANCE AND FLUORESCENCE)**

Spectral reflectance of the same leaf used for gas exchange was determined immediately after gas exchange measurement when the leaf was under identical conditions (described above) with a laboratory spectroradiometer (Monolight, Macam Photometrics, Livingston, Scotland).

The instrumentation consisted of a fibre optic probe attached to the leaf gas exchange chamber at a 60° angle (30° to the normal) and the Monolight spectroradiometer (model 6118). Reflectance spectra were calculated by dividing the spectral radiance of the leaf adaxial surface by the radiance of a 99 % calibrated reference reflectance standard (Spectralon, Labsphere, North Sutton, NH). The scan of the reference panel was made immediately after the leaf spectral measurement. Data were collected between 400 and 900 nm at 1 nm intervals. PRI was calculated as follows,

$$\mathrm{PRI} = (R_{550} - R_{530})/(R_{550} + R_{530})$$

where $R_{530}$ indicates the reflectance at 530 nm (the waveband of the xanthophyll signal) and $R_{550}$ indicates the reflectance at 550 nm (a reference waveband). This reference waveband differs slightly from that used in most recent studies (Gamon *et al.*, 1997) but is identical to that used in earlier studies (Gamon *et al.*, 1992, 1993, 1997, Penuelas, 1997). Referencing $R_{530}$ to $R_{550}$ has the effect of subtracting factors other than the xanthophyll cycle that can affect spectral reflectance in this region, such as chloroplast movement.

The efficiency of photosystem II (PSII) (for details see Genty *et al.*, 1989), was measured using a pulse modulated chlorophyll fluorescence meter equipped with a leaf clamp (FMS-2, Hansatech Instruments Ltd, Norfolk, England). The light was provided by the same halogen lamps that were used for the gas exchange and reflectance measurements. Fluorescence readings were taken immediately after reflectance and gas exchange measurements respectively. Because reflectance and fluorescence probes were of similar diameter, both techniques measured similar leaf areas and leaf regions. Each optical measurement was completed within two minutes, allowing reflectance and fluorescence to be measured under near-identical conditions. However, because of the different temporal and spatial scales of gas exchange, it was not possible to match exactly the time of measurement with reflectance and fluorescence, although the same leaves of each plant were used for all three measurements and conditions were uniform throughout.

## 2.3 RESULTS

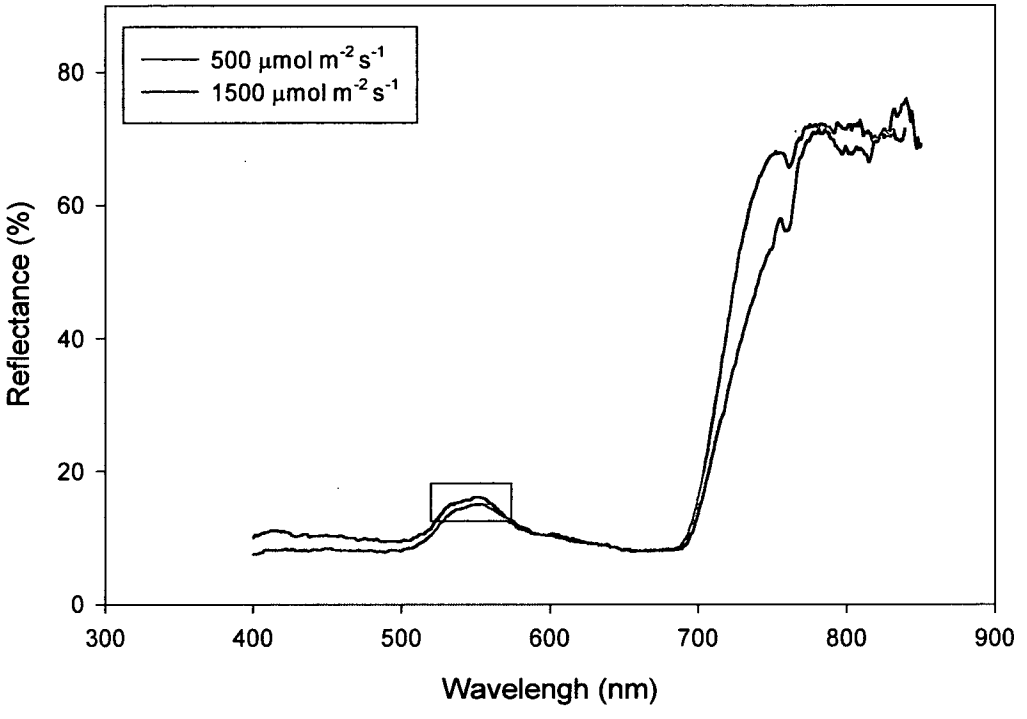


**Figure 2.2** Individual reflectance spectra in visible wavebands of leaves exposed to PPFDs of 500 µmol $m^{-2}$ $s^{-1}$ and 1500 µmol $m^{-2}$ $s^{-1}$. Each line is an individual scan. Both scans were on the same leaf, within 10 minutes of each other.

Transition from medium (500 µmol $m^{-2}$ $s^{-1}$) to high (1500 µmol $m^{-2}$ $s^{-1}$) PPFD caused a slight decline in leaf reflectance around 530 nm (Fig 2.2).

In the absence of normalisation, the reflectance at 530 nm did not yield any correlation with LUE (data not shown).

Gamon *et al.*, (1993) showed that the range of wavelengths that could be used for the calculation of PRI was from 517 – 539 nm, with the average for all species in his study being 531 nm. To locate the optimal wavelength to be used for the calculation of PRI in this species, PRI was recalculated with wavebands ± 5 nm of 531 nm. The

correlations between PRI and LUE were investigated. Figure 2.3 shows that the optimal wavelengths in this study were 530 and 531 nm, where the $R^2$ of the PRI : LUE relationship in both cases peaked at 0.55. PRI calculated using 529 nm produced an $R^2$ of 0.43, with 528 nm generating an $R^2$ of 0.41 and 532 nm generating an $R^2$ of 0.5. Beyond these peaks the strength of the PRI : LUE relationship clearly weakens.

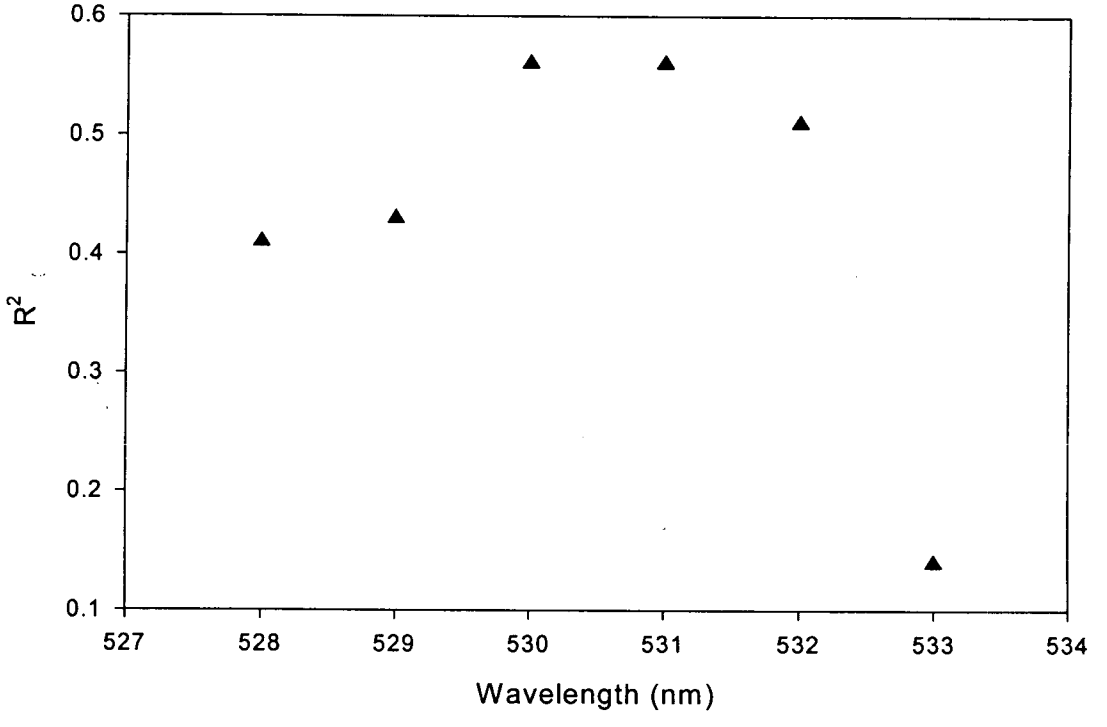


**Figure 2.3** A summary of the $R^2$ for the relationship between PRI and LUE when PRI is calculated using a range of wavelengths indicated on the x-axis, keeping the reference wavelength at 550 nm.

PRI showed a strong linear relationship ($R^2 = 0.55, p < 0.01$ Figure 2.4A) with LUE over the medium to high PPFD range (500 – 1500 μmol $m^{-2}$ $s^{-1}$). There was also a strong correlation between PRI and PS II efficiency, obtained from fluorescence measurements ($R^2 = 0.79, p < 0.01$ Figure 2.4 B).

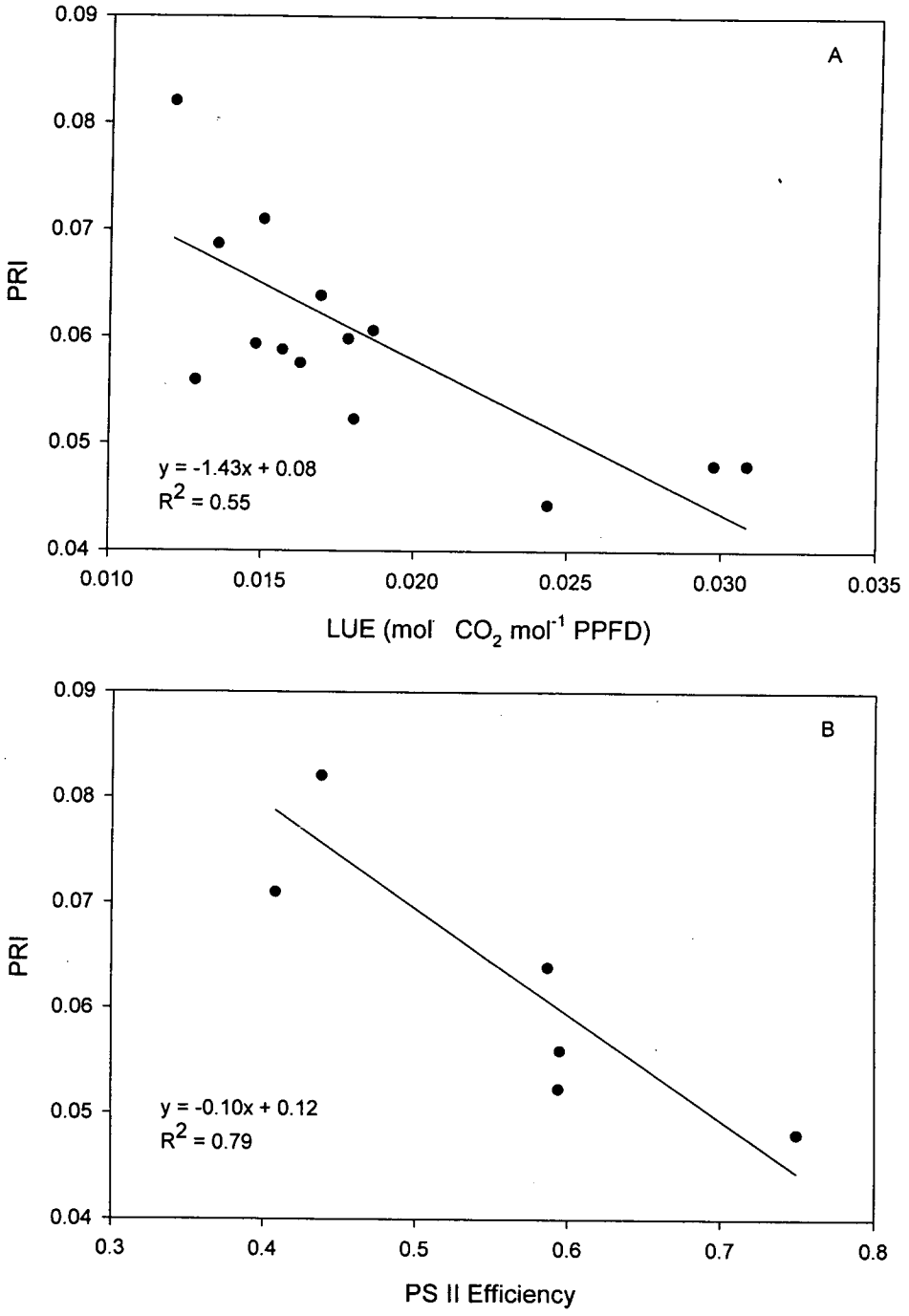


**Figure 2.4 A** Relationship between PRI and light use efficiency (LUE) for individual bean leaves over medium to high PPFD (500-1500 μmol $m^{-2}$ $s^{-1}$). Symbols represent spectral and gas exchange measurements from the same (individual) leaves. **B** Relationship between PRI and photosystem II (PSII) efficiency for individual bean leaves sampled over over medium to high PPFD (500-1500 μmol $m^{-2}$ $s^{-1}$). Symbols represent measurements of gas exchange and fluorescence from the same (individual) leaves

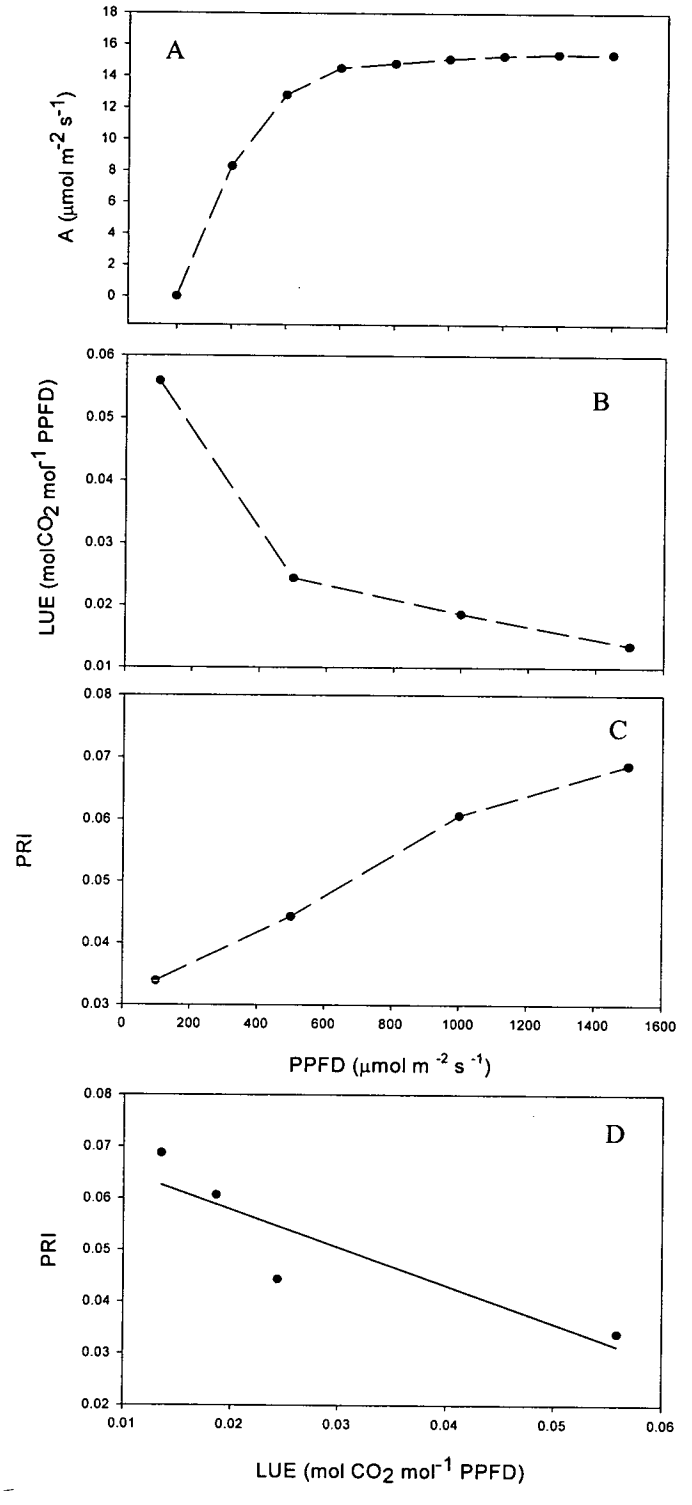


**Figure 2.5 A** Light response of leaf gas exchange (*A* = Assimilation), **B** photosynthetic light use efficiency **C**, leaf PRI and **D** the relationship between leaf PRI and LUE. Each point represents a measurement on an individual leaf. **B** and **C** were measured sequentially on the same leaf. Note graph A starts at 0 μmol $m^{-2}$ $s^{-1}$ and increments every 200 μmol $m^{-2}$ $s^{-1}$. B and C were measured at 100, 500, 1000 and 1500 μmol $m^{-2}$ $s^{-1}$.

The light response function shown in Figure 2.5 shows the familiar hyperbolic trend, typical of leaves of a $C_3$ species: steep at first and saturating at 800 – 1000 μmol $m^{-2}$ $s^{-1}$ (Figure 2.5A). The slope of this relationship (A/PPFD) defines the light use efficiency (LUE). It was high initially (0.05 - 0.06 mol $CO_2$ per mol absorbed photons) and then rapidly declined as light saturation approached (Figure 2.5B). The PRI decreased with light, in a near linear manner (Figure 2.5C). The relationship between PRI and LUE is shown in Figure 2.5D and whilst a linear fit generates an $R^2$ of 0.78 ($p > 0.1$) this result was not significant.

## 2.4 Discussion

The relationship between PRI and LUE and PS II efficiency supports the hypothesis that PRI can serve as an indicator of photosynthetic light use efficiency at this scale. Similar observations have been found by others using individual leaves within a species (e.g., Gamon *et al.*, 1992, Penuelas *et al.*, 1995, 1997, Fillela *et al.*, 1996) and across species of different functional types (Gamon *et al.*, 1997).

It has been suggested that the 531 nm "signal" consists of two spectral components (Penuelas *et al.*, 1995, Gamon *et al.*, 1997). Gamon and his co-workers (1997) found the dominance of a 545 nm component in low PPFD, with an appearance of a 526 nm component at higher PPFD. The contribution of two spectral components could explain previous reports of a non-linear relationship between PRI and LUE where samples were measured over a wide range of PPFDs (Penuelas *et al.*, 1995). Although Gamon *et al.*, (1990) first highlighted this, a recent paper has shown that these two spectral signals are active at different PPFDs, and can be separated in laboratory conditions (Gamon *et al.*, 1997).

The 545 nm component, which was apparent in the difference spectra, is related to chloroplast conformational changes associated with the build-up of the pH gradient, rather than to the conversion of violaxanthin to zeaxanthin. This conclusion was based on experimental work associating the generation of the thylakoid pH gradient with a change in absorbance at 540 nm (Heber, 1969, Bilger *et al.*, 1989, Bjorkman and Demmig Adams, 1994) and with a corresponding reflectance change near 539 nm (Gamon *et al.*, 1990). That the 545 nm component was initiated at lower PPFDs and progressively disappeared at higher PPFDs, suggests that it is not directly a result of xanthophyll pigment interconversion or the associated heat dissipation, but is more likely a result of light scattering changes associated with the initial build-up of the thylakoid pH gradient upon the sudden transition from darkness to low PPFD (Gamon *et al.*, 1997).

The 526 nm component, which appears at higher PPFD, is most likely caused by spectral changes associated with the conversion of violaxanthin to zeaxanthin. This conclusion can be drawn from evidence attributing a similar absorbance change near 515 nm (Bilger *et al*, 1989, Bjorkman and Demmig Adams, 1994) and a related reflectance change near 525 nm (Gamon *et al.*, 1990), to the production of zeaxanthin. Gamon *et al.*, (1997) further showed that PRI, when calculated using the 526 nm component at high light, was more strongly correlated to LUE than PRI calculated using 531 nm. Thus, the increased activity at PPFDs above 500 μmol $m^{-2}$ $s^{-1}$ of the 526 nm component is consistent with the function of xanthophyll cycle pigments as photoprotective pigments that serve to dissipate excess absorbed PPFD as heat (Demmig-Adams and Adams, 1994, Demmig-Adams *et al.*, 1996). In the linear, quantum yield region of the photosynthetic PPFD response curve, there is no need for such energy dissipation and thus no detectable contribution of the 526 nm component in sun acclimated leaves. Given this information, we chose 529 nm to represent our xanthophyll cycle wavelength. However, because no data were

acquired at low PPFD, it is not possible to confirm directly the existence of these two spectral components in this study.

It is therefore likely that the scatter in the PRI : LUE relationships presented here will be the result of factors that compete with the reductant generated by electron transport for processes other than carboxylation. For example, Photorespiration, the Mehler reaction (Harbison *et al.*, 1990) and nitrate reduction (Bloom *et al.*, 1989) are examples of such processes. The relationships presented here suggest that the photosynthetic apparatus is sufficiently regulated to maintain consistent relationships between PS II processes and carboxylation.

Previous studies have found the optimal waveband for the calculation of PRI to be centred at 531 nm (Gamon *et al.*, 1992, 1993, 1997, Penuelas *et al.*, 1997). Recalculating PRI using a range of wavelengths showed that 530 and 531 nm were the optimal wavebands for this study, with 532 nm also proving useful. Gamon *et al.*, (1993) suggested that the wavebands suitable for a calculation of PRI ranged from 517 – 539 nm, with the average being 531 nm. This was found in a study on 20 angiosperms. The optimal waveband in this study thus falls within the range outlined by Gamon. The exact position may vary between species as a result of leaf anatomy, optical errors that occur during measurement or simply instrument noise (Gamon *et al.*, 1993). Careful calibration however, should overcome the latter of these problems.

## 2.5 Conclusions

The results presented here show that reflectance, like fluorescence, can provide a non-destructive assessment of photosynthetic light use efficiency of plants grown under a range of PPFDs.

At the leaf level, a simple spectrometer that measures the reflectance in narrow wavebands centred around 530 nm and 550 nm could instantaneously calculate PRI and give an estimate of LUE in seconds. The lack of one universal waveband for calculating PRI suggests that the remote measurement of PRI may be complicated at larger spatial scales where the scene may be composed of a mixture of species and over a range of spatial scales. These issues are the focus of Chapters 3 and 4.

# 3. CANOPY PRI AND PHOTOSYNTHETIC LIGHT USE EFFICIENCY IN CANADIAN BOREAL FOREST.

## 3.1 INTRODUCTION

A number of studies have successfully shown that PRI tracks changes in leaf LUE in a range of species, under contrasting light and stress environments. The only canopy scale measurements that relate PRI to LUE are on small plots (~ 2 $m^2$) and single species (Gamon, 1992, 1997, Fillela *et al.*, 1996, Penuelas *et al.*, 1995, 1997). The step of relating PRI to a measure of LUE over larger forested areas has not been made.

Typically when scaling up to landscapes, factors such as Sun angle changes, complex canopy structure, understorey vegetation and soil can all influence the reflectance of a scene whether it be measured from a tower, aircraft or satellite sensor. It is therefore pertinent to know whether these influences will preclude PRIs use as a physiological indicator over heterogeneous canopies.

Extensive canopy spectral reflectance measurements were made from a helicopter platform and an eddy covariance system measured gas exchange over contrasting boreal forest canopies during the BOREAS experiment (Boreal Ecosystem Atmosphere Study, for overview see Sellers *et al.*, 1995b). These data provided an ideal opportunity to investigate the PRI:LUE relationship over large (~ 70 $m^2$) forested areas where canopy structure and understorey vegetation differed significantly between sites.

This chapter thus presents an evaluation of PRI as an indicator or photosynthetic LUE over a boreal forest canopy.

## 3.2 MATERIALS AND METHODS

### STUDY SITES

The BOREAS field experiment took place during 1994 on the northern and southern edges of the Canadian boreal forest. A Northern Study Area (NSA) was located near Thomson, Manitoba, and Southern Study Area (SSA) was located near Candle Lake, Saskatchewan (see Sellers *et al.*, 1995b for details) and specific sub-sites within the SSA were intensively studied during the growing season. A brief outline of the sites used in this study is included here:

### OLD BLACK SPRUCE

The site lies in the southern mixed forest zone about 100 km north of Prince Albert in Saskatchewan (53° 55' N, 105° 5' W, elevation 630 m), and has been described by Jarvis *et al.*, (1997). The terrain is essentially flat with pure and mixed stands of black (*Picea mariana* (Mill.) BSP) and white spruce (*Picea glauca* Moench.), jack pine (*Pinus banksiana* Lamb.), aspen, fen and lakes. The substratum is peat overlying glacial drift with an elevated water table so the surface is generally wet. The understorey is sparse with some low shrubs reaching ~1.5 m in height.

### OLD JACK PINE

The jack pine forest (*Pinus banksiana* Lamb.) stand grows in the SSA near Nipawin, Saskatchewan, Canada (53° 54' N, 104° 41' W, elevation 579 m) and has been described by Baldocchi *et al.*, (1997). The landscape is relatively flat (slope ~ 2 and 5 %) with pure and mixed stands of black (*Picea mariana* (Mill) BSP) and white spruce (*Picea glauca* Moench.), aspen, jack pine and fen The soil is a coarse textured, well drained sand. The ground was covered with an optically bright mat consisting of bearberry (*Arctostaphylos uva-ursi*), bog cranberry (*Vaccinium vitis-*

*idaea*), and lichens (*Cladina spp*).The understorey vegetation is sparse but there are isolated groups of alder (*Alnus crispa*).

### OLD ASPEN

The site is located in the SSA within Prince Albert National Park, Saskatchewan (53° 38'N, 106° 12'W, elevation 600 m) and has been described by Hogg *et al.*, (1997). It is an extensive, mostly pure, stand of trembling aspen (*Populus tremuloides* Michx) on an Orthic gray luvisol with a loam texture dominates the site. Beaked hazelnut (*Corylus cornutta* Marsh) dominates the understorey shrub layer and is approximately 2 m in height. Wild rose (*Rosa woodsii*) and alder (*Alnus crispa*) are found in intermittently.

### FEN

The fen study site is located in the southern study area, 115 km Northeast of Prince Albert, Saskatchewan (53° 57' N, 105° 57' W elevation 525 m). The fen study site is a minerotrophic, patterned fen surrounded by black spruce (*Picea mariana* (Mill.) BSP)) and jack pine (*Pinus banksiana* Lamb.) forests and has been described by Suyker *et al.*, (1997). Abundant herbaceous species throughout the fen included bogbean (*Menyanthes trifoliata*) and several sedge species (*Carex* and *Eriophorum spp*). Dominant woody plant species are 0.5 - 1.5 m tall bog birch (*Betula pumila*) and widely scattered, stunted tamarack trees (*Larix laricina*). Mosses whilst present are not abundant in this fen.

### CANOPY SPECTRAL REFLECTANCE DATA

The BOREAS remote sensing science group RSS-03 collected multiple remotely sensed data sets from a helicopter platform during the 1994 growing season. A description of the data acquisition is given as follows.

The National Aeronautics and Space Administration (NASA) Goddard Space Flight Center (GSFC) / Wallops Flight Facility (WFF) helicopter-based optical remote sensing system (Walthall *et al.*, 1996) was deployed to acquire canopy multispectral data with a portable spectroradiometer. A spectroradiometer (model SE-590, Spectron Engineering, Denver, Colorado) was mounted on a steel rack at nadir orientation. A 15-degree instantaneous field of view lens (IFOV) was fitted to yield a ground resolution of 79 m at the 300 m nominal altitude. The SE-590 had a spectral range of 362.7 to 1122.7 nm, with a usable range of 400 to 900 nm. Data are reported at 3 nm intervals calculated at the centre point of a five 3 nm bin running average.

Data were acquired on clear days (incident PPFD > 900 μmol $m^{-2}$ $s^{-1}$) whilst the helicopter hovered at each site for 1 - 2 minutes for each observation (consisting of an average of 20 - 25 scans). Observations were made in the spring, summer and autumn (Table 3.1).

**Table 3.1**. A summary of acquisition attributes of reflectance data set for the Southern Study Areas

| Site | Instrument | Observation date | Solar zenith angle (degrees) | Solar azimuth angle (degrees) | Range of temperature °C | Range of solar radiation $\mu mol\ m^{-2}\ s^{-1}$ |
|---|---|---|---|---|---|---|
| Old aspen | SE-590 | 31-May-94 | 53 | 103 | 17.7-18.3 | 992-1129 |
| | | 21-July-94 | 37 | 144 | 22.6-23.3 | 1339-1539 |
| | | 25-July-94 | 49 | 115 | 21.5-21.7 | 1343-1450 |
| | | 13-Sept-94 | 52 | 201 | 15.7-16.4 | 1077-1216 |
| Fen | SE-590 | 01-June-94 | 50 | 108 | 20.5-21.0 | 1043-1352 |
| | | 06-June-94 | 39 | 130 | 21.2-21.2 | 1445-1545 |
| | | 21-July-94 | 36 | 210 | 21.3-21.6 | 1222-1366 |
| | | 13-Sept-94 | 50 | 183 | 12.4-12.9 | 1021-1117 |
| Old jack pine | SE-590 | 31-May-94 | 43 | 121 | 15.9-16.7 | 1022-1192 |
| | | 06-June-94 | 44 | 118 | 21.0-21.2 | 1416-1545 |
| | | 21-July-94 | 39 | 222 | 25.4-25.7 | 1397-1476 |
| | | 24-July-94 | 44 | 127 | 21.1-21.4 | 1382-1498 |
| | | 13-Sept-94 | 51 | 190 | 18.9-19.5 | 1196-1271 |
| Old black spruce | SE-590 | 01-June-94 | 42 | 124 | 18.4-18.6 | 1399-1498 |
| | | 06-June-94 | 48 | 111 | 20.4-20.6 | 1361-1479 |
| | | 21-July-94 | 34 | 166 | 24.6-25.3 | 1500-1579 |
| | | 23-July-94 | 45 | 124 | 18.5-18.9 | 1216-1341 |
| | | 13-Sept-94 | 59 | 134 | 18.7-19.1 | 1177-1236 |

Radiometric calibration and spectral calibration procedures were performed before and after the field season to check for changes in sensor radiometric response. The SE-590 data were corrected to at-surface reflectances using the 6S atmospheric radiative transfer model and Sun photometer data.

PRI from the SE-590 data was formulated;

$$\text{PRI}_{\text{SE-590}} = (R_{569} - R_{529}) / (R_{569} + R_{529}) \qquad (1)$$

Where $R_{529}$ indicates the reflectance centred at 529 nm with upper and lower band limits of 536.5 nm and 521.5 nm (coinciding with the signal of the xanthophyll cycle) and $R_{569}$ indicates the reflectance centred at the 569 nm waveband with upper and lower band limits of 561.5 and 576.5 nm (a reference waveband). This differs

slightly from that used in previous studies, but still lies within the range of wavelengths considered applicable for the calculation of PRI (Gamon *et al.*, 1993). By referencing $R_{529}$ to $R_{569}$, this index normalises for factors which include pigment content and chloroplast movement both of which can affect the $R_{529}$ signal (Gamon *et al.*, 1993).

**Eddy Covariance Measurement of Fluxes**

Half-hour fluxes of momentum, sensible heat, water vapour and carbon dioxide (as well as meteorological variables) were measured at all sites using tower-mounted, eddy covariance systems continuously from May through September of the 1994 growing season. Full details of the theory and instrument set for each site are published elsewhere. For old black spruce see Jarvis *et al.*, 1997; old jack pine, Baldocchi *et al.*, 1997; old aspen, Blanken *et al.*, 1997; fen, Suyker *et al.*, 1997.

**Estimates of stand photosynthesis**

The $CO_2$ flux was partitioned into photosynthesis and respiration components by estimating daytime ecosystem respiration as functions of soil temperature. Following Goulden *et al*, (1997), night-time half-hour $CO_2$ fluxes at high windspeeds (friction velocity, $u^* > 0.2$) were plotted against soil temperature (at 5 cm) and the usual exponential function fitted, of the form,

$$A = ce^{bT_s}$$

where $A$ is carbon dioxide flux , $T_s$ is soil temperature, $c$ and $b$ are constants and e is the base of the natural logarithm. Daytime respiration was then calculated using this function and daytime soil temperatures. This was done for each month's night-time half hour flux data from May until September for each of the sites (data not shown).

Photosynthesis was then calculated as the daytime half-hour $CO_2$ fluxes after the respiration component had been removed (Lloyd and Taylor, 1994, Goulden *et al.*, 1997). Because the helicopter overpass occurred on clear bright days (PPFD > 900 μmol $m^{-2}$ $s^{-1}$), the $CO_2$ flux data for these periods were restricted to PPFD > 900 μmol $m^{-2}$ $s^{-1}$. Photosynthesis and incident PPFD were averaged above this PPFD and a daily LUE value computed from these averages according to the following,

$$\text{Canopy light use efficiency} = \frac{\text{Canopy photosynthesis } (\mu\text{mol } CO_2 \text{ m}^{-2} \text{ s}^{-1})}{\text{Incident PPFD } (\mu\text{mol photons m}^{-2} \text{ s}^{-1})}$$

## 3.4. RESULTS

Two mean representative reflectance spectra obtained from the SE-590 spectroradiometer, each representing coniferous or deciduous forest are shown in Figure 3.1 along with the two wavebands used for the calculation of PRI.

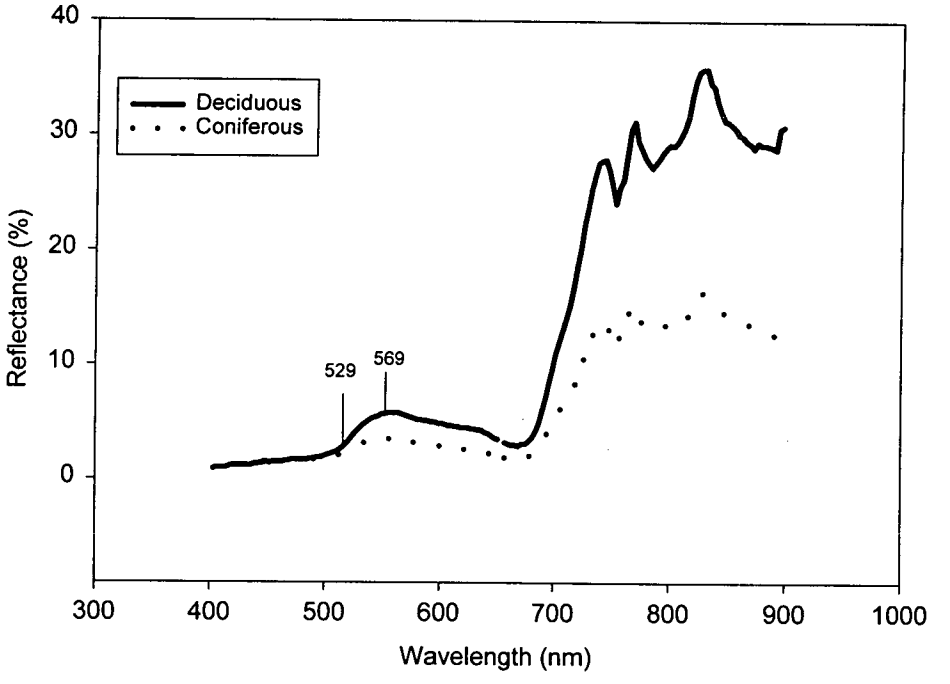


**Figure 3.1** Mean spectra of the coniferous and deciduous forest canopy from the BOREAS southern study area. Each curve represents the mean of 20-25 scans acquired by the helicopter mounted SE-590 spectroradiometer. Wavelengths used for PRI calculation are shown in the Figure.

In the absence of normalisation, the reflectance at 529 nm ($R_{529}$) yielded no clear correlation with LUE for the coniferous and deciduous species together (Figure 3.2A), or for the deciduous species (Figure 3.2B) and coniferous species (Figure 3.2C).

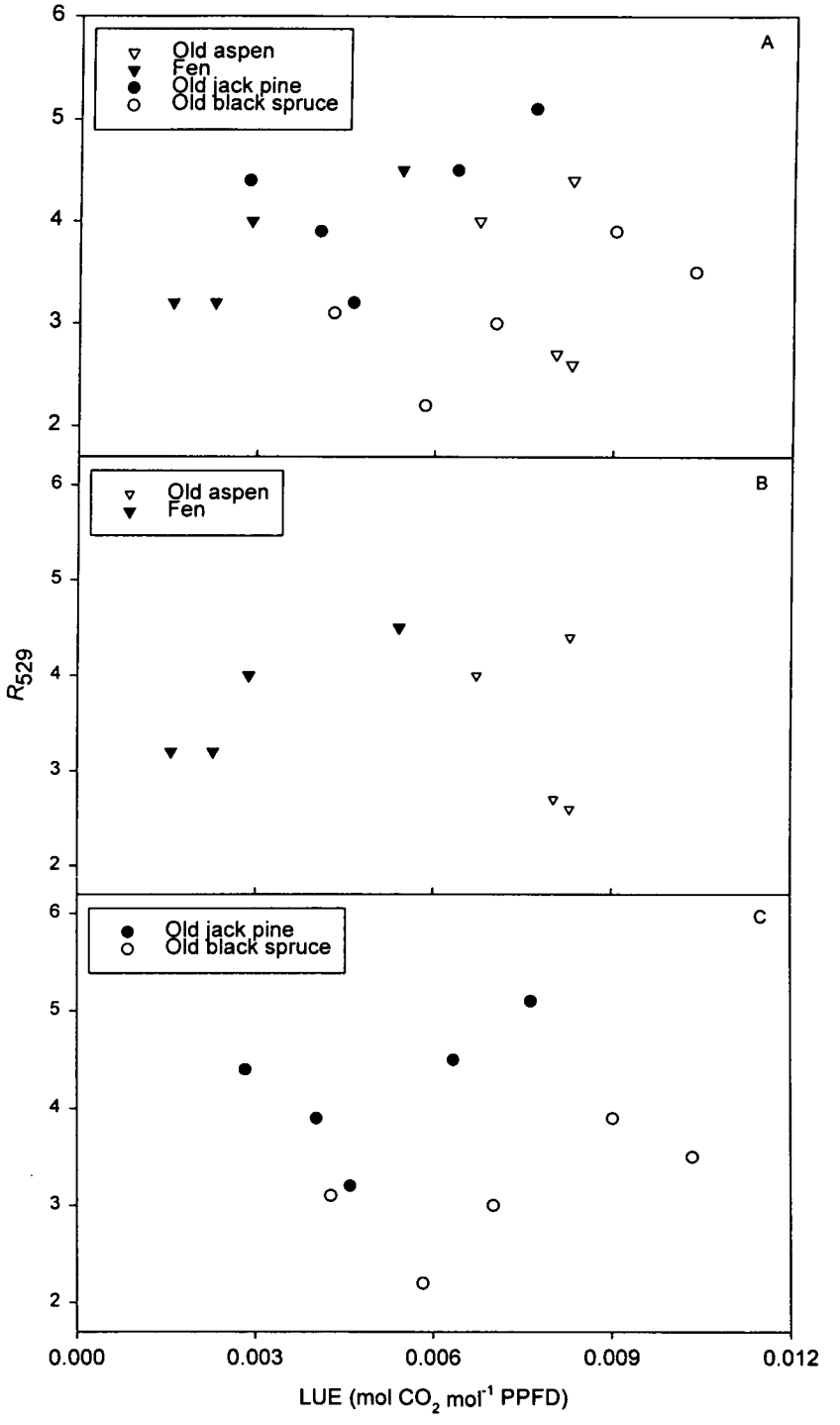


**Figure 3.2**. Relationship between reflectance (%) at 529 nm and canopy light use efficiency (LUE). Each point is an average of 20-25 spectral scans and four hours of canopy LUE data. A Four boreal forest species. B Two deciduous species. C Two coniferous species. Individual species are represented by the different symbols indicated.

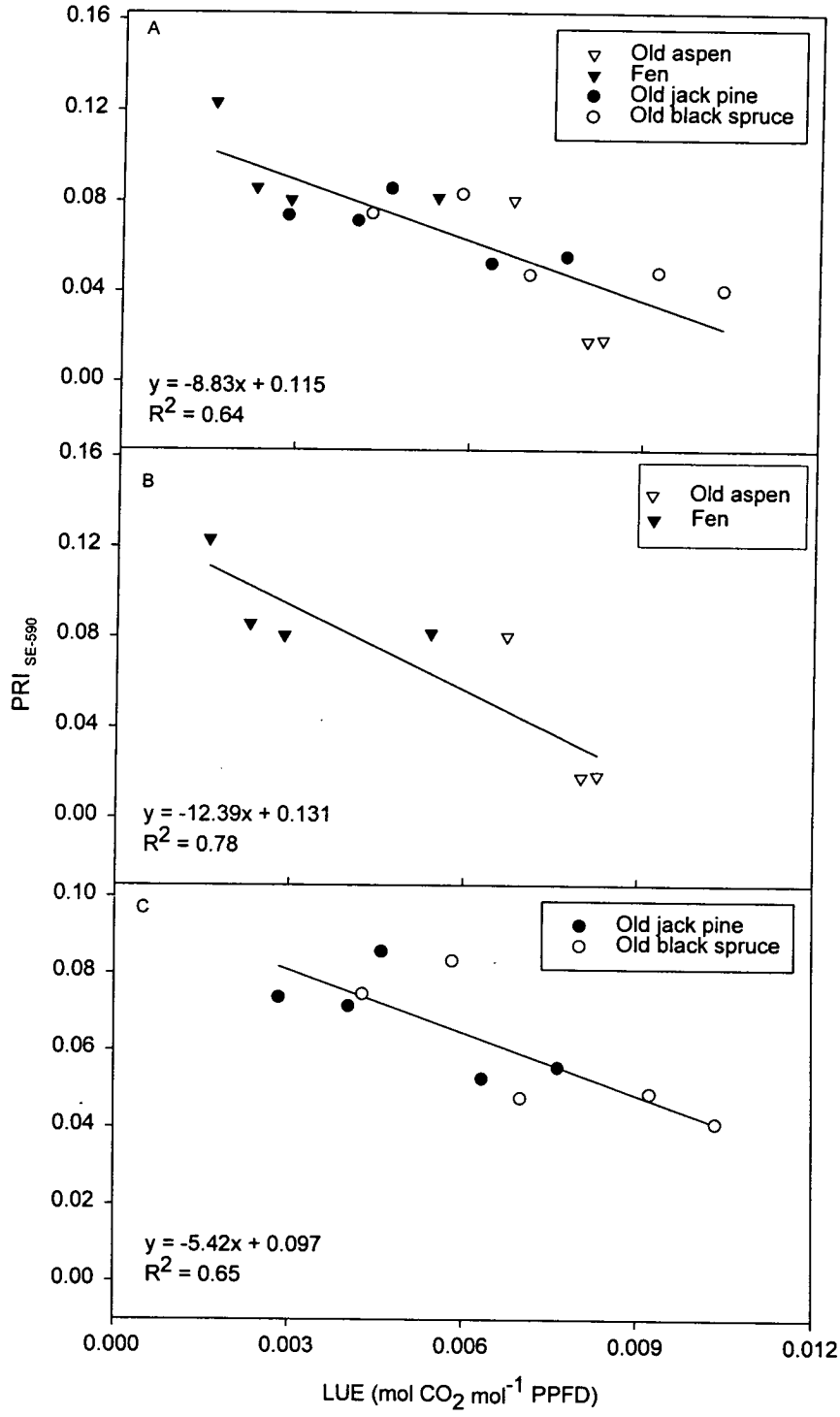


**Figure 3.3**. Relationship between the Photochemical Reflectance Index (PRI) and canopy light use efficiency (LUE) for boreal forest sites sampled in full Sun. Each point is an average of 20-25 spectral scans and four hours of canopy LUE data. A. Four boreal forest species B. Two deciduous species. C. Two coniferous species. Individual species are represented by different symbols indicated.

However, after normalisation midday top canopy $PRI_{SE\text{-}590}$ values were significantly correlated with canopy LUE across the four species sampled ($R^2 = 0.64$, $p < 0.05$, Figure 3.3A). The correlations were stronger when the species were divided into their functional groups. A linear relationship was apparent between $PRI_{SE\text{-}590}$ and LUE for the deciduous species ($R^2 = 0.78$, $p < 0.05$, Figure 3.3B) and coniferous species ($R^2 = 0.65$, $p < 0.05$, Figure 3.3C).

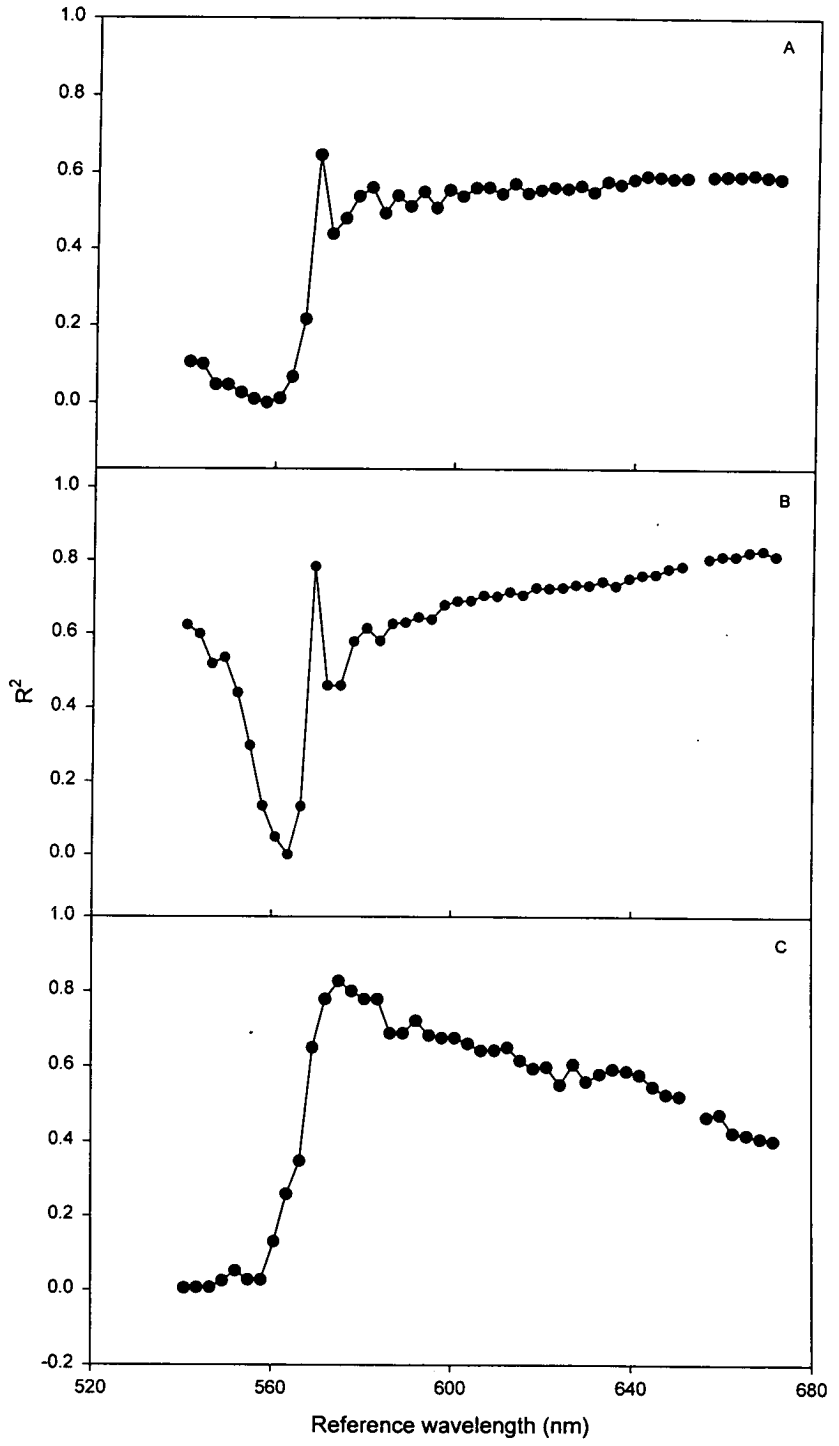


**Figure 3.4.** A summary of the $R^2$ coefficients for relationship between the Photochemical Reflectance Index (PRI) and canopy light use efficiency (LUE). A. Four boreal forest species. B. Two deciduous species. C. Two coniferous species. PRI was calculated using $R_{529}$ as the xanthophyll waveband with reference wavelengths ranging from 540 to 670 nm, at 3 nm intervals.

The $PRI_{SE-590}$ : LUE relationships were reassessed by calculating $PRI_{SE-590}$ using a range of reference wavelengths. Figure 3.4 shows a summary of the $R^2$ of the relationship between $PRI_{SE-590}$ and LUE. The peak of this graph would be the best combination of xanthophyll wavelength and reference wavelength for the estimation of LUE. A reference wavelength of 569 nm produces the best relationship between $PRI_{SE-590}$ and LUE. This is also the optimal reference waveband to use for the deciduous species (Figure 3.4B), but for the coniferous sites, the selection of a slightly longer reference wavelength generated a stronger relationship between $PRI_{SE-590}$ and LUE (Figure 3.4C). In this case, selecting a reference wavelength of 575 nm produced an $R^2$ of 0.82 in the relationship between $PRI_{SE-590}$ and LUE.

## 3. 5 DISCUSSION

### CANOPY PRI AND PHOTOSYNTHETIC LIGHT USE EFFICIENCY

The consistent relationship between $PRI_{SE-590}$ and LUE for canopies sampled in full sunlight (Figure 3.3A, B and C) supports the hypothesis that $PRI_{SE-590}$ provides a measure of PS II LUE across species and functional types. Similar observations have been made using individual leaves and small plots (~ 2 m) (Gamon *et al.*, 1990; Gamon *et al.*, 1992, Penuelas *et al.*, 1995, 1997; Fillela *et al.*, 1996; Gamon *et al.*, 1997), but this is the first time a relationship has been found between PRI and LUE over heterogeneous forest canopies.

Penuelas *et al.*, (1995) studied the relationship between PRI and PS II LUE in plants differing in phenology, habit and photosynthetic type, and found that the slope and intercept of the PRI : LUE relationship varied between species. The lack of a single relationship in their study is not surprising. Variation may arise from the environmental growth conditions, varying anatomy, morphology and pigmentation and diverse species differences. Such factors can dramatically influence the visible reflectance and PRI (Guyot, 1990).

Similar to the leaf scale analysis, the scatter in the relationship between $PRI_{SE-590}$ and LUE could be the result of several factors that can cause divergence between whole leaf assimilation and PS II LUE. These factors include the Mehler reaction, photorespiration (Harbison *et al.*, 1990) and nitrate reduction (Bloom *et al.*, 1989), all of which compete with carboxylation for reductant generated by electron transport. In the conditions of this study, the significant correlations between $PRI_{SE-590}$ and LUE within each functional group suggest that the overall photosynthetic systems were sufficiently regulated to maintain consistent relationships between PS II processes and carboxylation.

Consistent relationships between PRI and LUE for small plots (~ 2 m) do not always exist. Work by Gamon *et al.*, (1992) on sunflower canopies experiencing severe water stress showed a divergence between PRI and LUE, possibly owing to increased use of reductant by photorespiration and other processes besides carboxylation. Of the sites used in this study it is possible that a degree of water stress was experienced at the old jack pine site because of the free draining nature of the soil (Cuenca *et al.*, 1997), and some of the scatter in the $PRI_{SE-590}$ : LUE relationship could be attributed to this (Baldocchi *et al.*, 1997). But is has been argued that any stress that depresses photosynthesis, independent of high light, would necessitate the energy dissipating mechanism more since the rate of the dark reaction will not be able to match the pace of the light reaction. Thus there would exist a greater need for dissipation. This is an area that is under intense interest and the focus of Chapter 4.

## THE CALCULATION OF LUE : INCIDENT PAR (IPAR) VERSUS ABSORBED PAR (APAR).

It has been suggested that the calculation of LUE based on IPAR rather than APAR could potentially introduce an error into the calculation of LUE (Gallo and Daughtry, 1986, Russell, 1989, Gower *et al.*, 1999). Typically IPAR is within 4 % of APAR when canopies are closed. If LAI is low (~ 0.2) and the soil has a high reflectance (PAR reflectance = 0.5) then APAR may be 40 % larger than IPAR for a random canopy because additional PAR reflected from the soil is absorbed by the leaves. Results from a modelling study (Barton and North, 2000 *in press*) suggested that LUE, when calculated from IPAR, showed greater scatter with PRI than LUE calculated using APAR, using a hypothetical canopy with wide range of leaf areas. However the authors did not take into account the density of the canopy or different understories, other than two soil types. The issue of IPAR versus APAR will come into play when considering an open canopy that is not vegetated with photosynthesising understorey, such as lichen or dry soil. In tall fully green vegetation, such as forests, APAR and IPAR will be very similar since the leaves

reflect and transmit very little light in the visible wavelengths. However, when canopies have brown (senesced) leaves and woody boles and branches, APAR and IPAR will vary greatly with IPAR being greater than APAR. In these instances, use of APAR should prevail. In the context of the results presented here, all canopies were closed and had a LAI well above 2, which is the critical value whereby IPAR and APAR should not differ (Gower *et al.*, 1999).

### WAVELENGTH CHOICE FOR THE CALCULATION OF PRI

The wavelength chosen to signal activity of the xanthophyll cycle differs slightly from that used in previous studies (Gamon *et al.*, 1992, Penuelas *et al.*, 1995, Filella *et al.*, 1996, Gamon *et al.*, 1997). As the results from Chapter 2 indicated however, the width of the spectral response of the xanthophyll cycle is such that wavebands within $\pm$ 3 nm could be used (i.e. a total spectral window of 7 nm). The location of the wavebands generated by the SE-590 was such that 529 nm was closest to 531 nm.

$PRI_{SE\text{-}590}$ was recalculated using a range of reference wavelengths and correlated with LUE. Some surprising relationships emerged. When all the species were grouped together, the $R^2$ peaked at 0.645 when 569 nm was used as a reference. This was also the case for the deciduous species. However, the $PRI_{SE\text{-}590}$ data for the conifers were more strongly correlated with LUE when a slightly longer reference waveband of 575 nm was used. Gamon *et al.*, (1992) found that any reference waveband between 539 and 570 nm would be suitable for the calculation of $PRI_{SE\text{-}590}$ and statistical correlation with LUE data. Their results however, were for a single species, rather than the four species used in this study.

## EFFECTS OF BACKGROUND REFLECTANCE ON PRI

The effective use of periodic remotely sensed observations in landscape process studies depends on stable estimation of diurnally integrated conditions (Goward and Huemmrich, 1992). It has been widely documented that the reflectance measured from forest sites may vary with solar illumination angle, viewing angle, understorey or background reflectance and atmospheric effects, as well as intrinsic canopy variables such as phytomass and leaf area index of the dominant species (Kimes, 1980, Guyot, 1990, Ranson *et al.*, 1986, Huete, 1987, Goward and Huemmrich, 1995). Although the spectral data used in this study were acquired from a nadir orientation during conditions of highest possible solar elevation (approximately 40 – 60°), which would have minimised unstable calculations of PRI, a full sensitivity analysis of the PRI : LUE relationship is warranted. This is addressed in Chapter 5. The sites used in this study however had closed canopies and the likely influence of background materials would have been minimal.

## 3.6 CONCLUSIONS

The results presented here have demonstrated that $PRI_{SE-590}$ can serve as an index of photosynthetic light use efficiency over heterogeneous forest canopies. These results extend beyond earlier studies using individual leaves (Gamon *et al.*, 1992, Penuelas *et al.*, 1995, Fillela *et al.*, 1996) by showing that this index is well suited to sampling areas of ~ 70 $m^2$ in contrasting ecosystems at high PPFD. Consequently, it should be possible to derive methods of remotely estimating relative photosynthetic rates based on reflectance in the 529 nm spectral region.

The following chapter builds on the findings presented here by investigating the relationship between boreal forest PRI (measured from a helicopter system) and LUE (estimated from eddy covariance measurements). It specifically focuses on the forest during the transition from winter dormancy to spring when low temperatures and high light are considerable stress factors.

# 4. CANOPY PRI AND PHOTOSYNTHETIC LIGHT USE EFFICIENCY IN SIBERIAN BOREAL FOREST.

## 4.1 INTRODUCTION

The carotenoids of the xanthophyll cycle perform an essential role in the quenching of triplet state chlorophyll within the chloroplasts of all higher plants. The interconversion of the pigments that comprise the xanthophyll cycle has been found to provide the main pathway for thermal dissipation of excess absorbed energy (Demmig-Adams and Adams, 1992, Gilmore and Yamamoto, 1993, Pfundel and Bilger, 1994, Demmig-Adams *et al.*, 1996, Osmond *et al.*, 1999) thus maintaining a delicate balance between the capture of light and its utilisation in photosynthesis.

Optical techniques have been successfully used to track these changes in pigment concentrations and the corresponding change in the efficiency of photosynthesis in leaves (Gamon *et al.*, 1992, Penuelas *et al.*, 1995, Fillela *et al.*, 1996, Gamon *et al.*, 1997) and over whole canopies (Nichol *et al.*, 2000, and Chapter 3).

The work by Nichol *et al.*, (2000) demonstrated a good correlation between PRI, calculated from spectral data collected from a helicopter platform, and LUE, calculated from eddy covariance data, for four Canadian boreal forest canopies.

The functionality of this index remains to be tested over further canopies in a number of other ecosystems and under a variety of stress factors. Conifers are the most common evergreen plants in the temperate and subarctic northern hemisphere. They must endure severe stress in the form of low temperatures (< -50° C) combined with high light. This combination occurs especially in spring. Under these conditions photosynthetic consumption of excitation is blocked but leaves must retain their capacity to photosynthesise when favourable conditions return. Such winter stress causes severe inhibition of photochemical efficiency of PS II (Martin *et al.*, 1978b),

and severe photoinhibition often occurs in nature at freezing temperatures (Oquist and Ogren, 1985, Hallgren *et al.*, 1990, Ottander and Oquist, 1991, Ottander *et al.*, 1995).

This chapter addresses the utility of PRI as an indicator of LUE in four contrasting Siberian boreal forest canopies. It specifically focuses on the transition from late winter into spring and summer when the canopy moves from severe photoinhibition to full photosynthesis.

Extensive canopy spectral reflectance measurements were thus made over the late winter /spring period from a helicopter platform. Eddy covariance systems measured the gas exchange over four Siberian sites continuously during May to June 2000. These data provided the opportunity to investigate the relationship between PRI and LUE when the forest was making the transition from severe winter stress when photosynthesis rates were zero, to full canopy photosynthesis in the spring. A comparison of the data from this boreal forest could also be made with the data from Canada's boreal forest (as presented in Chapter 3).

In addition to this, a study was undertaken from a tower where measurements of top of the canopy reflectance were made along with eddy covariance measurements at a Siberian Scots pine stand with simultaneous sampling of needles for xanthophyll pigment determination.

## 4.2 Materials and Methods

### Study sites

The sites sampled are located on the east and west sides of the Yenesei river in Siberia. Sub sites within this area were being studied by colleagues at the Max-Planck Institute for Biogeochemistry as part of an ongoing field experiment into the carbon balance of the region. A brief description of the sites used in this study are outlined here.

### Scots Pine

The *Pinus sylvestris* L (Scots pine) stand (Plates 1A and B) lies about 40 km west of the Yenesei river (60° 45' N, 89° 23' E, elevation 90 m) at the eastern edge of the west Siberian lowland. The mean canopy height is 16 m. The forest occurs on alluvial sand dunes surrounded by sphagnum peat bogs and river meanders. The canopy is open with a LAI of 1.5 and the prominent understorey is dominated by lichens (*Cladina spp*, *Cladonia spp*)(Plate 1C), and intermittent ericoid shrubs (*Vaccinium spp.*).

### Bog

The bog (Plate 2) lies 30 km west of the Yenesei river (60° 45' N, 89° 23' E, elevation 80 m) at the eastern edge of the west Siberian lowland. The surface vegetation is located in distinct hummocks and hollows. Hummock vegetation on drier elevated patches is dominated by *Chamaedaphne calyculata,* labrador-tea (*Ledum palustre*), bog rosemary (*Andromeda polifolia*), rannoch-rush (*Scheuchzeria palustris*), cranberry (*Oxycoccus palustris*), Cloudberry (*Rubus chamaemorus*) and cottongrass (*Eriophorum vaginatum)* are also present, but not dominant. The hollow patches contain mostly sphagnum mosses, rannoch-rush (*Scheuchzeria palustris*), bog-sedge (*Carex limosa*), bog rosemary (*Andromeda polifolia*) and round-leaved sundew (*Drosera rotundifolia).*

**MIXED STAND**

The mixed stand (Plate 2) lies on the east side of the Yenesei river (61° 87' N, 89° 47' E, elevation 160 m). The terrain is essentially flat with a mix of *Abies siberica* (Siberian fir), *Picea abies* (Norway spruce), P*inus siberica* (Siberian pine), *Sorbus aucuparia* (Rowen) and *Betula pendula* (Silver birch). The forest occurs on loam to clay rich. Canopy height is approximately 22 m in height. The LAI was measured using an LAI-2000 Plant Canopy Analyser (LICOR, Lincoln NE, USA) on May 5$^{th}$ and June 25$^{th}$ and was 1.45 and 2.09 respectively. Understorey species include a mixture of shrubs, herbs, mosses and fern. These are listed in Table A of Appendix A.

**POLE STAND**

The pole stand (Plate 2) lies on the east side of the Yenesei river (61° 87' N, 89° 46 E, elevation 150 m). The terrain is essentially flat with mainly *Abies siberica* (Siberian fir) and intermittent *Picea abies* (Norway spruce), and *Pinus siberica* (Siberian pine). The mean canopy height is 22 m and occurs on loam to clay rich soil. The canopy LAI was 1.87, 2.97 and 2.85 on May 5$^{th}$, 10$^{th}$ and June 25$^{th}$ respectively. The mix of understorey species found at this site is similar to that at the mixed stand (Roeser, *pers. comm.*) and is given in Table A, Appendix A.

A

B

C

**Plate 1 A** Eddy covariance tower at the Scots pine stand. **B** View of the Scots pine canopy from the top of the tower. **C** Lichen understorey at the Scots pine site.

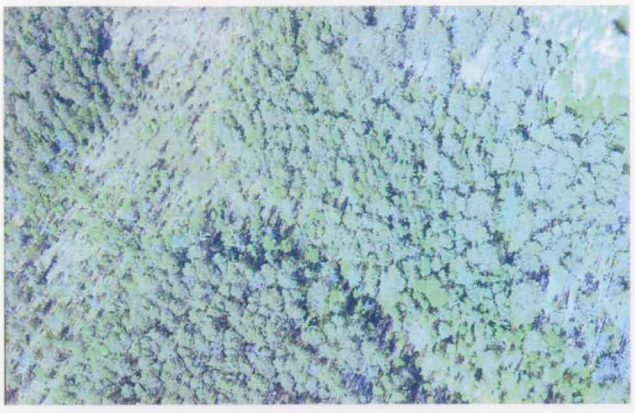

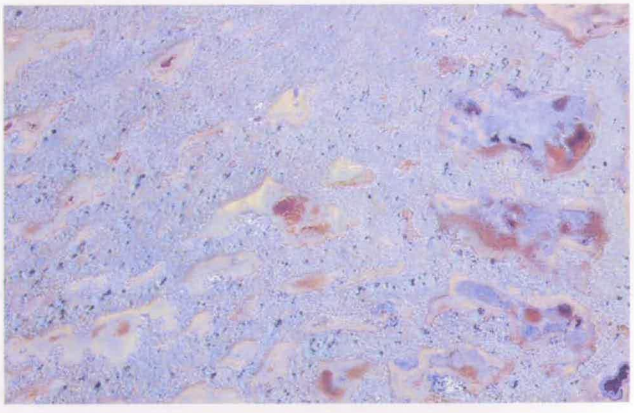

View of the Scots pine canopy from the helicopter (above left) the bog (above right) the pole stand (below left) and the mixed stand (below right).

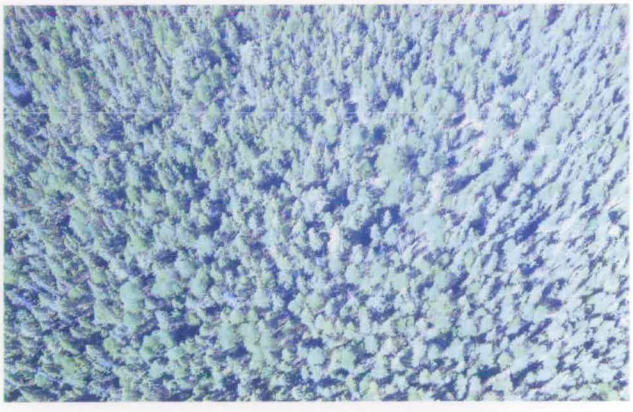

## CANOPY SPECTRAL REFLECTANCE DATA

### HELICOPTER MEASUREMENTS

A portable spectroradiometer (GER-1500, Geophysical & Environmental Research Corp., Milbrook, NY) was flown on a helicopter with the fibre optic probe mounted at nadir orientation on a steel mount through a hatch in the bottom of the helicopter. A twin axis spirit level was fixed to the mount as a visual level to aid manoeuvres during measurement. The fibre optic had a 23° instantaneous field of view (IFOV) and yielded a ground resolution of 122 m at the 300 m altitude.

The GER-1500 has a useable spectral range from 350 nm to 1050 nm with data being reported in 512 spectral bands.

Data were acquired on clear cloud free days whilst the helicopter hovered at each site for 1 - 2 minutes for each observation. Reflectances were calculated by normalising the canopy radiance by the radiance of a 99 % calibrated reflectance standard measured immediately before each flight (Spectralon, Labsphere, North Sutton, NH). Measurements were made around $\pm$ 2 hours of solar noon (consisting of an average of 32 scans). Observations were made from May 5$^{th}$ to June 15$^{th}$ when the canopy moved from zero photosynthesis (the winter condition) to full photosynthesis. Spectral calibration procedures were performed before and after the field season to check for changes in sensor radiometric response.

**Table 4.1** Summary of the dates and reflectance data acquisition with the range of temperature and solar radiation experienced during the observation period. Measurements were made around midday ± 2 hours of solar noon. Missing data points indicated with a dash. SZA is the solar zenith angle in degrees. Solar azimuth angle is also given in degrees. "Obs" date is observation date and temperature range is in degrees Celsius. The PPFD range is in μmol $m^{-2}$ $s^{-1}$.

| Site | Instrument | Obs date | Temp range | PPFD range | SZA | Azimuth |
|---|---|---|---|---|---|---|
| Scots pine | GER-1500 | 05/05/00 | 6.37-6.67 | 1450-1456 | 44 | 169 |
| | | 13/05/00 | 9.96-10.40 | 1415-1450 | 42 | 167 |
| | | 14/06/00 | 24.70-24.75 | 1546-1549 | 39 | 153 |
| | | 15/05/00 | - | - | 50 | 115 |
| | | 15/05/00 | - | - | 38 | 193 |
| Mixed | GER-1500 | 05/05/00 | 6.07-6.12 | 1430-1467 | 44 | 174 |
| | | 13/05/00 | 5.9-6.2 | 1219-1303 | 42 | 181 |
| | | 14/06/00 | 24.02-24.28 | 1565-1577 | 38 | 163 |
| | | 15/06/00 | 26.09-27.06 | 1344-1433 | 48 | 120 |
| | | 15/06/00 | 28.55-29.24 | 1421-1385 | 38 | 199 |
| Pole | GER-1500 | 05/05/00 | 6.85-7.04 | 1332-1339 | 44 | 183 |
| | | 13/05/00 | 5.9-6.2 | 1219-1303 | 42 | 181 |
| | | 14/06/00 | 24.28-24.33 | 1561-1577 | 38 | 166 |
| | | 15/06/00 | 27.06-27.79 | 1433-1529 | 47 | 124 |
| | | 15/06/00 | 28.59-29.24 | 1385-1391 | 39 | 202 |
| Bog | GER-1500 | 13/05/00 | 10.15-10.6 | 1309-1402 | 42 | 189 |
| | | 14/06/00 | 25.3-25.50 | 1549-1554 | 39 | 157 |
| | | 15/06/00 | - | - | 49 | 117 |
| | | 15/06/00 | - | - | 38 | 195 |

### TOWER SPECTRAL MEASUREMENTS

Measurements of the reflectance spectra of the Scots pine forest canopy were acquired from the north, south, east and west sides of the tower. The same open ended fibre optic probe used in the helicopter measurements was attached to the GER-1500 and positioned at the top of the tower (26 m, 8 m above the canopy) at an angle of 45 degrees to the normal so as to minimise the sensor "seeing " the flux tower itself. This yielded a (elliptical) spatial resolution of 27 $m^2$. An average of 4 spectral scans using this configuration were made for each measurement.

Diurnal measurements were made on clear cloud free days or when there was cloud below 20° on the horizon.

PRI from the GER-1500 data was formulated:

$$PRI = (R_{570} - R_{530})/(R_{570}+R_{530})$$

Where $R_{570}$ and $R_{530}$ are the reflectances in the spectral bands 570 nm and 530 nm respectively.

To follow the development of the canopy "greening up" from winter into spring, a (broadband) normalised difference vegetation index (NVDI) was also calculated from the helicopter GER-1500 data. To evaluate this change in greenness, an AVHRR-equivalent NDVI is defined as:

$$NDVI = (NIR-VIS)/(NIR+VIS)$$

Where NIR is the reflectance in the wavebands of the near infrared and VIS is the reflectance in the visible wavebands. This vegetation index is typically employed with AVHRR observations. The AVHRR equivalent VIS and NIR were derived from the spectra by averaging across appropriate wavelengths. The VIS AVHRR channel is computed from spectral data between 580 and 680 nm. The NIR AVHRR channel is computed from spectral data between 725 and 900 nm (described in Goward *et al*, 1994). The spectral data acquired by the GER-1500 were averaged to these waveband intervals, and NDVI calculated. This approach was taken to facilitate a later comparison with actual AVHRR computed NDVI values for the region.

**EDDY COVARIANCE MEASUREMENTS OF FLUXES**

Half hour fluxes of momentum, sensible heat, water vapour and carbon dioxide (and meteorological variables) were measured continuously at all four sites using tower-mounted eddy covariance systems operated by scientists from the Max-Planck

Institute in Jena. Full details of instrument set up and theory are presented elsewhere (Aubinet *et al.*, 2000).

At the Scots pine site, a second eddy covariance system was set up on the forest floor. Half-hour average fluxes of momentum, sensible heat, water vapour and carbon dioxide were measured continuously.

## ESTIMATES OF STAND PHOTOSYNTHESIS

### MIXED, POLE AND BOG

The $CO_2$ flux was partitioned into photosynthesis and respiration by estimating daytime ecosystem respiration as functions of air temperature. The procedure followed is the same as that used in Chapter 3. See Materials and Methods section (2.9) for details.

### SCOTS PINE

Estimates of canopy photosynthesis were made by subtracting the ecosystem respiration measured by the ground eddy system from the net $CO_2$ fluxes measured by the tower eddy covariance system.

Half-hourly values of canopy photosynthesis and incident PPFD were averaged during the period of the helicopter overflight (which was between 1230 and 1430 hours). Therefore, photosynthesis and PPFD were averaged for this period and an average canopy LUE was computed from these averages generating a midday average LUE value. This was calculated as follows:

$$\text{Canopy light use efficiency} = \frac{\text{Canopy photosynthesis } (\mu\text{mol } CO_2 \text{ m}^{-2} \text{ s}^{-1})}{\text{Incident PPFD } (\mu\text{mol photons m}^{-2} \text{ s}^{-1})}$$

**XANTHOPHYLL CYCLE PIGMENTS**

Top canopy needles of Scots pine (*Picea sitchensis*) were sampled for xanthophyll pigment analysis. Using a shotgun, top branches in full sunlight were shot down from three trees. One year old needles were selected and transferred to liquid nitrogen immediately for analysis in the laboratory. The growth of new needles in Scots pine starts around the beginning of May and usually terminates at the end of June. Therefore these needles were still at an early developmental stage and thus focus was placed on the first years needles, which are also well known to be responsible for the observed photosynthesis levels in early spring (Ottander *et al.*, 1995). The samples were analysed for pigment concentrations at the Research School of Biological Sciences, Australian National University.

Pigments were extracted in acetone with a mortar and pestle. The separation and quantification were by HPLC using a modified procedure of Gilmore and Yamamoto (1991). Details of this method are given in Appendix B. Relative concentrations of violaxanthin (V), antheraxanthin (A) and zeaxanthin (Z) were used to calculate the epoxidation state (EPS) of the xanthophyll cycle after Thayer and Bjorkman (1990) as

$$EPS = (Z+A)/(V+A+Z)$$

Pigment content was expressed on needle projected area basis.

The samples collected for pigment analysis were taken at the same time spectral data were being collected of the forest from the top of the tower.

## 4.3. RESULTS

### SEASONAL VARIATION IN LANDSCAPE SCALE LUE – A HELICOPTER STUDY

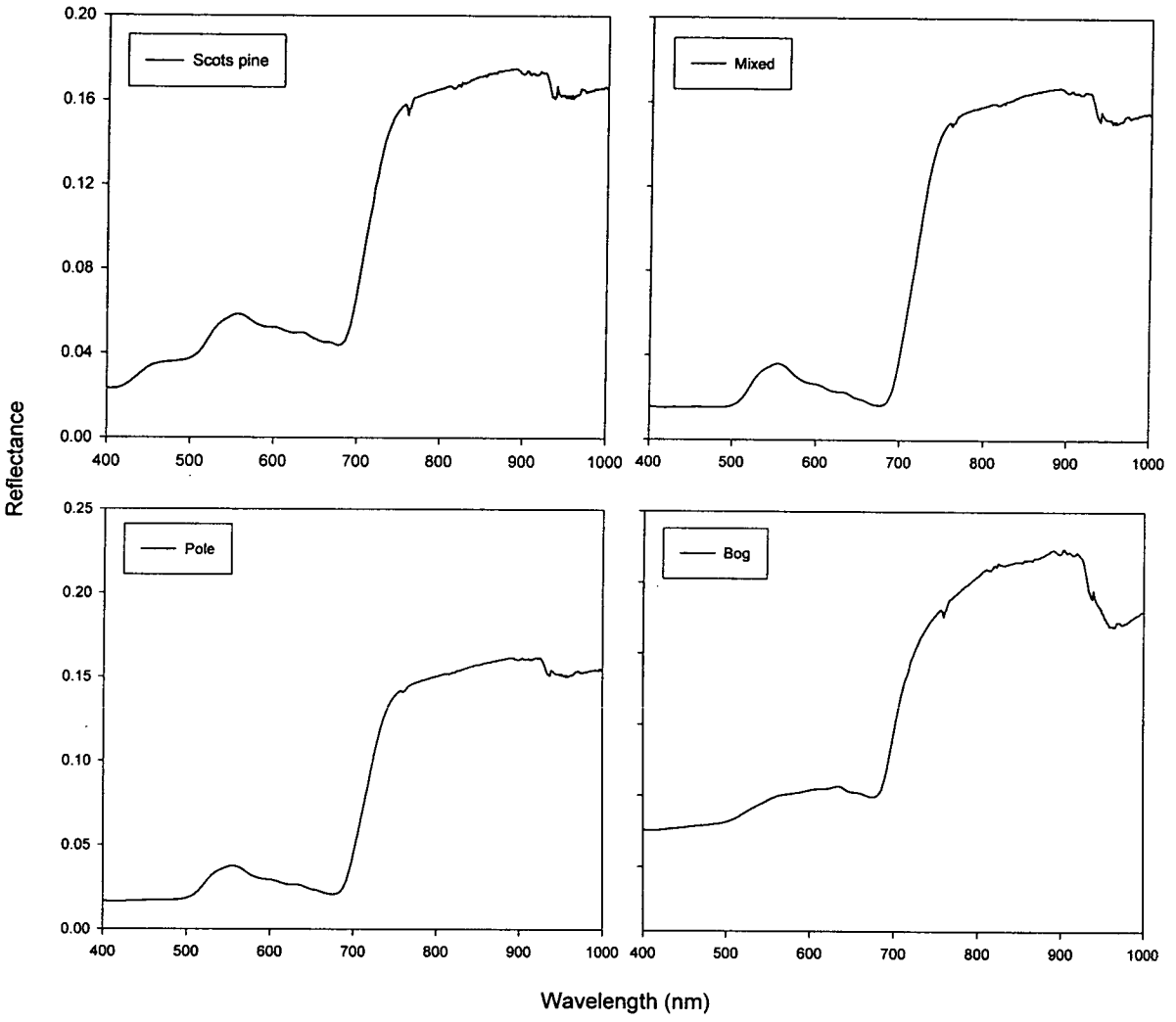


**Figure 4.1** Mean reflectance spectra of four Siberian boreal forest canopies acquired on June 14th by a helicopter mounted spectroradiometer (GER-1500). Each curve is the mean of 32 spectral scans.

Mean representative spectra for the four sites studied are given in Figure 4.1. All spectra exhibit the typical characteristics of vegetated canopies with the characteristic peak in the visible with the sharp increase into the near infrared at 700 nm. The Scots pine and bog have notably higher reflectances in the blue region of the spectrum. The reflectance of the Scots pine also shows a very small atmospheric absorption feature as seen by the dip at 680 nm, and to a lesser extent in the bog spectra.

The trend in $PRI_{HELI}$ (measured from the helicopter) values from the end of winter into the beginning of spring for the four stands is shown in Figure 4.2 and 4.3. Decreasing $PRI_{HELI}$ from the onset of snowmelt is apparent at all four sites. $PRI_{HELI}$ falls from 0.06 and 0.04 in the mixed and pole canopies respectively to 0.02 on June 15. The Scots pine however increases from 0.04 to 0.05 in the first weeks and then begins to decline from the 14$^{th}$ June. The values of $PRI_{HELI}$ for the bog are significantly higher and showed no change from May 13$^{th}$ to June 15$^{th}$. These changes in $PRI_{HELI}$ are mirrored in the calculated values of canopy light use LUE, which shows an inverse relationship to $PRI_{HELI}$. Increases in canopy LUE are observed in all four canopies from May 5$^{th}$ to June 14$^{th}$ (Figure 4.2).

The seasonal change in $NDVI_{HELI}$ (measured from the helicopter and hereafter "canopy greenness") is given in Figure 4.3 where the increase from May 5$^{th}$ to a plateau in June is visible in all four stands. This increase in canopy greenness is most apparent in the Scots pine stand which has the lowest value of 0.19 on May 5$^{th}$, increasing to 0.54 in June. The mixed and pole stands have the highest levels of greenness at the onset of snow-melt increasing to highs of 0.75 and 0.77 respectively.

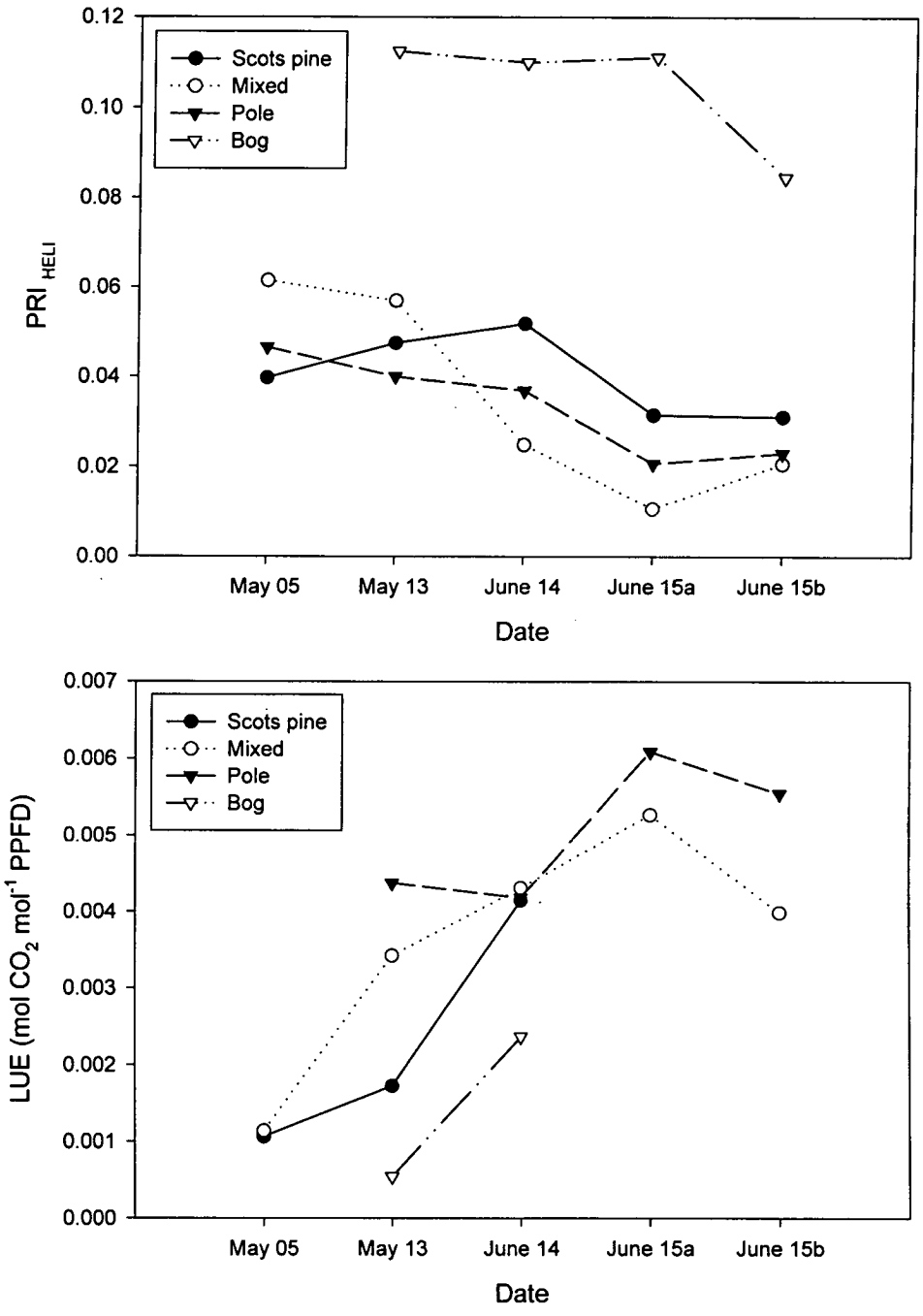


**Figure 4.2** Trend in the Photochemical Reflectance Index (PRI) during the winter-spring transition in four Siberian boreal forest canopies and canopy LUE over the same period. Missing points denote missing $CO_2$ flux data. June 15$^{th}$a represents measurements at 11am and June 15$^{th}$b represents measurements at 2.30pm.

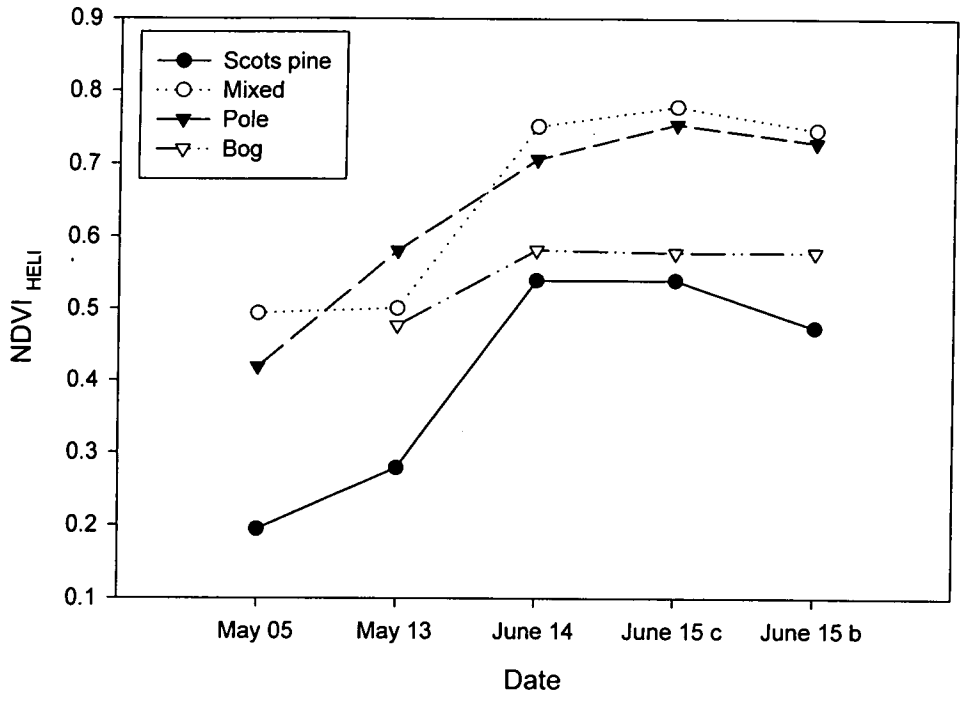


**Figure 4.3** Seasonal change in the Normalised Difference Vegetation Index (NDVI) for four Siberian boreal forest canopies. June 15$^{th}$a and b are as defined in 4.2.

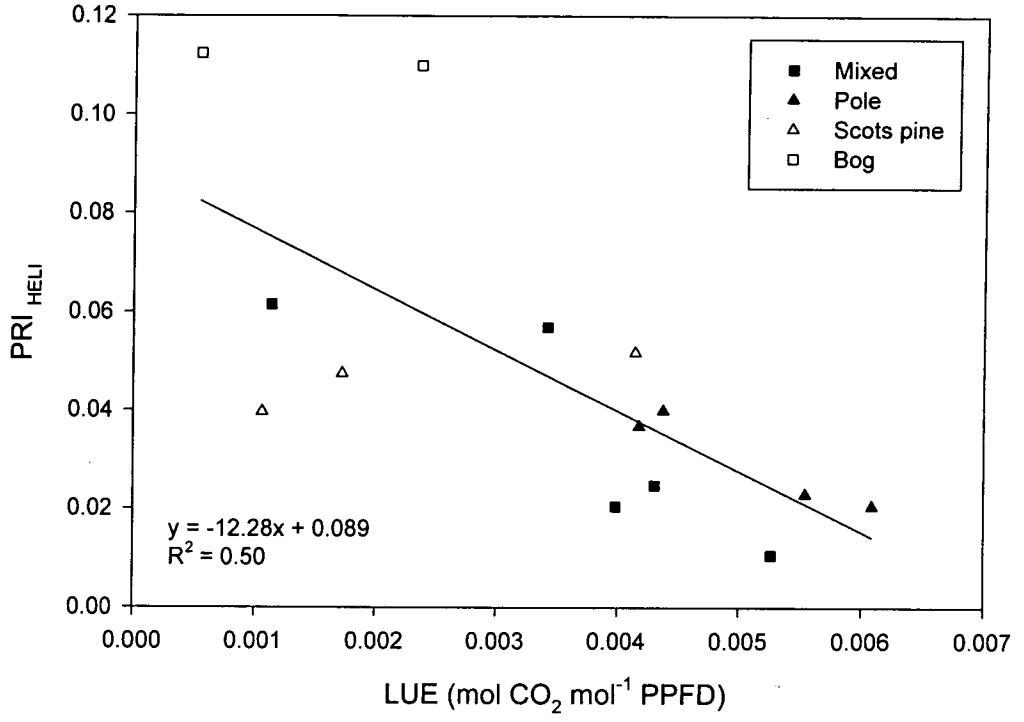


**Figure 4.4** Relationship between the Photochemical Reflectance Index (PRI) and canopy light use efficiency (LUE) in four Siberian boreal forest canopies sampled in full sun. Each point is the average of 32 spectral scans and 3 hours of eddy covariance data.

The relationship between $PRI_{HELI}$ and LUE is shown in Figure 4.4. Top canopy $PRI_{HELI}$ is moderately correlated with canopy LUE ($R^2 = 0.50$, $p < 0.01$) when the data from the four sites are combined. The Scots pine stand in particular exhibits a flat response between $PRI_{HELI}$ and LUE with PRI varying by only 0.01 for a change in LUE of 0.003 mol $CO_2$ $mol^{-1}$ PPFD.

The relationship between canopy LUE and $NDVI_{HELI}$ is shown in Figure 4.5 where a significant relationship is apparent between these two variables ($R^2 = 0.64$, $p < 0.001$).

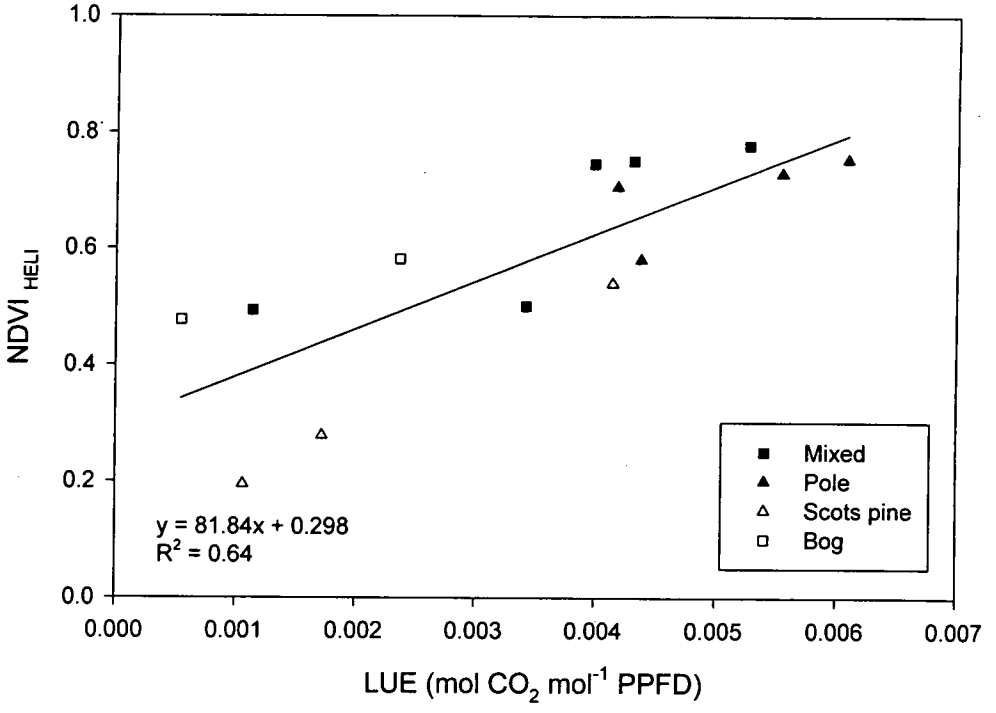


**Figure 4.5** Relationship between the Normalised Difference Vegetation Index (NDVI) and canopy light use efficiency (LUE) in four Siberian boreal forest canopies sampled in full sun. Each point is the average of 32 spectral scans and 3 hours of eddy covariance data.

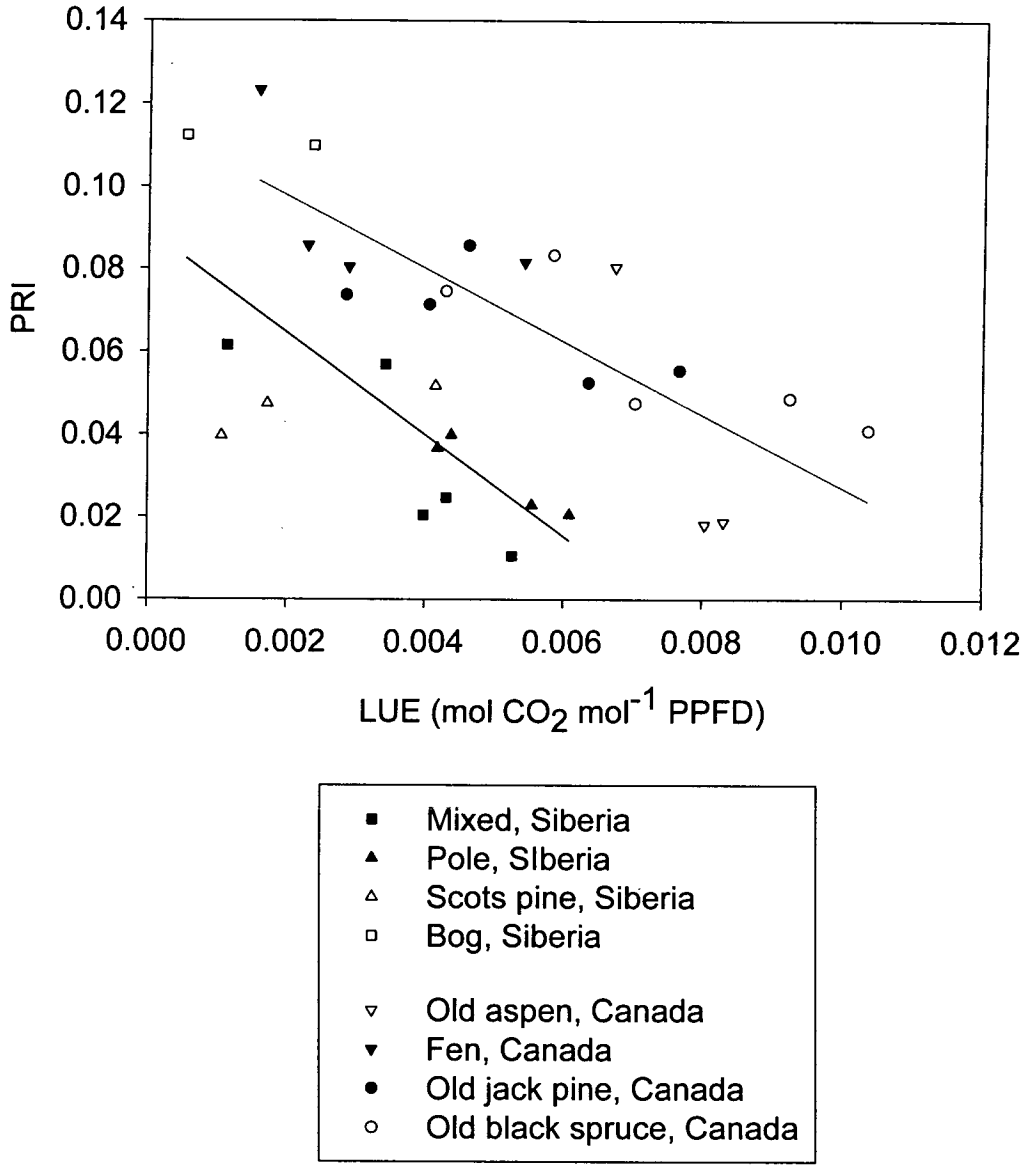


**Figure 4.6** Relationship between the Photochemical Reflectance Index (PRI) and canopy light use efficiency (LUE). Each Siberian point is an average of 32 spectral scans and 3 hours of eddy covariance data and each Canadian point is an average of 20-25 spectral scans and 4 hours of eddy covariance data.

Collating the PRI : LUE data set from the Canadian boreal forest (as presented in Chapter three) with the data from the Siberian boreal forest is shown in Figure 4.6. Two separate relationships between PRI and LUE clearly emerge when the data are pooled. The LUE values for the Siberian stands fall within the same range as the LUE values in Canada, but have lower values of PRI. Although the data for the Canadian forest represent a whole growing season, a significant difference exists between the two regression lines ($p$ = 0.01). Note for a single LUE value of 0.004 mol per $mol^{-1}$ absorbed PPFD, PRI values range from 0.02 to 0.08.

A comparison of the PRI values obtained in Siberia with those obtained at similar times in Canada are shown in Tables 1 and 2. From this, and Figure 4.6, it is apparent that for the same value of LUE, PRI varies by as much as 0.06.

**Table 4.2** Values of PRI and LUE in mol $CO_2$ per $mol^{-1}$ of absorbed PPFD (in brackets) for four Siberian boreal forest canopies (**A**) and for four Canadian boreal forest (**B**) and the early growing season (Canada) and winter spring transition (Siberia).

**A**

| | May 05 | May 13 | June 14 | June 15 am | June 15 pm |
|---|---|---|---|---|---|
| Scots pine | 0.0397 (0.001) | 0.0475 (0.002) | 0.0518 (0.004) | 0.0314 | 0.0310 |
| Mixed | 0.0615 (0.001) | 0.0570 (0.003) | 0.0248 (0.004) | 0.0106 (0.005) | 0.0205 (0.004) |
| Pole | 0.0465 | 0.0400 (0.004) | 0.0368 (0.004) | 0.0206 (0.006) | 0.0230 (0.005) |
| Bog | | 0.1124 | 0.1099 (0.0005) | 0.1100 (0.002) | 0.0844 |

**B**

| | May 31 | June 01 | June 06 |
|---|---|---|---|
| Old black spruce | | 0.0746 (0.004) | 0.0833 (0.005) |
| Old jack pine | 0.0737 (0.003) | | 0.0857 (0.005) |
| Old aspen | 0.0805 (0.007) | | |
| Fen | | 0.0805 (0.003) | 0.0857 (0.002) |

## SEASONAL CHANGE IN SCOTS PINE, LUE AND XANTHOPHYLL CYCLE PIGMENTS A TOWER STUDY

The seasonal change in the epoxidation state of the xanthophyll cycle and canopy LUE are shown in Figure 4.7. The needles that were sampled for xanthophyll pigment analysis were taken from the tops of the trees in Sun exposed positions. Therefore the spectral reflectance data taken from the brightest area of forest canopy from the tower at the time of pigment sampling was selected to represent those needles sampled for pigment analysis. The assumption here was that the response of the sun leaves sampled for pigment analysis would be the same as that generated (spectrally) for sunlit leaves in a different location, but similar orientation in the canopy. Data from the sun leaves could then be assumed to represent the spectra acquired from an area of canopy that was also being viewed by the sun. The LUE values were calculated from the eddy covariance data for the ½ hour interval during pigment sampling.

To test the operation of the xanthophyll cycle when the forest was still in winter dormancy, needles were sampled in full sunlight on the 15$^{th}$ April, when temperatures were around –10° C. The value of (Z+A)/(V+A+Z) in winter (Apr-15, Figure 4.7A) was at a maximum of 0.993. The beginning of May brought the onset of spring and this saw a fall in the relative quantities of xanthophyll cycle pigments in the de-epoxidised state from 0.916 on May 2$^{nd}$ to 0.698 on May the 13$^{th}$. This decrease in (Z+A)/(V+A+Z) was paralleled by a steady increase in canopy light use efficiency (Figure 4.7B), with the relation between the two being linear and significant ($R^2$ = 0.80, $p$ < 0.05). PRI, calculated from tower measurements of reflectance, demonstrated the characteristic inverse relationship (Z+A)/(V+A+Z). A plot of the relationship between PRI and (Z+A)/(V+A+Z) is shown in Figure 4.7C and whilst linear was not significant ($R^2$ = 0.87, $p$ = 0.1). A full description of the carotenoid composition is given in Appendix C.

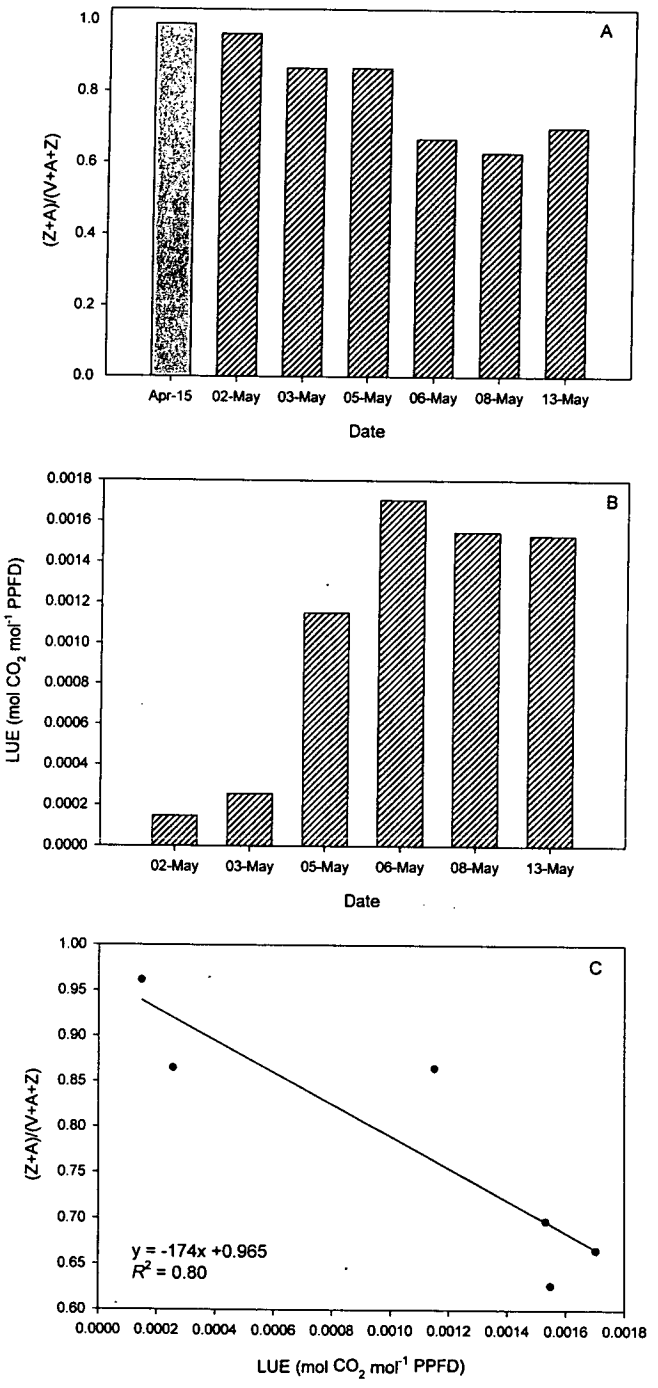


**Figure 4.7** The seasonal change in **A** the epoxidation state of the xanthophyll cycle (Z+A)/(V+A+Z) (measured from one year old needles) **B** photosynthetic light-use-efficiency (LUE) and **C** the relationship between the epoxidation state and LUE during the winter spring transition in a Siberian Scots pine forest canopy. Each LUE value is calculated from a ½ hour average of PPFD and flux data.

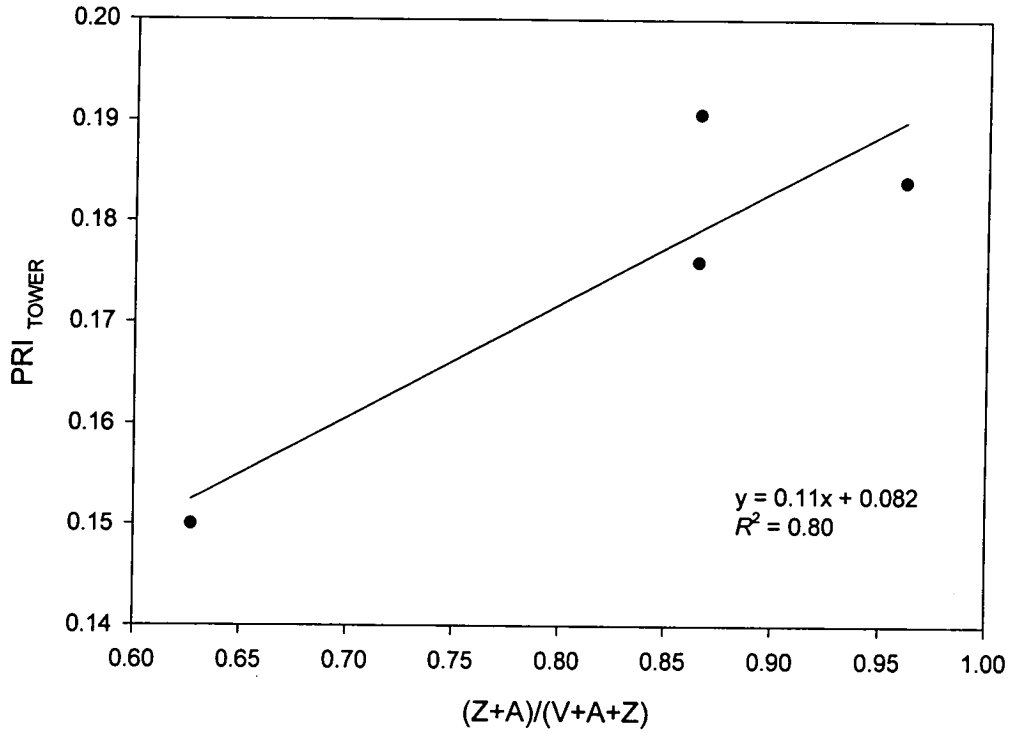


**Figure 4.8** Relationship between the epoxidation of the xanthophyll cycle (Z+A)/(V+A+Z) and the Photochemical Reflectance Index (PRI) calculated from tower measurements of Scots pine spectral reflectance. Each point is an average of 4 spectral scans. Each LUE value is calculated from a half-hour average of PPFD and flux data

## DIURNAL CHANGE IN SCOTS PINE PRI AND LUE A TOWER STUDY

A diurnal light response relationship of canopy photosynthesis, LUE, $PRI_{TOWER}$ and NDVI is shown in Figure 4.9. In this analysis, the spectral data correlated with the eddy covariance data, was chosen based on the location/direction of the flux footprint. To do this required checking the wind direction from the flux data. The flux measured by the eddy covariance system was from the region to the north of the tower (i.e. around 20-30°). Spectral scans taken in this area were selected from the measurements made throughout the day. The relationship between sun angle induced variation in the fluxes and reflectance could be investigated.

At 8am, high values of photosynthesis and PPFD resulted in a high canopy LUE and low value of PRI. Photosynthesis declined to a minimum around noon when PPFD was at its highest value of around 1400 μmol $m^{-2}$ $s^{-1}$, with LUE further decreasing. LUE continued to fall as the ratio of photosynthesis to PPFD decreased through the afternoon. $PRI_{TOWER}$, again, followed an inverse relationship to LUE. The relationship between PRI and LUE over the diurnal cycle was linear and highly significant ($R^2 = 0.97, p < 0.001$).

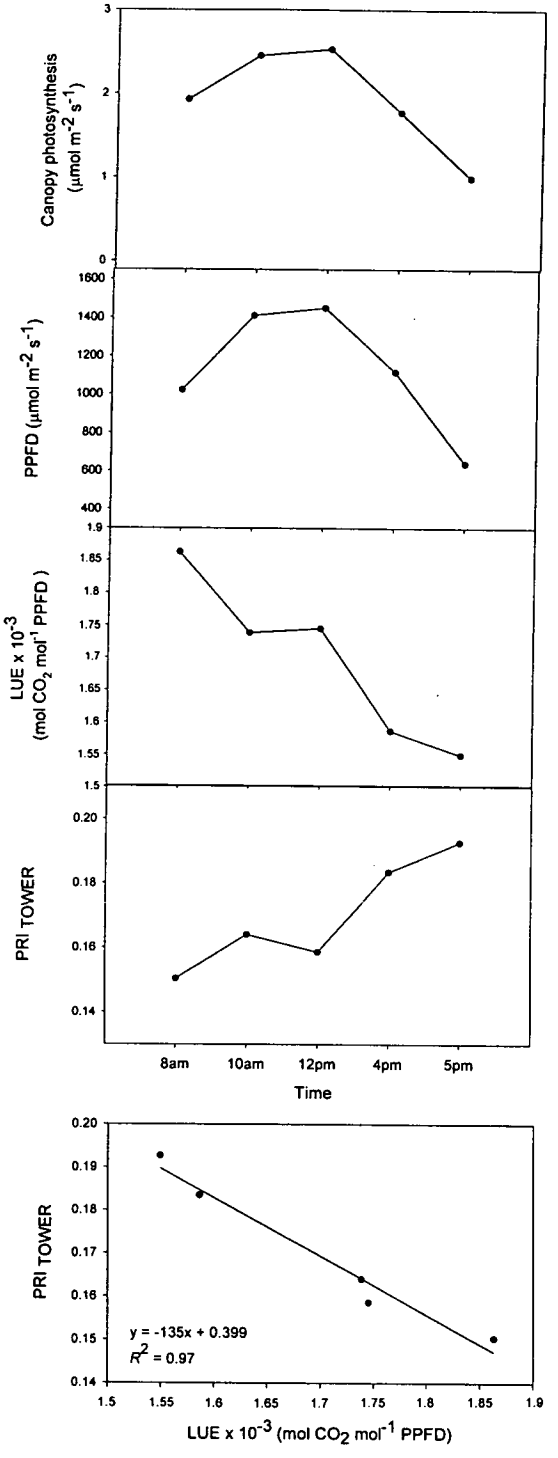


**Figure 4.9** Diurnal light response of canopy photosynthesis, incident PPFD, LUE, and PRI of a Scots pine canopy. Each spectral measurement is an average of 4 spectral scans with each LUE value being calculated from a half-hour average of PPFD and flux data.

## 4.5 DISCUSSION

### SEASONAL RESPONSES OF PRI, LUE AND NDVI : RESULTS FROM A HELICOPTER AND TOWER STUDY

The results presented here are a second application of PRI to measurements of photosynthetic light use efficiency of boreal forest. The first study by Nichol *et al.*, (2000)(Chapter 3) focused on a boreal forest canopy in Canada and demonstrated that PRI, also measured from a helicopter platform, correlated well with estimates of LUE calculated from eddy covariance measurements.

The study presented here took a further step by focusing on boreal forest in Siberia during a critical period where the climate, forest structure and understorey were changing rapidly during the spring. Previous studies have shown that the xanthophyll cycle works at its highest capacity during winter dormancy in evergreen species, including conifers (Ottander and Oquist, 1991, Adams *et al.*, 1994, Ottander *et al.*, 1995, Verhoeven *et al.*, 1996, Vogg *et al.*, 1998, Verhoeven *et al.*, 1999), when cellular structure changes dramatically and the xanthophyll cycle remains almost entirely in its de-epoxidised state (i.e. with maximum quantities of zeaxanthin) to effectively dissipate all of the absorbed energy as heat. The winter sample taken of the needles at the Scots pine site (Apr-15, Figure 4.7) supports this point. The value of (Z+A)/(V+A+Z) was 0.99, which is by far the highest value ever recorded for epoxidation of the xanthophyll cycle (Osmond, *pers comm*). Ottander *et al.*, (1995) reported winter values of 0.1 in *Pinus sylvestris* (the epoxidation state (EPS) was calculated as (0.5A+V)/(V+A+Z)) demonstrating that the xanthophyll cycle was maintaining very high concentrations of zeaxanthin. Adams *et al.*, (1994) also studied the winter dynamics of the xanthophyll cycle in overwintering leaves of *Pinus ponderosa* and reported EPS values of ~ 0.9, indicating major photoprotection and energy dissipation. Such high (or low) values of EPS have also been found in

other conifer species during the winter (Verhoeven *et al.*, 1996, Verhoeven *et al.*, 1999).

The change in $PRI_{HELI}$, LUE and $NDVI_{HELI}$ measured from the helicopter (Figures 4.2 and 4.3) and tower $PRI_{TOWER}$, LUE and (Z+A)/(V+A+Z) of the Scots pine stand (Figure 4.7) showed the four sites coming out of winter dormancy. The higher values of $NDVI_{HELI}$ and lower $PRI_{HELI}$ over the sampling period, between sites (Figure 4.2) suggested that the mixed and pole stands on the east side of the Yenesei had started to come out of winter dormancy before the Scots pine and bog on the west side, prior to my arrival. The lower (higher) values of $NDVI_{HELI}$ ($PRI_{HELI}$) on the west side compared to the east were probably a result of the faster melting of snow, building of chlorophyll and onset of photosynthesis. The main stimulus for recovery during post-dormancy is a combination of temperature and water status, and in stands of Scots pine such recovery typically occurs during April-May (Ottander and Oquist, 1991, Ottander *et al.*, 1995). As long as the water supply in the soil is frozen and unavailable, no active reaction centres of PS II are found in Scots pine (Tsel'niker and Chetverikov, 1988). Although favourable temperatures can stimulate the recovery of spring gas exchange, strong solar radiation at this time continues to promote daytime photoinhibition, which would explain why the changes in (Z+A)/(V+A+Z) are not dramatic and still high over this period. Part of this slow recovery is probably also due to the *de novo* synthesis of photosynthetic pigments and damaged proteins of PS II.

Although $NDVI_{HELI}$ increased rapidly in the sites studied here, the growth of the new years needles was not complete until the end of June and thus cannot explain the trend in "greenness". The increase in concentration of chlorophyll in current year needles is also slow, as mentioned, typically beginning in March and reaching a maximum in June (Ottander *et al.*, 1995). Therefore the increase in $NDVI_{HELI}$ is probably attributed to a combination of the redistribution of existing chlorophyll

stocks (which is around 40 % in winter needles) within current years needles and increasing leaf area. Certainly photosynthesis in Scots pine recovers before chlorophyll begins its increase to a summer maximum by the end of June (Ottander *et al*, 1995).

In agreement with the findings from Nichol *et al.*, (2000) a linear relationship between $PRI_{HELI}$ and LUE was also apparent for the four sites studied here, although the strength of the relationship was clearly weaker. This is likely to be the result of a combination of factors. Often where canopies are relatively open or have a low LAI, the influence of background materials reduces the sensitivity of a vegetation index to the biophysical variable under study. Of the canopies studied here, the Scots pine stand was open and exposed an understorey whose spectral characteristics were markedly different to that of the overstorey. Viewed from the helicopter the scene was a mixture of green canopy (with relatively low LAI) and bright lichen understorey. Spectral measurements of the lichen were made around the tower in May and June (data not shown) and the PRI value of the lichen was 0.04 and 0.05 respectively. As Table 1 shows, the scene $PRI_{HELI}$ for the Scots pine stand in May and June was 0.0475 and 0.0518. Clearly the scene $PRI_{HELI}$ was dominated by the lichen reflectance, and is the probable reason for a divergence in the relationship between $PRI_{HELI}$ and LUE. The mixed and pole stands lay closer to the regression line than the Scots pine or bog and together their relationship with LUE was stronger and significant ($R^2 = 0.67$)(data not shown). These two sites had dense canopies with a greater mix of species, and herbaceous understorey, so little interference would come from the background with a reflectance signal significantly different to that of the canopy.

The linear relation between LUE and $NDVI_{HELI}$ is most likely the result of a slowly changing LAI and build up and redistribution of chlorophyll in the current years needles. Therefore the linear increase in $NDVI_{HELI}$ and LUE during this time results

in an incidental relationship between the two variables that is most likely structural rather than physiological. It has been well established that NDVI is insensitive to short term fluctuations in photosynthesis in fully green canopies (Gamon *et al.*, 1995).

The merits of using absorbed PAR (APAR) over intercepted PAR (IPAR) in the calculation of LUE has been discussed in Chapter 3 and whilst this would not have caused significant error in the LUE computation at the Canadian sites, would have had an influence in the Scots pine site, and possibly to a lesser extent at the bog (due to the presence of water). The discussion in Chapter 3 explains this point in more detail.

**CANADIAN AND SIBERIAN BOREAL FOREST PRI AND LUE**

When the results from the boreal forests were collated, the slope of the relationship between PRI and LUE differed. Although the actual range of LUE values between Canada and Siberia (for the same time of year) were similar their corresponding values of PRI were very different. This is likely to be the result of a combination of factors. Of the canopies studied in Siberia, one (Scots pine) was relatively open with a bright understorey whose spectral characteristics were markedly different to that of the overstorey. Viewed from above the scene was a mixture of green canopy (with relatively low LAI) and a bright understorey of lichen. The results showed that the scene PRI was closer to that of lichen than green vegetation. The bog, whilst dominant in green mosses and shrubs (flowering was absent), was still flooded in places and had very high reflectance in the visible, with almost no difference in reflectance between the two wavebands. Thus the response to LUE was very flat.

The influence of the atmosphere may also have caused the values of PRI to differ between the two forests, when values of LUE were similar. An important consideration for remote sensing is the robustness of a calculated vegetation index to

atmospheric perturbation. The influence of the atmosphere on any remotely sensed observation is the result of a delicate balance between aerosol and molecular scattering and absorption by aerosols and atmospheric gases. Molecular scattering and absorption can be accounted for satisfactorily. It is practically constant in space and time and is given by Rayleigh's formulation (for details see Asrar, 1989). As Rayleigh's law states, "the scattering coefficient is inversely related to the fourth power of the wavelength" (i.e. as $\lambda^{-4}$) it will have a greater effect on the shorter waveband of 530 nm than the longer wavebands of 570 nm. This means that a top of the atmosphere PRI will be smaller than a top of canopy PRI. Thus a correction for Rayleigh scattering will be essential. As Barton and North (*in press*) demonstrated in their modelling study, top-of-the-atmosphere PRI differed from top- of-the-canopy PRI when Rayleigh scattering was not corrected for. This could explain why the tower measured PRIs were lower than the helicopter PRI values. However, the helicopter was seeing a combination of green canopy, lichen understorey and sunlit and shade background. Therefore, firm conclusions cannot be drawn.

Gaseous absorption is usually also minimised by choosing bands in atmospheric windows, and thus aerosol scattering and absorption are the main variables in the atmospheric effect. Depending on the reflectance features of the target, aerosol scattering is the main variable component of the atmospheric effect for dark surfaces (i.e. the visible for vegetation) whilst absorption is important for bright surfaces (i.e. vegetation in the NIR) (Asrar, 1989). A knowledge of the surface reflectance and the optical properties of the atmosphere must also be known.

The spectral data presented in Chapter 3 were atmospherically corrected but the data set presented here was not. There was no access to a Sun-photometer and whilst corrections/algorithms can be developed by viewing targets of known reflectance, finding a site suitable for this task was unsuccessful.

**DIURNAL VARIABILITY IN SCOTS PINE PRI AND LUE**

The diurnal measurements made of the Scots pine canopy clearly showed a close tracking of sun angle induced variation in canopy LUE by $PRI_{TOWER}$. This has also been found on smaller plots (Gamon *et al.*, 1992) and from modelling studies Barton and North (*in press*). First thing in the morning, incident PPFD is utilised with a higher degree of efficiency and as the sun's zenith increases towards solar noon the intensity increases, the efficiency of photosynthesis decreases and the de-epoxidised status of the xanthophyll cycle increases. That is, a greater proportion of the pool size of V+A+Z remains as zeaxanthin. This is evident from the change in $PRI_{TOWER}$.

An argument of spatial scale can clearly be made here. The specroradiometer measurements that were made from the tower were measuring an area of canopy 27 $m^2$, which is considerably smaller than the area of forest being sampled by the eddy covariance system (~ 1 $km^2$), and larger than the area sampled for xanthophyll cycle pigments, which can only be determined on a needle area basis. However, from the results presented, the assumptions made clearly hold. When viewing the seasonal change in $PRI_{TOWER}$, LUE and (Z+A)/(V+A+Z) (Figure 4.7) only sun exposed leaves were sampled for pigments and thus only sun exposed areas of the canopy were used to correlate spectral data with the pigment data. The eddy covariance system was also measuring $CO_2$ fluxes when the canopy was at light saturation.

## 4.5 CONCLUSIONS

This chapter demonstrated that the helicopter measured $PRI_{HELI}$ was linearly related to photosynthetic LUE when the data from four Siberian boreal forest canopies were combined, although the relationship was weaker than that found in similar boreal forest canopies in Canada. It is likely that a number of factors including leaf area index, understorey reflectance features and the atmosphere all played a role by

introducing variation in the observed relationship between $PRI_{HELI}$ and LUE at the canopy scale. The issue of atmospheric correction is relatively easy to solve with access to instrumentation and the necessary computer code (i.e. 6S atmospheric transport model), but the issue of canopy structure in sparse canopies needs to be considered further if PRI is to be applicable in sparse canopies.

The spectral measurements made of the Scots pine canopy from the tower clearly demonstrated the changing canopy LUE and proportions of the xanthophyll cycle pigments in the de-epoxidised state over the spring period and diurnal cycle, confirming the role of the xanthophyll cycle in photoprotection, and its measurement using remote sensing

# 5. PRI : A SENSITIVITY ANALYSIS USING THE SAIL MODEL

## 5.1 INTRODUCTION

A number of studies have demonstrated that the photochemical reflectance index (PRI) correlates well with photosynthetic light use efficiency (LUE) of both leaves (Gamon, 1992, 1997) and canopies (Fillela *et al.*, 1996, Nichol *et al.*, 2000). There appears to be a consistent relationship between PRI and LUE across species, functional types and nutrient treatments, apparent at all but the lowest light levels (~ 100 μmol $m^{-2}$ $s^{-1}$). These studies have further suggested that relative rates of photosynthesis could be derived from remotely sensed reflectance measurements.

However, reflectance measurements made over vegetated canopies are complex in nature and include a signal that is a function of both the canopy and background reflectances. Thus, a number of extraneous factors could exert their own influence on the reflectance of the scene, and overwhelm the signal of interest, in this case PRI. Whilst the design of a spectral vegetation index is such that it maximises sensitivity to the variable of interest (see Verstraete and Pinty, 1996), the influence of background materials on the scene is unavoidable when LAI is low, unless an appropriate correction is applied to the spectral data to subtract the contamination.

Simulations of light interactions in plant canopies have shown that the form of the relationship between a spectral vegetation index (e.g. NDVI or PRI) and various biophysical variables (e.g. LAI, biomass, $f_{APAR}$) could vary with changes in canopy architecture, optical properties of canopy components and as well as the optical properties of the background (for NDVI see: Baret and Guyot, 1991, Asrar *et al.*, 1992, Goward and Huemmrich, 1992, Roujean and Brean, 1995: for PRI see Barton and North, *in press*).

If landscape scale reflectance data are to be interpreted correctly for the determination of PRI and photosynthetic efficiency over large areas, a sound understanding of how the canopy and background materials affects the measurement of PRI itself must be obtained. A suitable model of canopy reflectance enables an exploration of how the optical properties of canopies may differ from that of leaves, and how this difference is influenced by canopy architecture and viewing angle.

Leaf scale reflectance and transmittance (as well as and background) measurements were made during the BOREAS experiment. The SAIL model was used to simulate canopy reflectance and then, by introducing realistic variations into the scene, I investigated the sensitivity of PRI to these changing conditions and identified the optimal conditions for its use.

## 5.2 Materials and Methods

### Leaf optical measurements

Reflectance and transmission measurements were made of individual needles from the of top of the old black spruce canopy on September 15th, 1994 by the BOREAS terrestrial ecology science group (TE-10) at the University of Nebraska. A brief description of the measurement setup is as follows.

Access to the top of the canopy was provided by a canopy access tower. Branch tips to be measured were excised from the trees and sealed in plastic bags with moist towels. After collection, samples were refrigerated until the measurements were conducted at room temperature in the field laboratory. Hemispherical reflectance and transmittance were measured at near normal incidence levels using an external light source and a LI-COR LI-1800 integrating sphere (Lincoln, Nebraska) attached to a

Spectron Engineering SE-590 spectroradiometer (Denver, Colorado). The reflectance and transmittance values, with the background used, are shown in Figure 5.1.

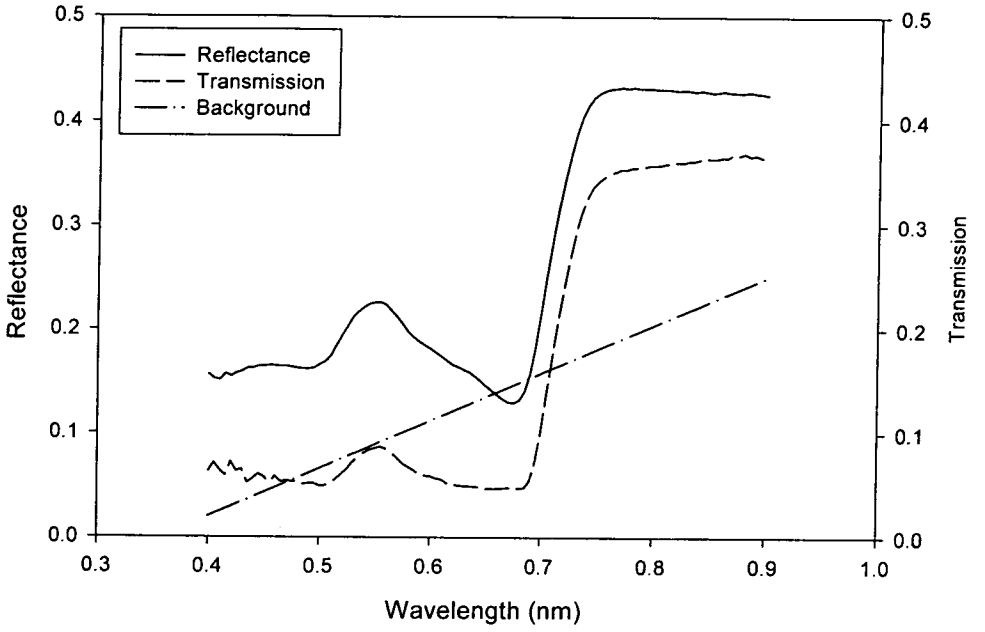


**Figure 5.1** Needle reflectance and transmittance (and background) data used in SAIL model calculations.

# MODELLING CANOPY REFLECTANCE

## THE SAIL MODEL

Of the many models used to simulate canopy bidirectional reflectance, the SAIL (Scattering from Arbitrarily Inclined Leaves) model adopts the simplist deterministic approach to produce a realistic estimate of canopy bidirectional reflectance (Alexander, 1983, Verhoef, 1984). The SAIL model is an extension of the Suits model (1972) which includes a range of leaf angle distributions rather than a single leaf angle. Because of this, the SAIL model produces a more realistic output of canopy bidirectional reflectance than the Suits model (Goward and Huemmrich, 1992).

The SAIL model is a 1-D model that assumes that the canopy consists of multiple layers and that the canopy is homogeneous and infinite in the $x$ and $y$ directions. The canopy is described by its leaf area index (LAI) and leaf angle distribution (LAD) and calculates the scene reflectance from flux streams (a downward (direct) specular, downward diffuse and upward diffuse), the size of which are determined by extinction and scattering coefficients. The extinction coefficients are in turn dependent on the canopy structure, in particular LAI and LAD.

Several primary variables describe the radiative transfer in the SAIL model (Goward and Huemmrich, 1992). These variables describe the two major elements in remotely sensed observation.

**a) Illumination and viewing conditions:**

1. Direct and diffuse composition of the incident radiation.
2. Solar zenith angle
3. Sensor view zenith and azimuth angles

**b) Canopy and landscape conditions**

1. Leaf area index
2. Canopy structure (leaf angle distribution)
3. Leaf optics (reflectance and transmission)
4. Background reflectance

Leaf area index (LAI) is one of the primary canopy variables that controls the spectral reflectance patterns and influences any calculated reflectance index. LAI values of 0.25, 0.5, 1.0, 2.0, 3.0, 4.0, 5.0, 6.0, 7.0 and 8.0 were selected to characterise this variable and thus generate a range of scene reflectances for differing canopy densities. The remaining variables for canopy and landscape conditions are shown in Table 5.1.

**Table 5.1** Parameter specifications for calculation of canopy reflectance in the SAIL model

| Illumination and Viewing Conditions | |
|---|---|
| Proportion direct radiance | 1.0 |
| Latitude | 40° N |
| Observation time | 1400 EST |
| Solar declination angle | 0.0° (equinox) |
| Solar zenith angle | 40° |
| Solar view zenith | 0° |
| **Canopy and Landscape Conditions** | |
| Leaf optical properties | User input |
| Leaf angle distribution | Spherical |
| Twig inclination angle | Planophile |
| Background spectral reflectance | Assigned |

**MODEL SIMULATION APPROACH**

The variables set for illumination and viewing conditions are also given in Table 5.1. Observations from a 2.00 pm local time for a northern latitude location during the solar equinox were simulated. The sensor was viewing in the nadir position (unless otherwise specified). This approximated the afternoon observations of the AVHRR overpass and is also relevant to Landsat sensor and SPOT sensor observations acquired at 10:00 am local time.

Senescent leaves, opaque stems and branch materials were not included (unless otherwise stated). This approximates to grasslands or typical temperate agricultural crops during the early and middle growth phases. This is the simplist vegetation canopy to represent in a radiative transfer model but represents only a fraction of the variability found in global vegetation systems. Further work addressing canopies with non-green materials, discontinuous canopies and areas with marked topographic relief is required.

The spectral vegetation index used in this study is the photochemical reflectance index (PRI) and was calculated from the simulated reflectances as follows,

$$\mathrm{PRI} = (R_{570} - R_{530}) / (R_{570} + R_{530}) \qquad (1)$$

Where $R_{570}$ and $R_{530}$ denotes the reflectance at 570 nm and 530 nm respectively.

In addition to the basic parameters specified in the model, realistic variations were introduced in the observations, one variable at a time. A brief description of each of the variables considered in the sensitivity study is given below. It should be noted that the leaf optics and background reflectances were held constant throughout, unless otherwise stated.

## SENSITIVITY STUDY USING SAIL

### INFLUENCE OF SOLAR ZENITH ANGLE

The solar zenith angle was varied (10 - 80°, at 10° increments) for a constant and changing canopy (i.e.LAI). Leaf optical properties and background reflectance were kept constant throughout. Reflectances were calculated for a nadir-looking sensor for all wavebands from 400-1200 nm.

### INFLUENCE OF BACKGROUND REFLECTANCE

To determine the influence of background reflectance on the PRI of the scene, five contrasting backgrounds were introduced into the calculation of reflectance. These were: illuminated ground vegetation, illuminated ground moss, illuminated debris and snow, shadow and snow. Scene reflectance was calculated for changing LAI with each background. The background reflectances used are presented in Figure 5.2, and were collected by the BOREAS remote sensing science group (RSS-19) at the University of York.

### INFLUENCE OF LEAF ANGLE DISTRIBUTION (LAD)

Leaf angle distribution will influence the radiation interaction with the canopy by both altering the penetration into the canopy, the distribution of light within the canopy and the transmission of light by the canopy (and thus to the ground sensor). The interaction between leaf angle and view angle will determine the depth of canopy from which the PRI signal is perceived. Six LADs were used (described in table 2) along with the basic parameter set (as described in table 1). Again,

reflectances are calculated for an at-nadir sensor. Leaf optical properties and background reflectance were kept constant throughout.

### INFLUENCE OF NON-GREEN MATERIAL

The presence of non-green material in scene reflectance was considered by altering the ratio of green leaf area to twig area, whilst leaf and background optical properties were kept constant. Canopy reflectance was also modelled for a canopy with no non-green material, for varying LAI.

### INFLUENCE OF IRRADIANCE QUALITY

Few terrestrial locations can be observed daily because of the interference of clouds and haze. The effect of such variable illumination conditions is of significance in growth analysis. In terms of the SAIL model, the proportion of incident irradiance which is direct (specular) versus diffuse can be varied. Under cloudy conditions the relative proportion of diffuse irradiance increases. Specular irradiance was varied between 0 (completely diffuse) and 1 (completely specular) for a changing canopy structure. Leaf optical properties and background reflectance were kept constant throughout.

### INFLUENCE OF VIEW ZENITH AND VIEW AZIMUTH

The view angles of many space borne sensors used in land use research can view up to $\pm$ 60 degrees from nadir. The SAIL model has limited ability concerning bidirectional specular scattering, so the results presented here addressing view angle and azimuth offer a limited representation of the problems encountered in off-nadir viewing (Deering, 1988, Deering *et al.*, 1999). The view azimuth angle was placed in the principle plane of the Sun, and sensor view angle was varied from 10 to 60° (representing the backscatter direction) and –10 to –60° (representing forward scatter). The co-ordinate system used is shown in Figure 5.2.

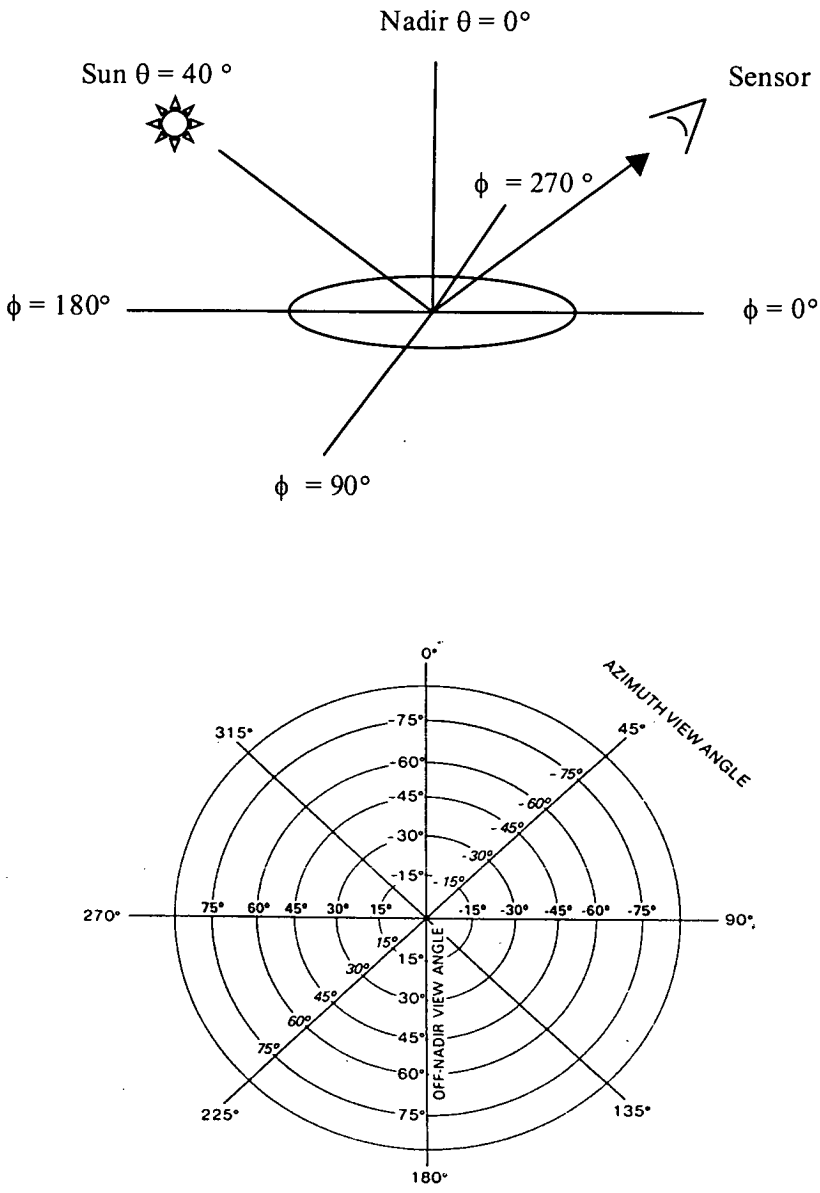


**Figure 5.2** Co-ordinate system describing solar and sensor angles, and polar plot showing scheme for plotting directional reflectance factors. The solar azimuth is always 180°. The sensors azimuth and off nadir are shown by ϕ and θ respectively. The distance from the origin in the polar plot represents the off-nadir viewing angle.

**Table 5.2** Fractions of leaf area in each zenith class for the six Leaf Angle Distributions used.

| LAD | 5° | 15° | 25° | 35° | 45° | 55° | 65° | 75° | 85° |
|---|---|---|---|---|---|---|---|---|---|
| Spherical | 0.015 | 0.045 | 0.074 | 0.100 | 0.123 | 0.143 | 0.158 | 0.169 | 0.174 |
| Extremophile | 0.216 | 0.167 | 0.092 | 0.026 | 0.000 | 0.026 | 0.092 | 0.167 | 0.216 |
| Plagiophile | 0.007 | 0.056 | 0.130 | 0.196 | 0.222 | 0.196 | 0.130 | 0.056 | 0.007 |
| Erectophile | 0.002 | 0.015 | 0.040 | 0.073 | 0.111 | 0.149 | 0.183 | 0.207 | 0.221 |
| Planophile | 0.221 | 0.207 | 0.183 | 0.149 | 0.111 | 0.073 | 0.040 | 0.015 | 0.002 |
| Uniform | 0.111 | 0.111 | 0.111 | 0.111 | 0.111 | 0.111 | 0.111 | 0.111 | 0.111 |

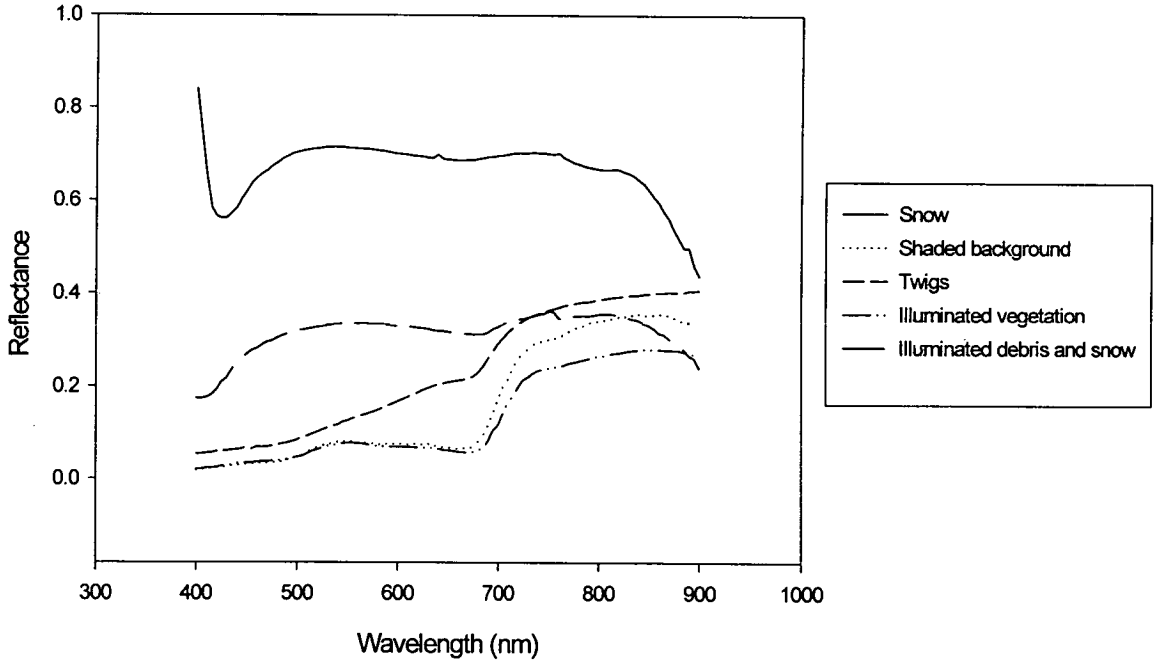


**Figure 5.3** Background reflectances used in SAIL model simulations .

## 5.3 RESULTS

### EFFECT OF SOLAR ZENITH ANGLE

The influence of changing solar zenith angle on PRI shown in Figure 5.4.

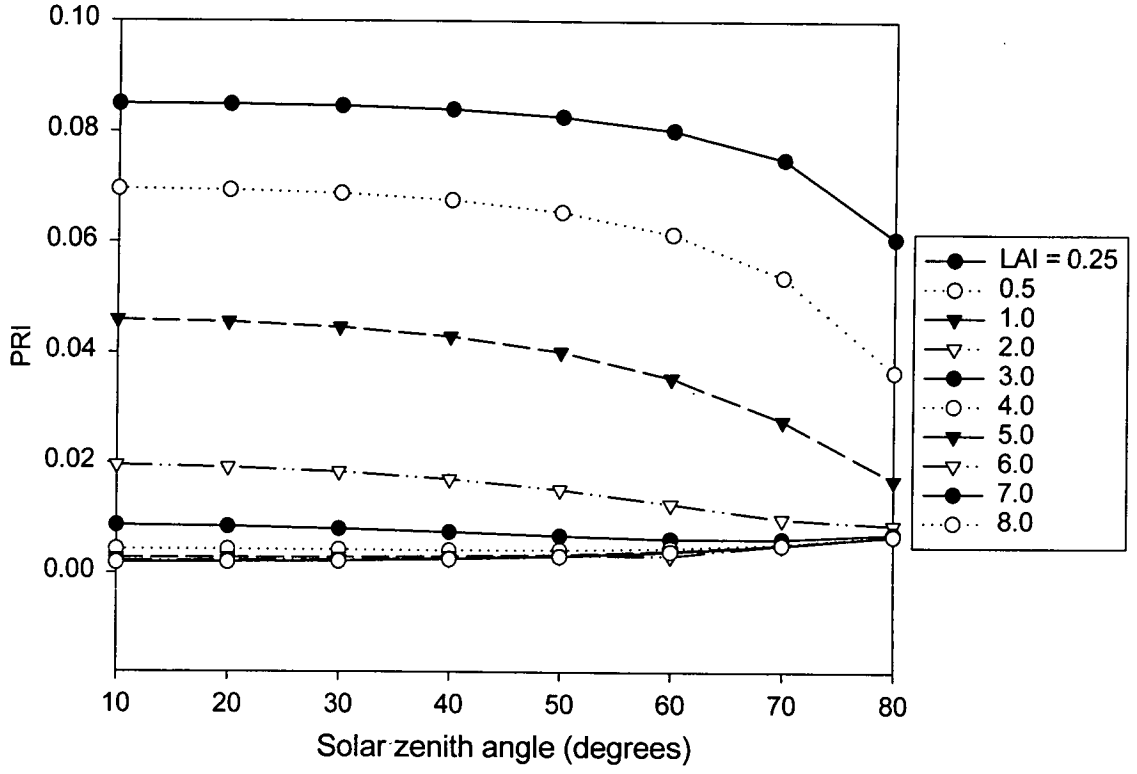


**Figure 5.4** Photochemical Reflectance Index PRI variations as a function of solar zenith angle and Leaf Area Index (LAI). A simulation using the SAIL model. Spherical leaf angle distribution. Leaf optics and soil reflectance held constant.

At high canopy cover (LAI 3-8), PRI showed little sensitivity to changing solar zenith angle up to 60° (Figure 5.4). Beyond this there was a slight increase in PRI for solar angles of 70 and 80°, but this change was marginal. However at intermediate LAIs (0.25-3) PRI was more sensitive to LAI (and probably background) than solar angle. This is apparent by the flat response in PRI over the range 10 - 50°. Beyond

50°, there was a slight increase in PRI. A decrease in PRI was evident at low to intermediate LAI beyond 50°. Clearly the influence of solar angle was more prominent at low canopy cover.

**Effect of background reflectance**

The influence of contrasting backgrounds to total scene PRI is given in Figure 5.5. At low values of LAI, there is a noticeable influence of background reflectance. For a constant LAI of 2, for example, PRI varies by 15% between backgrounds of illuminated moss and snow. Beyond an LAI of 4 however, the canopy is closed sufficiently to minimise interference from the understorey.

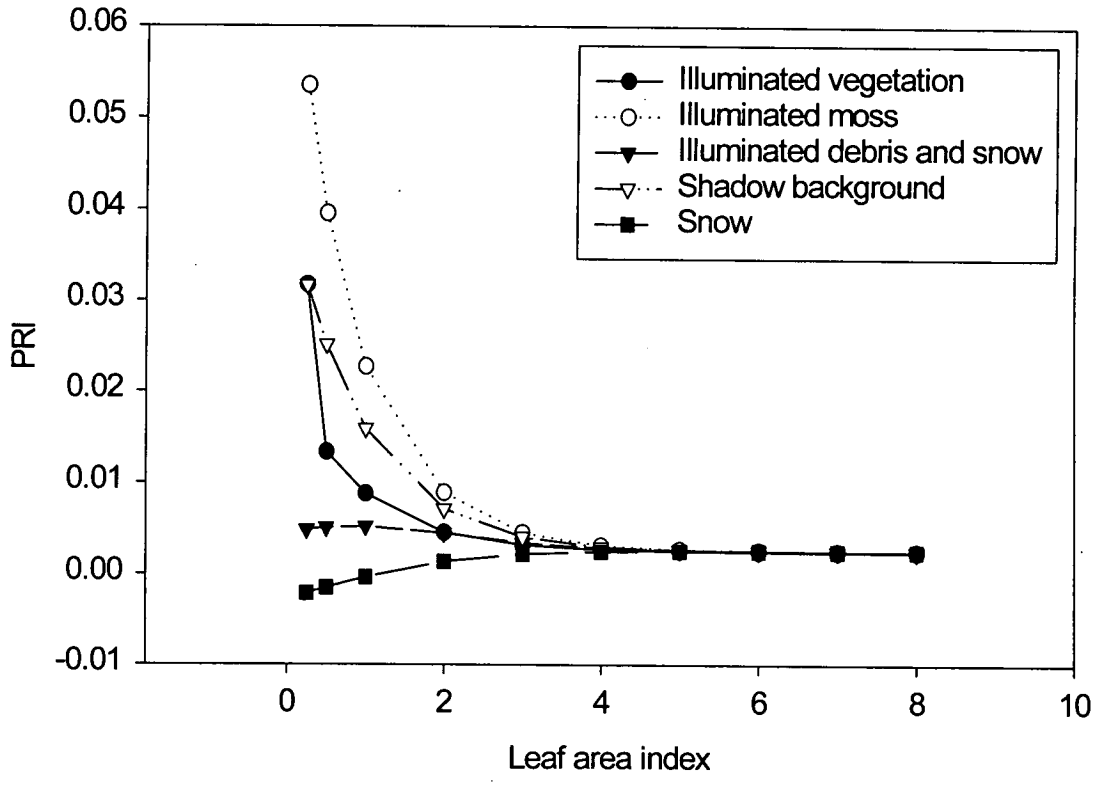


**Figure 5.5** Variations in the Photochemical Reflectance Index (PRI) with changing background reflectance properties. Leaf Area Index values range from 0.25 to 8. Spherical leaf angle distribution and leaf optics held constant.

## EFFECT OF CANOPY STRUCTURE

The effect of differing leaf angle distributions on scene PRI was investigated and is shown in Figure 5.6. The LADs considered here include spherical, with leaf angle frequency the same as for surface elements of a sphere, planophile, with horizontal leaves most frequent, extremophile, with oblique leaves least frequent, plagiophile, with oblique leaves most frequent, erectophile, with vertical leaves most frequent, and uniform, with the same proportion of leaves at all angles.

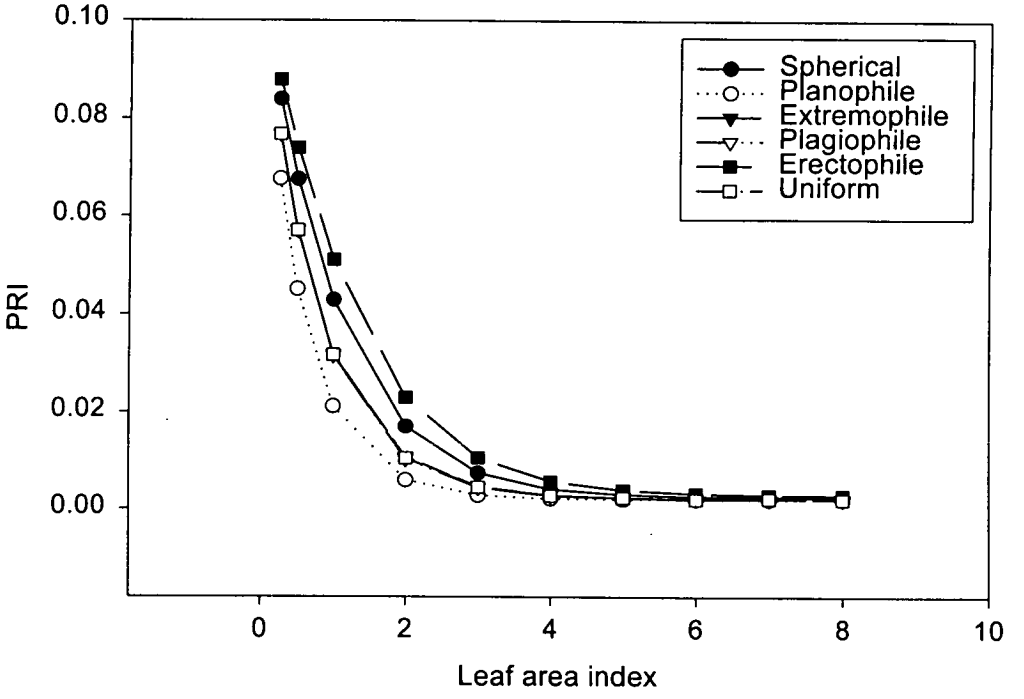


**Figure 5.6** PRI as a function of changing leaf angle distribution with LAI values ranging from 0.25 to 8. Leaf optics and soil reflectance held constant.

The effect of varying LAD on PRI was, again, influenced by canopy cover. At low to intermediate values of LAI (0.25 - 4), PRI values were within 30 % of each other. Out of all LADs analysed, the planophile distribution exhibited the lowest values of PRI and was less sensitive to the background than the erectophile for the same leaf area. That is, the response of PRI to LAI for a given LAD was the least when the

canopy consisted of flat leaves. However, when LAI was high enough, the LAD had little influence on a calculation of PRI.

### EFFECT OF NON-GREEN MATERIAL

The inclusion of twigs in the model is shown in Figure 5.7.The presence of non-green material only influenced PRI when LAI was low enough such that the twigs and background were the dominating reflectance feature. However, when the model was run without twigs, and thus only varying LAI, there was very little between the two sets of PRI values.

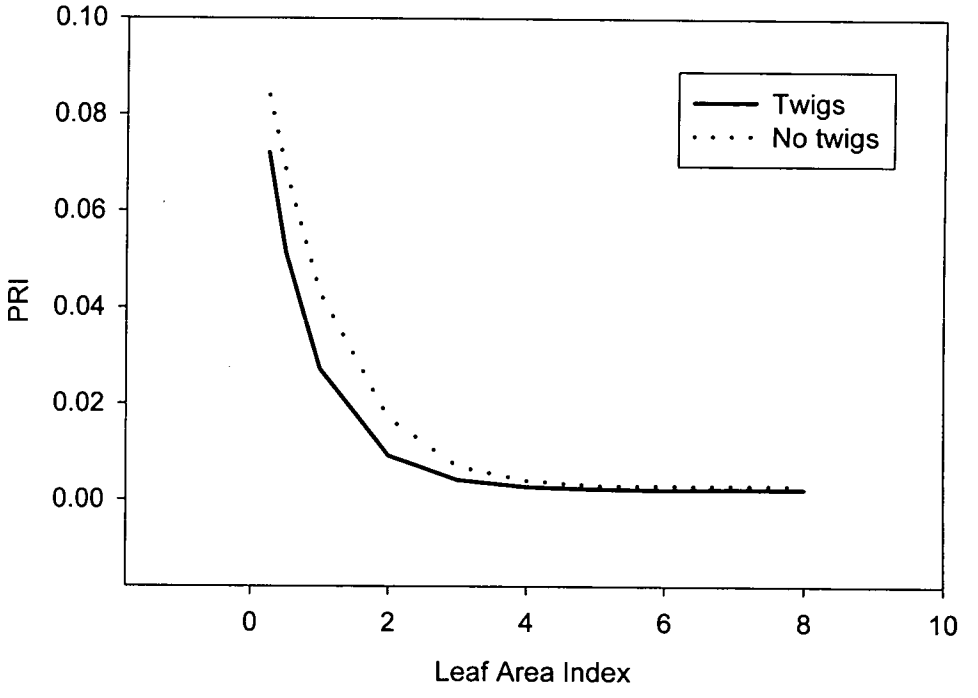


**Figure 5.7** Photochemical Reflectance Index (PRI) variations as a function of changing twig area. A simulation using the SAIL model. Spherical leaf angle distribution. Leaf optics and soil reflectance held constant.

**EFFECT OF IRRADIANCE QUALITY**

The effect of changing irradiance quality can be seen in Figure 5.8. At low values of LAI (incomplete canopy) there was clearly a strong influence of background reflectance, and little influence of changing the proportion of direct versus diffuse light, as indicated by the flat response over the range of LAIs. This was also the case at high canopy coverage where PRI was also flat across the range of LAI values simulated. The main factors influencing PRI were thus a combination of the LAI and background optical properties. With an incomplete canopy (LAI 0.25- 4), PRI varied by as much as 80%. Differences in PRI (for a constant LAI) with changing fraction of direct versus diffuse light varied only by ~ 5 %.

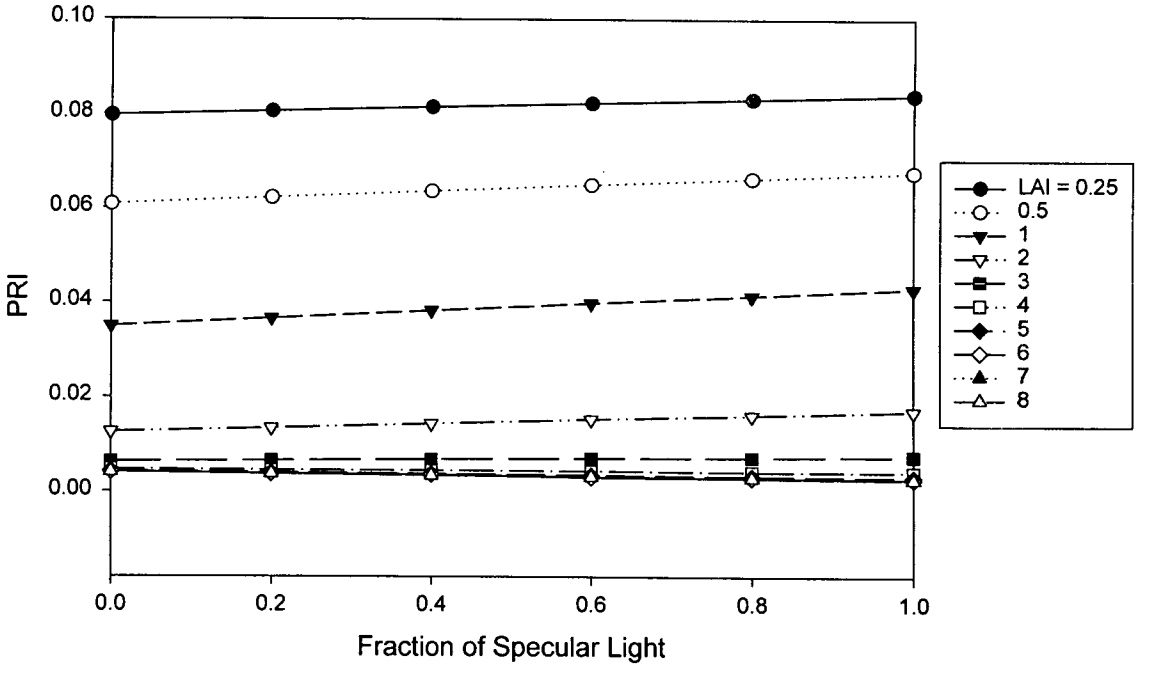


**Figure 5.8** Photochemical Reflectance Index (PRI) variations as function of the fraction of direct incident flux and leaf area index (LAI). A simulation using the SAIL model. Spherical leaf angle distribution. Leaf optics and soil reflectance held constant.

**EFFECT OF VIEW ZENITH AND AZIMUTH**

In this analysis the view angles were varied up to ± 60° from nadir, capturing the reflectances in the forward and backward scattering directions. The angles sampled were limited to ± 60° because currently there is no space-borne sensor that can view beyond these angles. For example, the AVHRR views around ± 60° from nadir. However, because the SAIL model has limitations when calculating the bidirectional specular scattering, the results presented here will not fully represent the problems encountered in off-nadir viewing (Deering, 1988).

The values of PRI in the forward scatter for a given LAI were consistently higher than those measured in the backscatter direction (Figure 5.9). For LAIs of 0.25 - 2 PRI was relatively constant across the view angles simulated in the forward scatter direction. At high canopy LAI there was a decrease in PRI as the view angle moved away from nadir.

For low LAIs in the backscatter direction there was a distinct decrease in PRI as the view angle moved away from nadir. However, at high LAIs PRI was insensitive to changing the view angle of the sensor, with a flat response across evident across the view angles simulated.

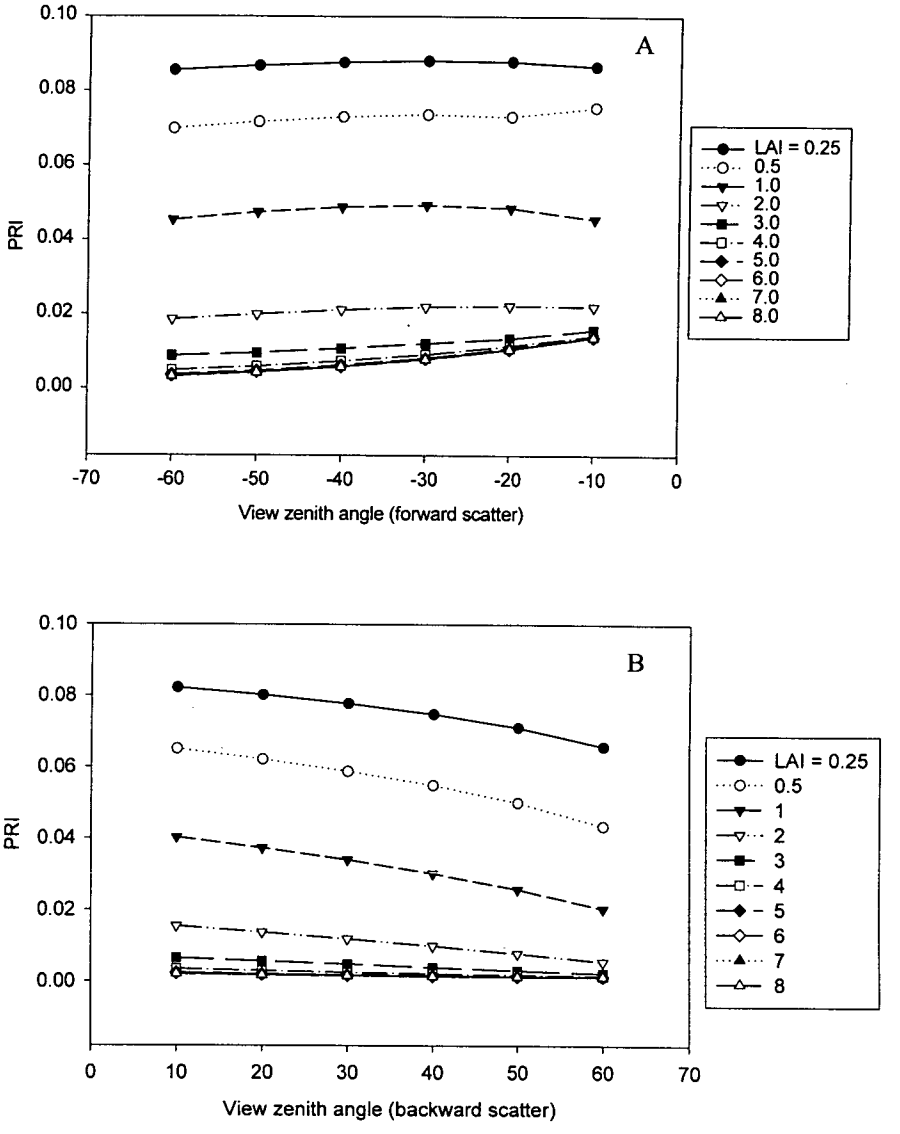


**Figure 5.9** Photochemical Reflectance Index (PRI) variations as a function of view zenith angle and leaf are index (LAI). View azimuth angle is in the principle plane. Positive angles indicating backward scattering (A), negative angles indicate forwardscattering (B). Spherical leaf angle distribution. Leaf optics and soil reflectance held constant.

## 5.3 DISCUSSION

Needle reflectance and transmittance data and background reflectance values were combined in the SAIL model to study the effects of extraneous factors on canopy reflectance. A number of authors have utilised this model for investigating the sensitivity of canopy reflectance and vegetation indices to the effects of background reflectance, canopy structure and Sun-sensor geometry (Goward and Huemmrich, 1992, Huemmrich, 1995, Weiss *et al.*, 2000). A combination of data collected during BOREAS in conjunction with a baseline data set (described in Table 1 and Figure 5.1) provided the means to investigate the sensitivity of PRI to a number of background variables.

From the results presented here, changing solar zenith angle, background reflectance, leaf angle distribution, non green material, and view zenith angles all lead to changes in canopy PRI for a given canopy structure. One feature common throughout was the influence of these factors at low values of LAI. For incomplete canopies, all of the above variables had a significant effect on canopy PRI with the most pronounced effects being for a changing solar zenith angle and background reflectance.

The surface reflectance of continuous vegetation changes in brightness with view angle, but shows a relatively small spectral shift (North *et al.*, 1999). Thus, any normalised vegetation index should show smaller angular variation than that of individual bands. However, when a sensor is at nadir there will invariably be a greater interference of background components such as soil (Gemmel and McDonald, 2000). In addition to interference from background components, it has been suggested that PRI may show greater angular variation with view zenith angle over other vegetation indices. This has been attributed to the fact that leaves viewed at different locations in the canopy will have different spectral responses based on the illumination they receive (Barton and North, *in press*). Thus, greater variation

could be expected with changing view angle for PRI as the sensor will be seeing leaves illuminated at different intensities at each angle. The results presented here do not show the expected variation with view angle, but this can probably be attributed to the lack of representation of scattering at off-nadir angles.

The difference in reflectance between the two wavebands used to calculate PRI is in the order of ~ 2%. Thus, the index may potentially be influenced by other sources which show a contrast in their spectral signal in this region. PRI is particularly sensitive to LAI because of the contrast in reflectance between the understorey and overstorey components. PRI of a dense green canopy in this instance is around 0.01. Of the backgrounds used in this study PRI varied greatly with shaded background (0.04), illuminated vegetation (0.02) and illuminated debris and moss (0.004). The likelihood that these backgrounds will influence PRI are determined by the probability that the sensor views a gap in the canopy. The probability that that the sensor will find a gap in the canopy will decrease with increasing view zenith angle, and so the effect of background reflectance being "seen" by the sensor will be a function of both solar zenith angle and view angle, LAD and LAI. The results here support this conclusion as do findings from Barton and North (*in press*). Thus significant error could be introduced into a computation of PRI in open canopies where the understorey dominates the reflectance of the scene. This could degrade the PRI : LUE relationship.

In relation to previous considerations, the influence of LAD, solar zenith angle and view angle are interrelated. The angle of the leaf normal relative to the sun will determine the intensity of light received at the leaf surface, and will influence the PRI and LUE of that leaf. The angle of this leaf relative to the sensor angle will determine the strength of the signal. Influence of LAD on canopy PRI has been found to be significant when the canopy was incomplete but when the canopy was closed, LAD have a significant effect. A modelling study by Barton and North (*in*

*press*) found that PRI was highly sensitive to LAD and sensor view zenith angles. This was particularly the case for extreme solar zenith angles (i.e. > 50°).

One factor likely to have an impact on remote sensing in this spectral region, but not considered in this analysis, is the influence of the atmosphere. As discussed in Chapter 4, the two wavebands used in the calculation of PRI will be affected by atmospheric scattering (Rayleigh) with the somewhat shorter wavelength representative of the xanthophyll cycle (530 nm) being influenced more than the reference waveband (570 nm). This means that when viewed from the top of the atmosphere PRI will be smaller than PRI measured metres above the canopy. The influence of aerosol scattering and absorption will not be so considerable because the wavebands are relatively close (~ 40nm) and the effect is likely to be same over the two wavebands (Barton and North, *in press*).

Depending on the remote sensing application, some but not all of the factors considered will come into play when investigating the relationship between PRI and LUE. For example, if the object of the exercise is to estimate LUE for a given ecosystem on a spatial rather than temporal scale, issues of canopy structure and background reflectance will present the obvious problems. If the canopy is closed, diurnal measurements of PRI will track the canopies response to changing Sun angle accordingly as presented earlier in this thesis (Chapter 4) and by Gamon *et al.*, (1992). At low canopy LAI however the issue of canopy structure will have to be resolved as background reflectances dominate the reflectance of the scene, through the effect of increasing or decreasing the scenes PRI value and causing a divergence in the relationship between the vegetation index and variable of interest.

A further issue to consider is the time response of de-epoxidation of the xanthophyll cycle. Gamon *et al.*, (1990) has shown that the onset of the signal is apparent in the spectra after 2 minutes, with 40 minutes being the time taken to reach the minimum reflectance (i.e. full de-epoxidation). Variations in illumination occur on smaller

timescales which may weaken the PRI : LUE relationship, depending on the time interval that measurements are taken.

The model used in this analysis approximates the reflectance of a horizontally homogeneous canopy. This assumption would not hold however for forest canopies where foliage is clumped and shadows cast. Although clearly not the optimal model for such a forest application, it was, at the time of analysis, the model that was most easily accessible

The output from SAIL can however be used in geometric-optical models which allows the landscape to be manipulated and investigation of such effects to be carried out. Although the model produces a reasonable approximation of homogeneous canopy reflectance, "hot spot" and low zenith angle patterns are poorly represented because no specular reflectance characteristic is included in the canopy or soil background. However, the model does generate reflectances of homogeneous canopies in the field (Goel, 1988, Jacquemond *et al.*, 1993, Weiss *et al.*, 2000), the purpose for which is was designed.

More powerful models that simulate canopy reflectance have become available in the past four years. An example of this is the FLIGHT model (North, 1996), and others, as discussed in Chapter 1. It calculates light interception and bidirectional reflectance using a Monte Carlo evaluation of photon transport. It also includes leaf scattering functions which allow the relations between the leaf surface and the light field to be simulated, which implicitly allows sunlit and shade leaves to be accommodated. The work carried out in this study using the SAIL model was conducted prior to the emergence of a number of these more powerful canopy models. Future work investigating the sensitivity of PRI will undoubtedly see these more recent models used.

## 5.4 CONCLUSIONS

Measured reflectances of needles and various backgrounds were incorporated into SAIL and the sensitivity of PRI calculated from the simulated canopy reflectance to extraneous variables was investigated.

The results showed PRI to be sensitive to a number of factors particularly when canopy cover was low (LAI $< 3$). These included solar zenith angle, view angle, LAD, and background reflectance. Because the influence of background reflectance at low LAI is so strong, the issue of canopy structure will have to be resolved if PRI is to be successfully applied over sparse canopies.

Further work is also warranted to assess the influence of such variables on PRI in more complex three-dimensional canopies.

# 6. GENERAL CONCLUSIONS

The general aim of this thesis was to explore the relationship between the light-use-efficiency of photosynthesis and the status of the xanthophyll cycle as assessed by remote sensing. The results in Chapter 2 confirmed that PRI is a useful indicator of photosynthetic LUE of individual leaves grown in a glasshouse under controlled conditions of temperature and light (Figure 2.4A and B). The application of PRI over forest canopies had not yet been investigated, and as such, was a key question addressed in this thesis. In the work reported in this thesis, it was possible to investigate PRI in boreal forests in two continents.

The BOREAS project was an international investigation implemented to improve the understanding of the interactions between the boreal forest and the atmosphere. A large data set emerged with remotely sensed measurements of Canadian boreal forest at a range of spatial and spectral scales. An intensive network of eddy covariance towers was also in operation monitoring forest $CO_2$ fluxes which provided a means to calculated a canopy LUE. This offered the opportunity to investigate the relationship between PRI and LUE over boreal forest where measurements of canopy reflectance and gas exchange were made at identical spatial scales.

$PRI_{SE\text{-}590}$ was calculated from spectral reflectance data collected from a helicopter-mounted spectroradiometer and correlated with LUE, calculated from eddy covariance measurements of $CO_2$ fluxes. Good correlations were found between $PRI_{SE\text{-}590}$ and LUE demonstrating that $PRI_{SE\text{-}590}$ is a useful indicator of forest LUE (Figure 3.3). This provided the first evidence that LUE could be estimated from PRI at the landscape scale.

This question was further addressed in the boreal forests of Siberia where a similar campaign was conducted. $PRI_{HELI}$ was calculated from spectral measurements made over four canopies from a helicopter platform and eddy covariance data were used to

calculate forest LUE. The campaign was conducted when the forest was coming out of winter dormancy from May to June 2000 when the forest was under considerable stress from low temperatures and high light. The results presented in Chapter 4 (Figures 4.4, 4.7, 4.9) also showed that $PRI_{HELI}$ correlated with LUE, although the strength of the relationship compared to that found in the Canadian forests was weaker. It is likely that factors such as background reflectance, a wide range of LAI values and the lack of an atmospheric correction all played a part in weakening the relationship between LUE and $PRI_{HELI}$. At low LAI, the canopy LUE is very low and PRI is the result of a combination of canopy and background reflectances. As LAI increases the LUE increases and PRI falls to a point whereby PRI is insensitive to a further change in LAI (Figure 5.7, Chapter 5). Thus at low LAI, PRI is sensitive to changing LAI and background reflectances. Because the values of LAI in Siberia were below 2, but greater than 3 in all Canadian sites, it is likely that PRI was detecting the change in LAI rather than LUE. The modelling results in Chapter 5 further highlighted the sensitivity of canopy PRI to changing variables.

PRI is capable of providing an estimate of forest LUE, although where canopies are sparse and understorey reflectances strong, as was found in Siberia, serious errors may be introduced into the calculation of PRI causing a divergence between PRI and LUE. Thus improvement of the sensitivity of this index is paramount if it is to be successfully applied across ecosystems and vegetation types.

The results in this thesis however are the first of their kind to relate PRI to LUE over forests. And whilst in certain situations PRI works well, a number of factors must be addressed if this index is to be applied across ecosystems successfully where canopy types are markedly different and understorey reflectances dominant. Routine measurement of the reflectance of forest canopies from eddy covariance towers would permit the interpretation of PRI over a number of contrasting canopies and understorey vegetation. Then it will be possible to determine whether the influence of background reflectance will need to be corrected for using site specific

information. This is an attractive possibility as it avoids the costs that are associated with aircraft campaigns.

The results presented in the preceding chapters have thus addressed some important questions concerning the remote sensing of physiological processes. The ability to probe directly the processes involved in photosynthesis using the spectral information of vegetation at 530 nm will undoubtedly continue to offer possibilities for measuring landscape scale processes. A sound understanding of the factors that influence PRI will also pave the way for refining this index such that its application can span across ecosystems and vegetation types.

The development of new satellites, remote sensing instruments and techniques will also provide access to data of high spectral and spatial resolution. Currently, of the systems carried on satellite and aircraft, there are a number of potentially useful sensors that should be useful for calculating a meaningful PRI. The Hyperion Instrument, carried on the EO-1 (Earth Observation) spacecraft, the Moderate Resolution Imaging Spectrometer (MODIS) which is carried aboard the EOS-AM and PM satellites and the MEdium Resolution Imaging Spectrometer (MERIS). MERIS is due to be launched in 2001 aboard the European ENVISAT satellite will generate global data sets with a spatial resolution of 300m and spectral resolution (of programmable wavebands) of 1.8 nm.

Of the sensors carried on aircraft, the Airborne Visible Infrared Imaging Spectrometer (AVIRIS) which is carried on the NASA ER-2 aircraft and the Compact Airborne Imaging Spectrometer (CASI), also carried aboard an aircraft should prove useful for determination of PRI.

### LINKING THE RESULTS TO MODELS

The issue of background reflectance and its effect on scene reflectance, and PRI, will be best investigated through the use of radiative transfer models. Little work has

been carried out to investigate the sensitivity of PRI to background reflectances (Chapter 5 and Barton and North, *in press*), and as such, a model such as FLIGHT (North, 1996) (and others discussed in Chapter 1) would be suitable for this task. It calculates canopy light interception and bidirectional reflectance using Monte Carlo evaluation of photon transport (Disney *et al.*, *in press*). The scene modelled by FLIGHT can be used to construct a large number of possible scenes and can be used at a variety of scales from continuous vegetation to detailed stand. Thus, by introducing variability into model runs, a large database of scene visualisations and their associated reflectance values could be generated and thereby a corresponding value of PRI for each scene.

The Farquhar model of photosynthesis is used in many forest models, including HYDRALL (Magnani, Mencuccini and Grace, 2000). HYDRALL is driven by climatological data, typically by those generated by global circulation models. It photosynthesises and "grows" in relation to the climate and water supply. The photosynthetic submodel consists of the Farquhar equations and a representation of stomatal response to the environment. However, the xanthophyll cycle is not represented in the photosynthesis model itself. It could be possible to utilise PRI measurements to modify the photosynthetic sub-model such that it could lead to a more realistic simulation of photosynthesis rates under conditions of high irradiance.

Ultimately, extending small-area techniques to large areas involves a number of challenges that can only be addressed with both theoretical and empirical studies at a range of scales. Remote sensing has led to importance advances in our understanding of photosynthesis and continues to offer exciting prospects for the future.

# BIBLIOGRAPHY

Adams, W. W., and Demmig-Adams, B. (1992) Operation of the xanthophyll cycle in higher plants in response to diurnal changes in incident light. *Planta* **186** : 390-398.

Adams, W. W., Demmig-Adams, B. (1994) Carotenoid composition and down regulation of photosystem II in three conifer species during the winter. *Physiologia Plantarum* **92** : 451-458.

Alexander, L. (1983) *SAIL Canopy Model Fortran Software.* Lyndon B. Johnson Space Center, NASA Technical Report JSC – 18899, Houston, Texas.

Andrieu, B., Baret, F., Jacquemoud, S., Malthus, T. and Steven, M. (1997) Evaluation of an improved version of SAIL Model for simulating bidirectional reflectance of sugar beet canopies. *Remote Sensing of Environment* **60** : 247-257.

Asner, G. P. (1998) Biophysical and biochemical sources of variability in canopy reflectance. *Remote Sensing of Environment* **64** : 234-253.

Asner, G. P., Wessman, C. A. and Schimel, D. S. and Archer, S. (1998b) Variability in leaf and litter optical properties: implications for BRDF model inversions using AVHRR, MODIS and MISR. *Remote Sensing of Environment* **63** : 243-257.

Asrar, G. (1989) *Theory and Applications of Optical Remote Sensing,* John Wiley & Sons, New York.

Asrar, G., Myneni, R. B. and Choudhury, B. J. (1992) Spatial heterogeneity in vegetation canopies and remote sensing of absorbed photosynthetically active radiation : a modelling study. *Remote Sensing of Environment* **41** : 85-103.

Aubinet, M., Grelle, A., Ibrom, A., Rannik, U., Moncrieff, J., Foken, T., Kowalski, A. S, Martin, P. H., Berbigier, P., Bernhofer, C., Clement, R., Elbers, J., Granier, A., Grunwald,T., Morgenstern, K., Pilegaard, K., Rebmann, C., Snijders, W., Valentini, R., Vesala, T. (2000) Estimates of the annual net carbon and water exchange of forests: The EUROFLUX methodology. *Advances in Ecological Research* **30**: 113-175.

Baldocchi, D. D., Vogel, C. A. and Hall, B. (1997) Seasonal variation of energy and water vapour exchange rates above and below a boreal jack pine forest canopy. *Journal of Geophysical Research* **102** : 28,939-28,951.

Baret, F. and Guyot, G. (1991) Potential and limits of vegetation indices for LAI and APAR assessment. *Remote Sensing of Environment* **35** : 161-173.

Barton, C. V. M. and North, P. R. J. A modelling study of the relationship between the Photochemical Reflectance Index and light use efficiency. Scaling from leaf to canopy. *Remote Sensing of Environment. (in press).*

Beck, E., Hansen, J., Heim, R., Schafer, Vogg, G., Leborgne, N., Teulieres, C and Boudet, A. M. (1995) Cold hardening and dehardening of evergreen trees. In: Sandermann, H, Bonnet-Masimbert, M (Eds) *EUROSILVA – Contribution to Forest Tree Physiology*. INRA Editions No 76, Paris, France. pp 171-193

Bilger, W., Bjorkman, O. and Thayer, S. S. (1989) Light induced spectral absorbance changes in relation to photosynthesis and the expoxidation state of xanthophyll cycle components in cotton leaves. *Plant Physiology* **91** : 542-551.

Bjorkman, O and Demmig, B. (1987) Photon yield of $O_2$ evolution and chlorophyll fluorescence characteristics at 77 K among vascular plants of diverse origins. *Planta* **170** : 489-504.

Bjorkman, O. and Demmig-Adams, B. (1994) Regulation of photosynthetic light energy capture, conversion and dissipation in leaves of higher plants. In: Schulze E-D, Caldwell, M. M. (Eds) Ecophysiology of Photosynthesis. Ecological Studies 100. Springer, Berlin Heidelbeig New York, pp 17-47.

Blanken, P. D., Black, T. A., Yang, P. C., den Hartog, G., Neumann, H. H., Nesic, M. D,. Novak, R., Staebler, R. and Lee, X. (1997) Energy balance and canopy conductance of a boreal aspen forest: partitioning overstorey and understorey components. *Journal of Geophysical Research* **102** : 28, 915 – 28, 927.

Bloom, A. J., Calswell, R. M., Finazzo, J., Warner, R. L. and Weissbart, J. (1989) Oxygen and carbon dioxide fluxes from barley shoots depends on nitrate assimilation. *Plant Physiology* **91** : 352-356.

Bonan, G. B. (1993) Importance of leaf area index and forest type when estimating photosynthesis in boreal forests. *Remote Sensing of Environment* **43** : 303-314.

Brugnoli, E. and Bjorkman, O. (1992) Chloroplast movements in leaves: Influence on chlorophyll fluorescence and measurements of light-induced absorbance changes related to $\Delta$pH and zeaxanthin formation. *Photosynthesis Research* **32** : 23-35.

Chen, J. M. (1996) Evaluation of vegetation indices and a modified simple ratio for boreal applications. *Canadian Journal of Remote Sensing* **22** : 229-242.

Ciais, P, Tans, P. P, Trolier, M., White, J. W. C. and Francey, R.J. (1995) A large northern hemisphere terrestrial $CO_2$ sink indicated by 13C/12C of atmospheric $CO_2$. *Science* **269** : 1098-1102.

Cuenca, R. H., Stangel, D. E. and Kelley, S. F. (1997) Soil water balance in a Boreal forest. *Journal of Geophysical Research* **102** : 29,935-29,365.

Curran, P. J. (1983) Mulitspectral remote sensing for the estimation of green leaf area index. *Philosophical Transactions of the Royal Society Series A* **309** : 257-270.

Curran, P. J., Dungan, J. L., Macler, B. A., Plummer, S. E. and Peterson, D. L. (1992) Reflectance spectroscopy of fresh whole leaves for the estimation of chemical concentration. *Remote Sensing of Environment* **39** : 153-166.

Curran, P. J., Dungan, J, L. and Gholtz, H. L. (1992) Seasonal LAI in slash pine estimated with Landsat TM. *Remote Sensing of Environment* **39** : 3-13.

Dawson, T. P., Curran, P. J. and Plummer, S. E. (1998) LIBERTY – Modelling the effects of leaf biochemical concentration on reflectance spectra. *Remote Sensing of Environment* **65** : 50-60.

Dawson, T. P., Curran, P .J., North, P, R. J. and Plummer, S. E. (1999) The propagation of foliar biochemical absorption features in forest canopy reflectance: A theoretical analysis. *Remote Sensing of Environment* **67** : 147-159.

Deering, D. W. (1988) PARABOLA directional field radiometer for aiding in space sensor data interpretation, in *Recent Advances in Sensors, Radiometry, and Data Processing for Remote Sensing,* Society of Photo-Optical Instrumentation Engineers, pp 249-261.

Deering, D. W., Eck, T. F, and Banerjee, B. (1999) Characterisation of the reflectance anisotropy of three boreal forest canopies in spring-summer. *Remote Sensing of Environment* **67** : 203-229.

Demmig-Adams, B (1990) Carotenoids and photoprotection in plants: a role for the carotenoid zeaxanthin. *Biochimica et Biophysica Acta* **1024** : 1-24.

Demmig-Adams, B. and Adams, W. W. (1990) The carotenoid zeaxanthin and "high-energy state quenching" of chlorophyll fluorescence. *Photosynthesis Research* **25** : 187-197.

Demmig-Adams, B. and Adams, W. W. (1992) Photoprotection and other responses of plants to light stress. *Annual Review of Plant Physiology and Molecular Biology.* **43** : 599-626.

Demmig-Adams, B and Adams, W. W. (1993) The xanthophyll cycle. In: Young, A. and Britton, G. (Eds) Carotenoids in Photosynthesis. Chapman and Hall, London. pp 206-251.

Demmig-Adams, B and Adams, W. W. (1994) Capacity for energy dissipation in the pigment bed in leaves with different xanthophyll cycle pools. *Australian Journal of Plant Physiology* **21** : 575-588.

Demmig-Adams, B, Adams, W. W., Logan, B. A. and Verhoeven, A. S. (1995) Xanthophyll cycle-dependent energy dissipation and flexible PS II efficiency in plants acclimated to light stress. *Australian Journal of Plant Physiology* **22** : 249-261.

Demmig-Adams, B., Gilmore, A. M. and Adams, W, W III. (1996) In vivo functions of carotenoids in higher plants. *Federation of the American Society of Experimental Biology Journal* **10** : 403-412.

Demmig-Adams, B., and Adams, W. W. (1996) The role of xanthophyll cycle carotenoids in the protection of photosynthesis. *Trends in Plant Science* **1** : 21-26.

Demmig-Adams, B., and Adams, W. W. (1996) Xanthophyll cycle and light stress in nature: uniform response to excess direct sunlight among higher plant species. *Planta* **198** : 460-470.

Demmig-Adams, B. (1998) Survey of thermal energy dissipation and pigment composition in sun and shade leaves. *Plant Cell and Environment* **39** : 474-482.

Demmig-Adams, B, Moeller, D. L., Logan, B. A. and Adams, W. W (1998) Positive correlation between levels of zeaxanthin + antheraxanthin and degree of photoinhibition in shade leaves of *Schefflera arboricola* (Hayata) Merrill. *Planta* **205** : 367-374.

Disney, M. I., Lewis, P. and North (*in press*) Monte Carlo ray tracing in optical canopy reflectance modelling. *Remote Sensing Reviews*.

Fassnacht, K, S., Gower, S. T., MacKenzie, M. D., Nordheim, E. V. and Lillesand, T. M. (1997) Estimating the Leaf Area Index of north central Wisconsin forests using Landsat Thematic Mapper. *Remote Sensing of Environment* **61** :229-245.

Field, C.B., Behrenfield, M. J., Randerson, J.T. and Falkowski, O. (1998) Primary production of the biosphere. Integrating terrestrial and oceanic components. *Science* **281** : 237-240.

Fillela, I., Amaro, J. L. and Penuelas, J. (1996) Relationship between photosynthetic radiation-use efficiency of barley canopies and the photochemical reflectance index (PRI). *Physiological Plantarum* **96** : 211-216.

Fourty, Th., Baret, F., Jacquemond, S., Schmuck, G. and Verdebout, J. (1996) Leaf optical properties with explicit description of its biochemical composition: direct and inverse problems. *Remote Sensing of Environment* **56** : 104-117.

Frank, H. A., Cua, A., Chynwat, V., Young, A., Gosztola, D. and Wasielewski, M. R. (1994) Photophysics of the carotenoids associated with the xanthophyll cycle in photosynthesis. *Photosynthesis Research* **41** : 389-395.

Gallow, K. P. and Daughtry, C. S. T. (1986) Techniques for measuring intercepted and absorbed photosynthetic active radiation in corn canopies. *Agronomy Journal* **85** : 752-756.

Gamon, J. A., Field, C. B., Bilger. W., Bjorkman, O., Freeden, A. and Penuelas, J. (1990) Remote sensing of the xanthophyll cycle and chlorophyll fluorescence in sunflower leaves and canopies. *Oecologia* **85** : 1-7.

Gamon, J. A., Fillela, I. and Penuelas, J. (1993) The dynamic 531 nanometer Δ reflectance signal: a survey of 20 angiosperm species. *Current Topics in Plant Physiology* **8** : 172-177.

Gamon, J. A., Penuelas, J. and Field, C. B (1992) A narrow waveband spectral index that tracks diurnal changes in photosynthetic efficiency. *Remote Sensing of Environment* **41** : 35-44.

Gamon, J, A, Field, C. B., Goulden, M., Griffin, K., Hartley, A., Joel, G., Penuelas, J. and Valentini, R. (1995) Relationships between NDVI, canopy structure and photosynthetic activity in three Californian vegetation types. *Ecologicial Applications*. **5** : 28-41.

Gamon, J. A., Serrano, L. and Surfus, J. S. (1997) The photochemical reflectance index: an optical indicator of photosynthetic radiation use efficiency across species, functional types, and nutrient levels. *Oecologia* **112** : 492-501.

Gemmell, F. and McDonald, A. J (2000) View zenith angle effects on the forest information content of three spectral indices. *Remote Sensing of Environment* **72** :139-158.

Genty, B., Briantais, J. M. and Baker, N. R. (1989) The relationship between the quantum yield of photosynethetic electron transport and photochemical quenching of chlorophyll fluorescence. *Biochimica et Biophysica Acta* **990** : 87-92.

Gilmore, A. M. and Yamamoto, H. Y. (1991) Resolution of lutein and zeaxnthin using a nonecapped, lightly carbon-loaded C-18 high performance liquid chromatograph column. *Journal of Chromatography* **543** : 137-145.

Gilmore, A. M. and Yamamoto, H. Y. (1992) Dark induction of zeaxanthin-dependent nonphotochemical fluorescence quenching mediated by ATP. *Proceedings of the National Academy of Sciences* **89** : 1899-1903.

Gilmore, A. M. and Yamamoto, H. Y. (1993) Linear models relating xanthophylls and lumen acidity to non-photochemical fluorescence quenching. Evidence that antheraxanthin explains zeaxanthin-independent quenching. *Photosynthesis Research.* **35** : 67-78

Gilmore, A. M., Mohanty, N. and Yamamoto, H. Y. (1994) Epoxidation of zeaxanthin and antheraxanthin reverses nonphotochemical quenching of photosystem II chlorophyll-*a* fluorescence in the presence of a transthylakoid ΔpH. *FEBS Letter* **350** : 271-274.

Gilmore, A. M. (1997) Mechanistic aspects of xanthophyll cycle-dependent photoprotection in higher plant chloroplasts and leaves. *Physiologia Plantarum* **99** : 197-209.

Goel, N, S. (1988) Models of vegetation canopy reflectance and their use in estimation of biophysical parameters from reflectance data. *Remote Sensing of Environment* **4** : 1-212.

Goulden, M. L., Daube, B. C., Fan, S-M., Sutton, A., Bazzaz, J. W., Munger, S. C. and Wofsy S. C. (1997) Physiological responses of a black spruce forest to weather. *Journal of Geophysical Research.* BOREAS Special Issue **102** 28,987-28,966.

Goward, S. N. and Huemmrich, K. F. (1992) Vegetation canopy PAR absorptance and the Normalised Difference Vegetation Index: An assessment using the SAIL Model. *Remote Sensing of Environment* **39**: 119-140.

Goward, S. N., Huemmrich, K. F. and Waring, R. H. (1994) Visible-near infrared spectral reflectance of landscape components in Western Oregon. *Remote Sensing of Environment* **47** : 190-203.

Goward, S.N. and Dye, D.G. (1996) Global biospheric monitoring with remote sensing. In: Gholtz, H.L., Nakane, K and Shimoda, H. (Eds) *The Use of Remote Sensing in the Modelling of Forest Productivity.* Forestry Sciences 50. Kluwer Academic Publishers, The Netherlands. pp 241-272.

Gower, S. T., Kucharik, C. J. and Norman, J. M. (1999) Direct and indirect estimation of Leaf Area Index, $F_{PAR}$ and Net Primary Production of terrestrial ecosystems. *Remote Sensing of Environment* **70** : 29-51.

Green, R. O., Eastwood, M, L., Sarture, C. M., Chrien, T. G., Aronsson, M., Chippendale, B. J., Faust, J. A., Pavri, B. E., Chovit, C. J., Solis, M., Olah, M. R. and Williams, O. (1998) Imaging spectroscopy and the Airborne Visible/Imaging Spectroradiometer (AVIRIS). *Remote Sensing of Environment* **65** : 227-248.

Guyot, G. (1990) Optical properties of vegetation canopies. In: Steven M. D., Clark J. A, (Eds) *Applications of Remote Sensing in Agriculture.* London, Butterworths, pp 19-44.

Hallgren, J-E., Lundmark, T and Strand, M. (1990) Photosynthesis of Scots pine in the field after night frosts during the summer. *Plant Physiology and Biochemistry* **28** : 437-445.

Hansen, J, Vogg, G. and Beck, E. (1996) Assimilation, allocation and utilisation of carbon by 3-year old Scots pine (*Pinus sylvestris* L.) trees during winter and early spring. *Trees* **11** : 83-90.

Harbison, J., Genty, B. and Baker, N. R. (1990) The relationship between $CO_2$ assimilation and electron transport in leaves. *Photosynthesis Research* **25** : 213-224.

Heber, U. (1969) Conformational changes of chloroplasts induced by illumination of leaves in vivo. *Biochimica et Biophysica Acta* **180**: 302-319.

Hogg, E. H., Black, T. A., den Hartog, G., Neumann, H. H., Zimmerman, R, Hurdle, P,. Blanken, P. D., Nesic, Z., Yang, P. C., Staebler, R. M., McDonald, K. C. and Oren R. (1997) A comparison of sap flow and eddy fluxes of water vapour from a boreal deciduous forest. *Journal of Geophysical Research.* BOREAS Special Issue **102** : 28,929-28,937.

Horton, P. and Ruben, A. V. (1992) Regulation of photosystem II. *Photosynthesis Research* **34** : 375-385.

Horton, P., Ruben, A. V., and Walters, R. G. (1994) Regulation of of light harvesting in green plants. *Plant Physiology* **106** : 415-420.

Huemmrich, K. F. (1995) An Analysis of Remote Sensing of the Fraction of Absorbed Photosynthetically Active Radiation in Forest Canopies. Ph. D.Thesis. University of Maryland, College Park, USA.

Huete, A. R. (1987) Soil and sun angle interactions on partial canopy spectra. *International Journal of Remote Sensing* **8** : 1307-1317.

Huete, A. R. (1998) A comparison of vegetation indices over a global set of TM images for EOS-MODIS. *Remote Sensing of Environment* **59** : 440-451.

Jackson, R.D. (1983) Spectral indices in n-space. *Remote Sensing of Environment* **13** : 1401-1429

Jacquemond, S. and Baret, F. (1990) PROSPECT: a model of leaf optical properties spectra. . *Remote Sensing of Environment* **34** : 75-91.

Jacquemond, S., Baret, F. and Hanocq, J. F. (1992) Modeling spectral and bidirectional soil reflectance. *Remote Sensing of Environment* **41** : 123-132.

Jarvis, P. G., Massheder, J. M., Hale, S. E., Moncrieff, J. B., Rayment, M. B. and Scott, S. L. (1997) Seasonal variation of carbon dioxide, water vapour and energy exchanges of a boreal black spruce forest. *Journal of Geophysical Research* **102** : 28,953-28,966.

Jenson, J. R (1983) Biophysical remote sensing. *Annals of the Association of American Geographers* **73** : 111-132.

Joel, G., Gamon, J. A. and Field, C. B. (1997) Production efficiency in sunflower: the role of nitrogen and water stress. *Remote Sensing of Environment* **62** : 176-188.

Keeling, C.D., Bacastow, R.B., Carter, A. F *et al.* (1989) A three-dimensional model of atmospheric $CO_2$ transport based on observed winds, 1. Analysis of observational data. In: Peterson, D. H. (Ed) *Aspects of Climate Variability in the Pacific and the Western Americas.* Geophysical. Monographs, 55. American Geophysical Union, Washington DC, p 363.

Kimes, D. S. (1980) Vegetation reflectance as a function of solar zenith angle. *Photogrammic Engineering and Remote Sensing* **46** : 1563-1573.

Koniger, M, Harris, G. C., Virgo, A. and Winter, K. (1995) Xanthophyll-cycle pigments and photosynthetic capacity in tropical forest species: a comparative field study on canopy, gap and understorey plants. *Oecologia* **104** : 280-290.

Krause, G. H. (1988) Photoinhibition of photosynthyesis. An evaluation of damaging and protective mechanisms. *Physiologia Plantarum* **74** : 566-574.

Leverenz, J. W. and Oquist, G. (1987) Quantum yields of photosynthesis at high temperatures between – 2°C and 35° C in cold tolerant $C_3$ plant (*Pinus sylvestris*) during the course of one year. *Plant Cell and Environment* **10** : 278-295.

Levitt, J. (1980) *Responses of Plants to Environmental Stresses: Vol 1. Chilling, Freezing and High Temperature Stresses*. Academic Press, New York.

Li, X-P., Bjorkman, O., Shih, C., Grossman, A. R., Rosenquist, M., Jansson, S. and Niyogi, K. K. (2000) A pigment-binding protein essential for regulation of photosynthetic light harvesting. *Nature* **403**: 391-395.

Linder, S. and Troeng, E. (1980) Photosynthesis and transcription of a 20-year old Scots pine. In *Structure and Function of Northern Coniferous Forests – An Ecosystem Study*, Ecological Bulletins, Vol 32. Swedish Natural Science Research Council, Stockholm. pp. 165-181

Long, S. P., Humphries, S. and Falkowski, P. G. (1994) Photoinhibition of photosynthesis in nature. *Annual Review of Plant Physiology and Molecular Biology* **45** : 633-662.

Lloyd, J. and Taylor, J. A. (1994) On the temperature dependence of soil respiration *Functional Ecology* **8** : 315-323.

Ludlow, M. M. and Powles, S. B. (1988) Effects of photoinhibition induced by water stress on growth in yield of grain sorghum. *Australian Journal of Plant Physiology* **15** : 178-194.

Lundmark, T,. Hallgren J-E. and Heden, J. (1988) Recovery from winter depression of photosynthesis in pine and spruce. *Trees* **2** : 110-114.

Martin, B., Martensson, O. and Oquist, G. (1978b) Seasonal effects on photosynthetic electron transport and fluorescence properties in isolated chloroplasts of *Pinus sylvestris*. *Physiologia Plantarum* **44** : 102-109.

Magnani, F., Mencuccini, M. and Grace, J. (2000) Age-related decline in stand productivity: the role of structural acclimation under hydraulic constraints. *Plant Cell and Environment* **23** : 251-263.

McDonald, A. J., Gemmell, F. M. and Lewis, P. E. (1998) Investigation of the utility of spectral vegetation indices for determining information on coniferous forests. *Remote Sensing of Environment* **65** : 155-169.

Mellis, A. (1991) Dynamics of photosynthetic membrane composition and function. *Biochimica et Biophysica Acta* **1058** : 87-106.

Myneni, R. B., Ross, J. and Asrar, G. (1989) A review on the theory of photon transport in plant canopies. *Agriculture and Forest Meteorology* **45** : 1-153.

Nichol, C. J., Huemmrich, K. F., Black, T. A., Jarvis, P. G., Walthall., C. L., Grace, J. and Hall, F. G. (2000) Remote sensing of photosynthetic light use efficiency of boreal forest. *Agriculture and Forest Meteorology* **101** : 131-142.

North, P. R. J., Briggs, S. A., Plummer, S. E. and Settle, J. J. (1999) Retrieval of land surface bidirectional reflectance and aerosol opacity from ASTR-2 multi angle imagery. *IEEE Transactions on Geoscience and Remote Sensing* **37** : 526-537.

North, P. R. J. (1996) Three-dimensional forest light interaction model using a Monte-Carlo method. *IEEE Transactions on Geoscience and Remote Sensing* **34** : 946-956.

Oquist, G. and Ogren, E. (1985) Effects of winter stress on photosynthetic electron transport and energy distribution between two photosystems of pine as assayed by chlorophyll fluorescence kinetics. *Photosynthesis Research* **7** : 19-30.

Osmond, C. B. and Grace, S. C. (1995) Perspectives on photoinhibition and photorespiration in the field: quintessential inefficiencies of the light and dark reactions of photosynthesis? *Journal of Experimental Biology* **46** : 1351-1362.

Osmond, C. B., Anderson, J. M., Ball, M. C. and Egerton, J. J. G. (1999) Compromising efficiency: the molecular ecology of light resource utilisation in plants. In: Press, M. C., Scholes, J. D. and Barker, M.G (Eds) *Physiological Plant Ecology*, Blackwell Science Ltd, Oxford. pp 1-25

Ottander, C. and Oquist, G. (1991) Recovery of photosynthesis in winter-stressed Scots pine. *Plant Cell and Environment* **14** : 345-349.

Ottander, C., Campbell, D. and Oquist, G. (1995) Seasonal changes in photosystem II organisation and pigment composition in *Pinus sylvestris*. *Planta* **197** : 176-183.

Owens, T. G. (1996) Processing of excitation energy by antenna pigments. In: *Photosynthesis and the Environment.* (Ed). Baker, N. Kluwer Academic Publications, NL. pp 1-23

Pell, E. J. and Steffen, K. L. (1991) *Active Oxygen /Oxidatative Stress and Plant Metabolism.* American Society of Plant Physiology, Rockville, MD.

Penuelas, J., Filella, I. and Gamon, J. A. (1995) Assessment of the photosynthetic radiation use efficiency with spectral reflectance. *New Phytologist* **131** : 291-296.

Penuelas, J., Llusia, J., Pinol., J. and Fillela, I. (1997) Photochemical reflectance index and leaf photosynthetic radiation-use-efficiency assessment in Mediterranean trees. *International Journal of Remote Sensing* **18** : 2863-2868.

Peterson, D. L., Spanner, M. A,. Running, S. W. and Teuber, K. B. (1987) Relationships of Thematic Mapper simulator data to leaf area index of temperate coniferous forests. *Remote Sensing of Environment* **22** : 323-341.

Pfundel, E. and Bilger, W. (1994) Regulation and possible function of the violaxanthin cycle. *Photosynthesis Research* **42** : 89-109.

Prince, S. D. (1991) Global Primary Production: a remote sensing approach. *Journal of Biogeography* **22**: 815-835.

Ranson, K. J., Daughtry, C. S. T. and Biehl, L. L. (1986) Sun angle, view angle, and background effects on spectral response of simulated Balsam Fir canopies. *Photogrammic Engineering and Remote Sensing* **52** (5) : 649-658.

Roujean, J. L. and Breon, F. M. (1995) Estimating PAR absorbed by vegetation from bidirectional reflectance measurements. *Remote Sensing of Environment* **51** : 375-384.

Ruben, A. V. and Horton, P. (1992) Mechanism of ΔpH dependent dissipation of absorbed excitation energy by photosynthetic membranes. 1. Spectroscopic analysis of isolated light-harvesting membranes. *Biochimica et Biophysica Acta* **1102** : 30-38.

Running, S. W., Baldocchi, D. D., Turner, D. P., Gower, S. T., Bakwin, P. S. and Hibbard, K. A. (1999) A global terrestrial monitoring network integrating tower fluxes, flask sampling ecosystem modeling and EOS satellite data. *Remote Sensing of Environment* **70** : 108-127.

Runyon, J. Waring, R. H., Goward, S. N. and Welles, J. M. (1994) Environmental limits on net primary productivity and light use efficiency across the Oregon transect. *Ecological Applications* **4** : 226-237.

Russell, G., Jarvis, P. G. and Monteith, J. L. (1989) Absorption of radiation by canopies and stand growth. In: Russell, G, Marshall, B and Jarvis, P. G. (Eds) *Plant Canopies: Their Growth, Form and Function*. Cambridge University Press, Cambridge. pp 21-40.

Schindler, C and Lichtenthaler, H. K. (1996) Photosynthetic $CO_2$-Assimilation, Chlorophyll fluroescence and Zeaxanthin Accumulation in Field Grown Maple Trees in the course of a Sunny and Cloudy Day. *Journal of Plant Physiology* **148** : 399-412.

Schimel, D.S. (1998) The carbon equation. *Nature* **393** : 208-209.

Sellers, P. J., Hall, F. H., Margolis, H., Kelly, B., Baldocchi, D., Denhartog, G., Cihlar, J., Ryan, M. G., Goodison, B., Crill, P., Ranson, K. J., Lettenmaier, D., Wickland, D. E. (1995b) The Boreal-Ecosystem-Atmosphere-Study (BOREAS): An overview and early results from the 1994 field year. *Bulletin of the American. Meteorological. Society.* **76** (9): 1549-1577.

Sellers, P. J., Bounoua L., Collatz G. J., Randall, D. A., Dazlich, D. A., Los, S. O., Berry, J. A., Fung, I., Tucker, C. J, Field, C. B, Jensen, T. G. (1996) Comparison of radiative and physiological effects of doubled atmospheric $CO_2$ on continental climate. *Science* **271** : 1402-1406.

Sellers, P. J., Hall, F. G., Kelly, R. D., Black, T. A, Baldocchi, D., Berry, J., Ryan, M., Ranson, K. J., Crill, P, M., Lettenmaier, D. P., Margolis, H., Cihlar, C., Newcomer, J., Fitzjarrald, D., Jarvis, P. G., Gower, S. T., Halliwell, D., Williams, D., Goodison, B., Wickland, D. E. and Guertin, F. (1997) BOREAS in 1997: Experiment overview, scientific results and future directions. *Journal of Geophysical Research* **102** : 28,731-28,769.

Siefermann-Harms, D. (1987) The light harvesting and photoprotective functions of carotenoids in photosynthetic pigments. *Physiological Plantarum* **69** : 561-568.

Spanner, M.A., Johnson, L., Miller, J., McCreight, R., Freemantle, J., Runyon, J. and Gong, P. (1994) Remote sensing of seasonal leaf area index across the Oregon transect. *Ecological Applications* **4** : 258-271.

Strahler, A. H. (1994) Vegetation canopy modelling: recent developments and remote sensing perspectives. *Proceedings of the Sixth International Symposium on Physical Measurements and Signatures in Remote Sensing.* CNES, Paris, pp 593-600.

Suits, G. (1974) The calculation of the directional reflectance of a vegetative canopy. *Remote Sensing of Environment* **2** : 117-125.

Sukyer, A. E., Verma, S. B. and Arkebauer, T. J. (1997) Season-long measurement of carbon dioxide exchange in a boreal fen. *Journal of Geophysical Research* **102** : 29,021-29,028.

Tans, P. P., Bakwin, P.S. and Guenther, D.W. (1990) Observational constraints on the global atmospheric $CO_2$ budget. *Science* **247** : 1431-1438.

Thayer, S. S. and Bjorkman, O. (1990) Leaf xanthophyll content and composition in sun and shade determined by HPLC. *Photosynthesis Research* **23** : 331-343.

Townsend, J. G. R and Justice, C. O. (1981) Utility of AVHRR NOAA-6 and NOAA-7 for vegetation mapping. *Matching Remote Sensing Technologies and Applications*. Remote Sensing Society, London pp 97 – 107.

Tsel'iker, Y. L. and Chetverikov, A. G. (1988) Dynamics of chlorophyll content and amounts of reaction centres of photosystems 1 and 2 in *Pinus sylvestris* L. and *Picea abies* Karst. Needles during a year. *Photosynthetica* **22** : 483-490.

Tucker, C. J. (1979) Red and photographic infrared linear combinations for monitoring vegetation. *Remote Sensing of Environment* **8** : 127-150.

Turner, D. P., Cohen, W. B., Kennedy, R. E., Fassnacht, K. S. and Briggs, J. M. (1999) Relationships between leaf area index and Landsat TM spectral vegetation indices across three temperate zone sites. *Remote Sensing of Environment* **70** : 52-68.

Verhoeven, A. S., Adams, W.W., Demmig-Adams, B. (1996) Close relationship between the state of the xanthophyll cycle and photosystem II efficiency during recovery from winter stress. *Physiologia Plantarum* **96** : 567-576.

Verhoeven, A. S., Adams, W.W., Demmig-Adams, B. (1999) The xanthophyll cycle and acclimation of *Pinus ponderosa* and *Malva neglecta* to winter stress. *Oecologia* **118** : 277-287.

Verhoef, W. (1984) Light scattering by leaf layers with application to canopy reflectance modelling: the SAIL model. *Remote Sensing of Environment* **16** : 125-141.

Verstraete, M. M. and Pinty, B. (1996) Designing Optimal Indexes for Remote Sensing Applications. IEEE Transactions on Geoscience and Remote Sensing **34** : 1254-1265.

Vogg, G., Heim, R., Hansen, J. and Beck, E. (1998) Frost hardening and photosynthetic preformance of Scots pine (*Pinus sylvestris* L.) needles I. Seasonal changes in the photosynthetic apparatus and its function. *Planta* **204** : 193-200.

Walthall, C., Williams, D. L., Markham, B., Kalshoven, J. and Nelson, R. (1996) Development and present configuration of the NASA GSFC/WFF helicopter based remote sensing system. International Geosciences and Remote Sensing Symposium. Lincoln, Nebraska, USA.

Watling, J. R., Robinson, S. A., Woodrow, I. E. and Osmond, C. B. (1997) Responses of rainforest understorey plants to excess light during sunflecks. *Australian Journal of Plant Physiology* **24** : 17-25.

Weiss, M., Baret, F., Myneni, R. B., Pragnere, A. and Knyazikhin, Y. (2000) Investigation of a model inversion technique to estimate canopy biophysical variables from spectral and directional reflectance data. *Agronomie* **20** : 3-22.

Williams, D. L. (1989) The radiative transfer characteristics of spruce (*Picea mariana*): implications relative to the canopy microclimate. Ph. D.Thesis. University of Maryland, College Park, USA.

Woodrow, I. E., Ball, J. T. and Berry, J. A. (1990) Control of photosynthetic carbon dioxide fixation by the boundary layer, stomata and ribulose 1,5-biphosphate carboxylase/oxygenase. *Plant Cell and Environment* **13** : 339-347.

Yamamoto, H. Y. (1979) Biochemistry of the violaxanthin cycle in higher plants. *Pure Applied Chemistry* **51** : 639-648.

## APPENDIX A

**Table A** showing list of species found under the canopy at the mixed and pole stands on the east side of the Yenesei.

| Species | Mixed and pole stands |
|---|---|
| *Vaccinium myrtillus L.* | + |
| *Vaccinium vitis-idaea* L. | |
| *Maianthemum bifolium* (L.) F. W. SCHM. | + |
| *Trientalis europaea* L. | + |
| *Linnaea borealis* L. | + |
| *Rosa rugosa* THUNB. | + |
| *Oxalis acetosella* L. | + |
| *Geranium sylvaticum* L. | + |
| *Allium ursinum* L. | + |
| *Rubus saxatilis* L. | + |
| *Paris quadrifolia* L. | + |
| *Anemone sibirica* L. | |
| *Pyrola* spec. | |
| *Ledum groenlandicum* OEDER | |
| *Prunus padus* L. | |
| *Calamagrostis purpurea* TRIN. | + |
| *Milium effusum* L. | |
| *Dryopteris dilatata* (HOFFM.) GRAY | |
| *Gymnocarpium dryopteris* (L.) NEWM. | + |
| *Equisetum sylvaticum* L. | + |
| *Lycopodium annotinum* L. | + |
| *Lycopodium complanatum* L. | |
| *Cladonia* | |
| *Hylocomium splendens* (HEDW.) B.S.G. | + |
| *Pleurozium schreberi* (BRID.) MITT. | |
| *Dicranum* spec. HEDW. | |

# APPENDIX B

## XANTHOPHYLL PIGMENT EXTRACTION

The procedure used for extracting the xanthophyll cycle pigment (used in Chapter 4) is a modified version of Gilmore and Yamamoto (1991). The details are as follows:

Each sample (50mg dry weight) was ground in 2ml 80% acetone + 3ml 100% acetone with a mortar and a pestle. Then the samples were centrifuged for 5 min (6500 x g, 4C). The supernatant was filtered (4mm Nylon Syringe Filters, 0.45μm, Waters Corporation). 40μl sample was injected into the HPLC system (Waters 510 HPLC pump, Waters 490 detector). Pigment separation was performed using a Spherisorb ODS-1 column (5μm, 250mm x 4.6mm, Alltech Associates) + a guard column (5μm, 10mm x 4.6mm, Alltech Associates). The solvent mixtures were: (A) acetonitrile-methanol-Tris (72:12:5) and (B) methanol-hexane (4:1). Tris buffer (pH 8.0, HCl) was 0.1M. All solvents were HPLC grade. The gradient program was as follows:

0-8.5 min: 100% solvent A, flow-rate 2.0 ml/min.
8.5-11.0 min: linear gradient to 100% solvent B, flow-rate 2.0ml/min.
11.0-18.0 min: 100% solvent B, flow-rate 1.2ml/min.
18.0-19.0 min: linear gradient to 100% solvent A, flow-rate 1.2ml/min.
19.0-20.0 min: 100% solvent A, flow-rate 2.0ml/min.

Pigments were detected at 440nm.
Conversion factors for peak area ($m^2$) to pmol per injection were:
Neoxanthin: 10408.
Violaxanthin: 14340.
Antheraxanthin: 10408.
Lutein: 10408.

Zeaxanthin: 10800.

Chl b: 20699.

Chl a: 19601.

beta-caro: 11598.

# APPENDIX C

Tables **A** and **B** give the carotenoid composition of the sun exposed needles sampled from May 2nd to May 13th. Chl-a and Chl-b are chlorophylls a and b respectively, Neo = neoaxanthin, Vio = violaxanthin, Ant = antheraxanthin, Lut = lutein, Zea = zeaxanthin, β-Car = betacarotene and (V+A+Z) = combined pool size of violaxanthin, antheraxanthin and zeaxanthin.

| **A** | | Chl μmol/gLEAF | | Carotenoids, μmol/gLEAF | | | | | |
|---|---|---|---|---|---|---|---|---|---|
| Date | Time | Chl-a | Chl-b | Neo | Vio | Ant | Lut | Zea | β-Car |
| 02-May | 1610 | 0.3914 | 0.17 | 0.0205 | 0.0039 | 0.0106 | 0.1693 | 0.0857 | 0.0848 |
| 03-May | 1030 | 0.3585 | 0.12 | 0.0165 | 0.0016 | 0.0139 | 0.1603 | 0.0601 | 0.0936 |
| 05-May | 1330 | 0.3551 | 0.13 | 0.0175 | 0.0103 | 0.0130 | 0.1482 | 0.0528 | 0.1035 |
| 06-May | 1530 | 0.4361 | 0.15 | 0.0210 | 0.0268 | 0.0150 | 0.1750 | 0.0382 | 0.1127 |
| 08-May | 1530 | 0.3710 | 0.17 | 0.0215 | 0.0223 | 0.0120 | 0.1585 | 0.0256 | 0.0795 |
| 13-May | 1430 | 0.4361 | 0.23 | 0.0287 | 0.0149 | 0.0122 | 0.1832 | 0.0223 | 0.0966 |

| **B** | | | Carotenoids, mmol/mol Chla+b | | | | | | |
|---|---|---|---|---|---|---|---|---|---|
| Date | Time | Chla/Chlb | Neo | Vio | Ant | Lut | Zea | β-Car | V+A+Z |
| 02-May | 1610 | 2.3647 | 36.838 | 6.9223 | 19.108 | 304.05 | 153.83 | 152.27 | 0.9615 |
| 03-May | 1030 | 2.9565 | 34.415 | 24.111 | 28.898 | 334.10 | 125.30 | 195.16 | 0.8648 |
| 05-May | 1330 | 2.7399 | 36.010 | 21.169 | 26.760 | 305.70 | 108.83 | 213.60 | 0.8650 |
| 06-May | 1530 | 2.9323 | 35.919 | 45.753 | 25.763 | 299.16 | 65.362 | 192.79 | 0.6657 |
| 08-May | 1530 | 2.1663 | 39.738 | 41.149 | 22.072 | 292.29 | 47.127 | 146.69 | 0.6271 |
| 13-May | 1430 | 1.9340 | 43.342 | 22.581 | 18.452 | 276.93 | 33.655 | 146.03 | 0.6977 |

## LIST OF PUBLICATIONS

The publication that follows is based on work presented in Chapter 3 of this thesis.

Nichol, C. J., Huemmrich, K. F., Black, T. A., Jarvis, P. G., Walthall, C. L., Grace, J. and Hall, F. G. (2000) Remote sensing of photosynthetic light use efficiency of boreal forest. *Agricultural and Forest Meteorology* **101** : 131-142.

ELSEVIER

Agricultural and Forest Meteorology 101 (2000) 131–142

AGRICULTURAL AND FOREST METEOROLOGY

www.elsevier.com/locate/agrformet

# Remote sensing of photosynthetic-light-use efficiency of boreal forest

Caroline J. Nichol [a,*], Karl F. Huemmrich [b,1], T. Andrew Black [c,2], Paul G. Jarvis [a,3], Charles L. Walthall [d,4], John Grace [a,5], Forrest G. Hall [b,6]

[a] *Institute of Ecology and Resource Management, University of Edinburgh, EH9 3JU, Scotland, UK*
[b] *NASA Goddard Space Flight Center, Code 923, Greenbelt, MD 20771, USA*
[c] *Department of Agricultural Sciences, University of British Columbia, Vancouver, Canada V6T 1Z4*
[d] *United States Agricultural Research Service, Remote Sensing Laboratory, Beltsville, MD 20707, USA*

Received 12 April 1999; received in revised form 22 November 1999; accepted 23 November 1999

**Abstract**

Using a helicopter-mounted portable spectroradiometer and continuous eddy covariance data we were able to evaluate the photochemical reflectance index (PRI) as an indicator of canopy photosynthetic light-use efficiency (LUE) in four boreal forest species during the Boreal Ecosystem Atmosphere experiment (BOREAS). PRI was calculated from narrow waveband reflectance data and correlated with LUE calculated from eddy covariance data. Significant linear correlations were found between PRI and LUE when the four species were grouped together and when divided into functional type: coniferous and deciduous. Data from the helicopter-mounted spectroradiometer were then averaged to represent data generated by the Airborne Visible Infrared Imaging Spectrometer (AVIRIS). We calculated PRI from these data and relationships with canopy LUE were investigated. The relationship between PRI and LUE was weakened for deciduous species but strengthened for the coniferous species. The robust nature of this relationship suggests that relative photosynthetic rates may be derived from remotely-sensed reflectance measurements. 

*Keywords:* Xanthophyll cycle; AVIRIS; Photochemical reflectance index; Eddy covariance

## 1. Introduction

Remote sensing offers an important landscape and regional perspective on vegetation structure and function (Asner et al., 1998). Much remote sensing of vegetation has made use of broad band sensors to derive indices of vegetation cover, such as the normalised difference vegetation index (NDVI) (Tucker, 1979). Although NDVI often correlates well with biomass, leaf area index (LAI) and fraction of absorbed photosynthetically active radiation (FAPAR), it often fails to capture physiological processes that occur on fine temporal and spectral scales. For example, drought tolerant evergreens can undergo significant changes in photosynthetic light-use efficiency (LUE), without

* Corresponding author. Tel.: +44-131-650-5744; fax: +44-131-662-0478.
*E-mail addresses:* caroline.nichol@ed.ac.uk (C.J. Nichol), karl.huemmrich@gsfc.nasa.gov (K.F. Huemmrich), ablack@interchange.ubc.ca (T.A. Black), pjarvis@ed.ac.uk (P.G. Jarvis), cwalthal@asrr.arsuda.gov (C.L. Walthall), jgrace@ed.ac.uk (J. Grace), fghall@ltpmail.nasa.gov (F.G. Hall).
[1] Tel.: +301-286-4862; fax: +301-286-0239.
[2] Tel.: +604-822-2730; fax: +604-822-8639.
[3] Tel.: +44-131-650-5426; fax: +44-131-662-0478.
[4] Tel.: +301-504-6074; fax: +301-504-5031.
[5] Tel.: +44-131-650-5400; fax: +44-131-662-0478.
[6] Tel.: +301-286-2974; Fax: +301-286-0239.

0168-1923/00/$ – see front matter 
PII: S0168-1923(99)00167-7

an equivalent change in NDVI (Running and Nemani, 1988). Photosynthesis can change from day to day or hour to hour depending on the response of the leaves to a naturally fluctuating environment, with no significant changes in canopy architecture or NDVI (Tenhunen et al., 1987).

Pioneering work has shown how the reflectance of leaves may contain a signal for photosynthetic efficiency, and therefore provide a new method to detect changes in photosynthesis using remote sensing. Photosynthetic LUE is defined here as $CO_2$ uptake divided by the incident photosynthetic photon flux density (PPFD) and since the 1930s it has been known to decline at high PPFD as photosynthesis becomes light-saturated. More recently it has been found that when the photosynthetic system receives excess excitation energy from sunlight, the xanthophyll cycle is affected. The carotenoid violaxanthin is converted to zeaxanthin via de-epoxidase reactions (Yamamoto, 1979). Recent experimental work has shown a close correlation between xanthophyll pigment interconversion and the dissipation of excess energy in the pigment bed associated with photosystem II (PS II) (for reviews see Pfundel and Bilger, 1994; Demmig-Adams and Adams, 1994; Demmig-Adams et al., 1996). Recent evidence indicates that the conversion of the pigment violaxanthin to the photoprotective pigment zeaxanthin acts to lower the energy level of the lowest excited singlet state below that of chlorophyll-*a*, thus providing a sink for the excess excitation energy (Frank et al., 1994; Owens, 1996).

The interconversion of the xanthophyll cycle pigments can be detected in leaves through a change in the absorbance at 505–515 nm (Bilger et al., 1989) or the reflectance at 531 nm (Gamon et al., 1990, 1993). Because the pigments of the xanthophyll cycle are so closely linked to the LUE of PS II, a reflectance index that incorporates reflectance at 531 nm could provide a remote indicator of photosynthetic function. Gamon et al. (1990) formulated the photochemical reflectance index (PRI), incorporating reflectance at 531 nm (the xanthophyll cycle signal) and a reference wavelength (Gamon et al., 1992).

A number of studies beginning in the late 1980s explored the relationships between PRI and photosynthetic LUE at the leaf and small plot level. Measurements on individual leaves have demonstrated that PRI, calculated from narrow waveband data, was closely related to $\Delta F/Fm'$, a fluorescence-based indicator of PSII LUE, as well as LUE calculated from gas exchange measurements in leaves from a wide range of species (Penuelas et al., 1995). Fillela et al. (1996) and Gamon et al. (1997) have further presented evidence that PRI provided a widely applicable index of leaf LUE across species, functional types and nutrient levels.

The only canopy scale measurements that exist are on small plots ($\sim 2\,m^2$) and single species. Gamon et al. (1992) measured reflectance of sunflower plants with a portable spectroradiometer from a height of 4 m with wide-angle optics, allowing reflectance measurements over an area of diameter 1 m (consisting of 8–10 plants). This work showed that PRI closely tracked diurnal changes in photosynthetic LUE in control and nitrogen stressed canopies, but not in water stressed canopies that were undergoing severe wilting (Gamon et al., 1992).

Such observations suggest that measurement of reflectance by remote sensing in these spectral regions should also be useful for inferring canopy-scale LUE over regional and larger areas. However, at this time no work has been done to relate canopy PRI to LUE over areas of tens of meters. We have investigated the use of PRI as an index of LUE over contrasting canopy types. Extensive canopy reflectance and eddy covariance measurements of gas exchange were made over boreal forest during the BOREAS experiment (Boreal Ecosystem Atmosphere Study, for overview see Sellers et al., 1995) and provided the opportunity to investigate the PRI:LUE relationship over larger ($\sim 70\,m^2$) forested areas.

We report in this paper an evaluation of PRI as an indicator or photosynthetic LUE. We begin by describing the sites sampled in the boreal forest and the data set used, then proceed to outline the analysis approach for PRI:LUE. Finally, we present the results of this analysis and draw a number of conclusions regarding future directions.

## 2. Materials and methods

### 2.1. Study sites

The BOREAS field experiment took place during 1994 on the northern and southern edges of the Cana-

dian boreal forest. A Northern Study Area (NSA) was located near Thomson, Manitoba, and Southern Study Area (SSA) was located near Candle Lake, Sask. (see Sellers et al., 1995b for details) and specific sub-sites within the SSA were intensively studied during the growing season. A brief outline of the sites used in this study is included here.

### 2.2. Old black spruce

The site lies in the southern mixed forest zone about 100 km north of Prince Albert in Sask. (53°55′N, 105°5′W, elevation 630 m), and has been described by Jarvis et al. (1997). The terrain is essentially flat with pure and mixed stands of black (*Picea mariana* (Mill.) BSP) and white spruce (*P. glauca* Moench.), jack pine (*Pinus banksiana* Lamb.), aspen, fen and lakes. The substratum is peat overlying glacial drift with an elevated water table so the surface is generally wet. The understorey is sparse with some low shrubs reaching ~1.5 m in height.

### 2.3. Old jack pine

The jack pine forest (*Pinus banksiana* Lamb.) stand grows in the SSA near Nipawin, Sask., Canada (53°54′N, 104°41′W, elevation 579 m) and has been described by Baldocchi et al. (1997). The landscape is relatively flat (slope ~2 and 5%) with pure and mixed stands of black (*P. mariana* (Mill.) BSP) and white spruce (*P. glauca* Moench.), aspen, jack pine and fen. The soil is a coarse textured, well drained sand. The ground was covered with an optically bright mat consisting of bearberry (*Arctostaphylos uva-ursi*), bog cranberry (*Vaccinium vitis-idaea*), and lichens (*Cladina* spp.).The understorey vegetation is sparse but there are isolated groups of alder (*Alnus crispa*).

### 2.4. Old aspen

The site is located in the SSA within Prince Albert National Park, Sask. (53°38′N, 106°12′W, elevation 600 m) and has been described by Hogg et al. (1997). It is an extensive, mostly pure, stand of trembling aspen (*Populus tremuloides* Michx.) Orthic gray luvisol with a loam texture dominates the site. Beaked hazelnut (*Corylus cornutta* Marsh) dominates the understorey shrub layer and is approximately 2 m in height. Wild rose (*Rosa woodsii*) and alder (*A. crispa*) are found in intermittently.

### 2.5. Fen

The fen study site is located in the SSA, 115 km northeast of Prince Albert, Sask. (53°57′N, 105°57′W, elevation 525 m). The fen study site is a minerotrophic, patterned fen surrounded by black spruce (*P. mariana* (Mill.) BSP)) and jack pine (*Pinus banksiana* Lamb.) forests and has been described by Sukyer et al. (1997). Abundant herbaceous species throughout the fen included bogbean (*Menyanthes trifoliata*) and several sedge species (*Carex* and *Eriophorum* spp.). Dominant woody plant species are 0.5–1.5 m tall bog birch (*Betula pumila*) and widely scattered, stunted tamarack trees (*Larix laricina*). Mosses whilst present are not abundant in this fen.

### 2.6. Canopy spectral reflectance data

The National Aeronautics and Space Administration (NASA) Goddard Space Flight Center (GSFC)/Wallops Flight Facility (WFF) helicopter-based optical remote sensing system (Walthall et al., 1996) was deployed to acquire canopy multispectral data with a portable spectroradiometer. A spectroradiometer (model SE-590, Spectron Engineering, Denver, Colorado) was mounted on a steel rack at nadir orientation and processed to an atmospherically corrected at-surface reflectance. A 15° instantaneous field of view lens (IFOV) was fitted to yield a ground resolution of 79 m at the 300 m nominal altitude. The SE-590 had a spectral range of 362.7–1122.7 nm, with a usable range of 400–900 nm. Data are reported at 3 nm intervals calculated at the centre point of a five 3 nm bin running average.

Data were acquired on clear days (incident PPFD>900 $\mu$mol $m^{-2}$ $s^{-1}$) whilst the helicopter hovered at each site for 1–2 min for each observation (consisting of an average of 20–25 scans). Observations were made in the spring, summer and autumn (Table 1). Radiometric calibration and spectral calibration procedures were performed before and after the field season to check for changes in sensor radiometric response. The SE-590 data were corrected

Table 1
Summary of the dates of the reflectance data acquisition with the range of temperature and solar radiation experienced during the observation periods

| Site | Instrument | Observation date | Range of temperature °C | Range of solar radiation $\mu mol\ m^{-2}\ s^{-1}$ |
|---|---|---|---|---|
| Old aspen | SE-590 | 31-May-94 | 17.7–18.3 | 992–1129 |
| | | 21-July-94 | 22.6–23.3 | 1339–1539 |
| | | 25-July-94 | 21.5–21.7 | 1343–1450 |
| | | 13-Sept-94 | 15.7–16.4 | 1077–1216 |
| Fen | SE-590 | 01-June-94 | 20.5–21.0 | 1043–1352 |
| | | 06-June-94 | 21.2–21.2 | 1445–1545 |
| | | 21-July-94 | 21.3–21.6 | 1222–1366 |
| | | 13-Sept-94 | 12.4–12.9 | 1021–1117 |
| Old jack pine | SE-590 | 31-May-94 | 15.9–16.7 | 1022–1192 |
| | | 06-June-94 | 21.0–21.2 | 1416–1545 |
| | | 21-July-94 | 25.4–25.7 | 1397–1476 |
| | | 24-July-94 | 21.1–21.4 | 1382–1498 |
| | | 13-Sept-94 | 18.9–19.5 | 1196–1271 |
| Old black spruce | SE-590 | 01-June-94 | 18.4–18.6 | 1399–1498 |
| | | 06-June-94 | 20.4–20.6 | 1361–1479 |
| | | 21-July-94 | 24.6–25.3 | 1500–1579 |
| | | 23-July-94 | 18.5–18.9 | 1216–1341 |
| | | 13-Sept-94 | 18.7–19.1 | 1177–1236 |

to at-surface reflectances using the 6S atmospheric radiative transfer model and sun photometer data.

PRI from the SE-590 data was formulated:

$$I_{PR\,SE-590} = (R_{569} - R_{529})/(R_{569} + R_{529}) \quad (1)$$

where $R_{529}$ indicates the reflectance centred at 529 nm with upper and lower band limits of 536.5 and 521.5 nm (coinciding with the signal of the xanthophyll cycle) and $R_{569}$ indicates the reflectance centred at the 569 nm waveband with upper and lower band limits of 561.5 and 576.5 nm (a reference waveband). This differs slightly from that used in previous studies, but still lies within the range of wavelengths considered applicable for the calculation of PRI (Gamon et al., 1993). By referencing $R_{529}$ to $R_{569}$, this index normalises for factors which include pigment content and chloroplast movement both of which can affect the $R_{529}$ signal (Gamon et al., 1993).

### 2.7. A simulation of AVIRIS data

The Airborne Visible Infrared Imaging Spectrometer (AVIRIS) (for details see Green et al., 1998) is flown aboard the NASA ER-2 aircraft at an altitude of 20 km and acquires data in 224 contiguous channels of the shortwave spectrum (400–2500 nm). It measures at a larger spatial scale than the helicopter producing a ground coverage of $\sim$120 $km^2$ with a 20 m spatial resolution and spectral resolution of 10 nm. Since this instrument uses new technology that may be amenable for measuring the status of the xanthophyll cycle (but as yet is untested) the data generated by the SE-590 were averaged to those wavebands generated by the AVIRIS instrument (waveband information supplied by Green, NASA, JPL). The SE-590 data were thus averaged to the mid-point of each band, as is standard practice with hyperspectral sensors. PRI was thus calculated:

$$I_{PR\,AVIRIS} = (R_{570.5} - R_{530.5})/(R_{570.5} + R_{530.5}) \quad (2)$$

where $R_{570.5}$ indicates the reflectance over the range of 566–575 nm and $R_{530.5}$ indicates the reflectance over the range 526–535 nm. $R_{570.5}$ was the closest available reference waveband to that used in the computation of PRI from the helicopter data (Eq. (1)).

### 2.8. Eddy covariance measurement of fluxes

Half-hour fluxes of momentum, sensible heat, water vapour and carbon dioxide (as well as meteorological variables) were measured at all sites

using tower-mounted, eddy covariance systems continuously from May through September of the 1994 growing season. Full details of the theory and instrument set for each site are published elsewhere. For old black spruce see (Jarvis et al., 1997; old jack pine, Baldocchi et al., 1997; old aspen, Blanken et al., 1997; fen, Sukyer et al., 1997).

### 2.9. Estimates of stand photosynthesis

The $CO_2$ flux was partitioned into photosynthesis and respiration components by estimating daytime ecosystem respiration as functions of soil temperature. Following Goulden et al. (1997), night-time half-hour $CO_2$ fluxes at high windspeeds (friction velocity, $u^*>0.2$) were plotted against soil temperature (at 5 cm) and the usual exponential function fitted, of the form,

$$A = ce^{bT_s}$$

where $A$ is carbon dioxide flux , $T_s$ is soil temperature, $c$ and $b$ are constants and e is the base of the natural logarithm. Daytime respiration was then calculated using this function and daytime soil temperatures. This was done for each month's night-time half-hour flux data from May until September for each of the sites (data not shown). Photosynthesis was then calculated as the daytime half-hour $CO_2$ fluxes after the respiration component had been removed (Lloyd and Taylor, 1994). Because the helicopter overpass occurred on clear bright days (PPFD>900 $\mu mol\, m^{-2}\, s^{-1}$), the $CO_2$ flux data for these periods were restricted to PPFD>900 $\mu mol\, m^{-2}\, s^{-1}$. Photosynthesis and incident PPFD were averaged above this PPFD and a daily LUE value computed from these averages according to the following:

$$\text{Canopy light-use efficiency} = \frac{\text{Canopy photosynthesis}}{\text{Incident photosynthetic photon flux density}}$$

## 3. Data analysis

### 3.1. Correlating PRI with LUE data

Relationships between PRI and field measured estimates of photosynthetic LUE were investigated with linear regression analysis. This was done for the four sites sampled and then with respect to functional group. Relationships between the simulated AVIRIS data and LUE were also investigated with linear regression analysis for all species sampled and with respect to functional type.

## 4. Results

Two mean representative reflectance spectra obtained from the SE-590 spectroradiometer, each representing coniferous or deciduous forest are shown in Fig. 1 along with the two wavebands used for the calculation of PRI.

In the absence of normalisation, the reflectance at 529 nm ($R_{529}$) yielded no clear correlation with LUE for the coniferous and deciduous species together (Fig. 2A), or for the deciduous species (Fig. 2B) and coniferous species (Fig. 2C). However, after normalisation midday top canopy $PRI_{SE\text{-}590}$ values were significantly correlated with canopy LUE across the four species sampled ($R^2=0.64$, $p<0.05$, Fig. 3A). The correlations were stronger when the species were divided into their functional groups. A linear relationship was apparent between $PRI_{SE\text{-}590}$ and LUE for the deciduous species ($R^2=0.78$, $p<0.05$, Fig. 3B) and coniferous species ($R^2=0.65$, $p<0.05$, Fig. 3C).

The $PRI_{SE\text{-}590}$:LUE relationships were reassessed by calculating $PRI_{SE\text{-}590}$ using a range of reference wavelengths. Fig. 4A shows a summary of the $R^2$ of the relationship between $PRI_{SE\text{-}590}$ and LUE. The peak of this graph would be the best combination of xanthophyll wavelength and reference wavelength for the estimation of LUE. A reference wavelength of 569 nm produces the best relationship between $PRI_{SE\text{-}590}$ and LUE. This is also the optimal reference waveband to use for the deciduous species (Fig. 4B), but for the coniferous sites, the selection of a slightly longer reference wavelength generated a stronger relationship between $PRI_{SE\text{-}590}$ and LUE (Fig. 4C). In this case, selecting a reference wavelength of 575 nm produced an $R^2$ of 0.82 in the relationship between $PRI_{SE\text{-}590}$and LUE.

When the reflectance data from the SE-590 were averaged to simulate data generated by the AVIRIS instrument, scatter was introduced into the relationship between $PRI_{AVIRIS}$ and LUE. The $PRI_{AVIRIS}$:LUE

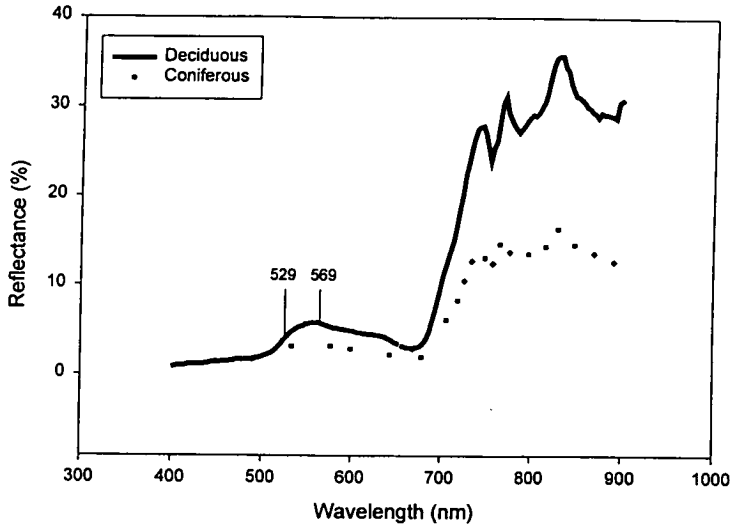


Fig. 1. Mean spectra of the coniferous and deciduous forest canopy from the BOREAS southern study area. Each curve represents the mean of 20–25 scans acquired by the helicopter mounted SE-590 spectroradiometer. Wavelengths used for PRI calculation are shown in the Figure.

relationship across the four species were significantly linearly correlated ($R^2$=0.46, $p$<0.05, Fig. 5A). The relationship between $PRI_{AVIRIS}$ and LUE was weakened within the deciduous species ($R^2$=0.38, $p$<0.05, Fig. 5B) but strengthened within the coniferous species ($R^2$=0.78, $p$<0.05, Fig. 5C).

## 5. Discussion

### 5.1. Canopy PRI and photosynthetic LUE

The consistent relationship between $PRI_{SE-590}$ and LUE for canopies sampled in full sunlight (Fig. 3A–C) supports the hypothesis that $PRI_{SE-590}$ provides a measure of PS II LUE across species and functional types. Similar observations have been made using individual leaves and small plots (~2 m) (Gamon et al., 1990, 1992, 1997; Penuelas et al., 1995, 1997; Fillela et al., 1996), but this is the first time a relationship has been found between PRI and LUE over heterogeneous forest canopies.

Penuelas et al. (1995) studied the relationship between PRI and PS II LUE in plants differing in phenology, habit and photosynthetic type, and found that the slope and intercept of the PRI:LUE relationship varied between species. The lack of a single relationship in their study is not surprising. Variation may arise from the environmental growth conditions, varying anatomy, morphology and pigmentation and diverse species differences. Such factors can dramatically influence the visible reflectance, and PRI (Guyot, 1990).

The scatter in the relationship between $PRI_{SE-590}$ and LUE could be the result of several factors that can cause divergence between whole leaf assimilation and PS II LUE. These factors include the Mehler reaction, photorespiration (Harbison et al., 1990) and nitrate reduction (Bloom et al., 1989), all of which compete with carboxylation for reductant generated by electron transport. In the conditions of this study, the significant correlations between $PRI_{SE-590}$ and LUE within each functional group suggest that the overall photosynthetic systems were sufficiently regulated to maintain consistent relationships between PS II processes and carboxylation.

Consistent relationships between PRI and LUE at the small plot scale (~2 m) do not always exist. Work by Gamon et al. (1992) on sunflower canopies experiencing severe water stress showed a divergence between PRI and LUE, possibly owing to increased use of reductant by photorespiration and other processes besides carboxylation. Of the sites used in this study it is possible that a degree of water stress was experienced at the old jack pine site because of the free draining nature of the soil (Cuenca et al., 1997), and

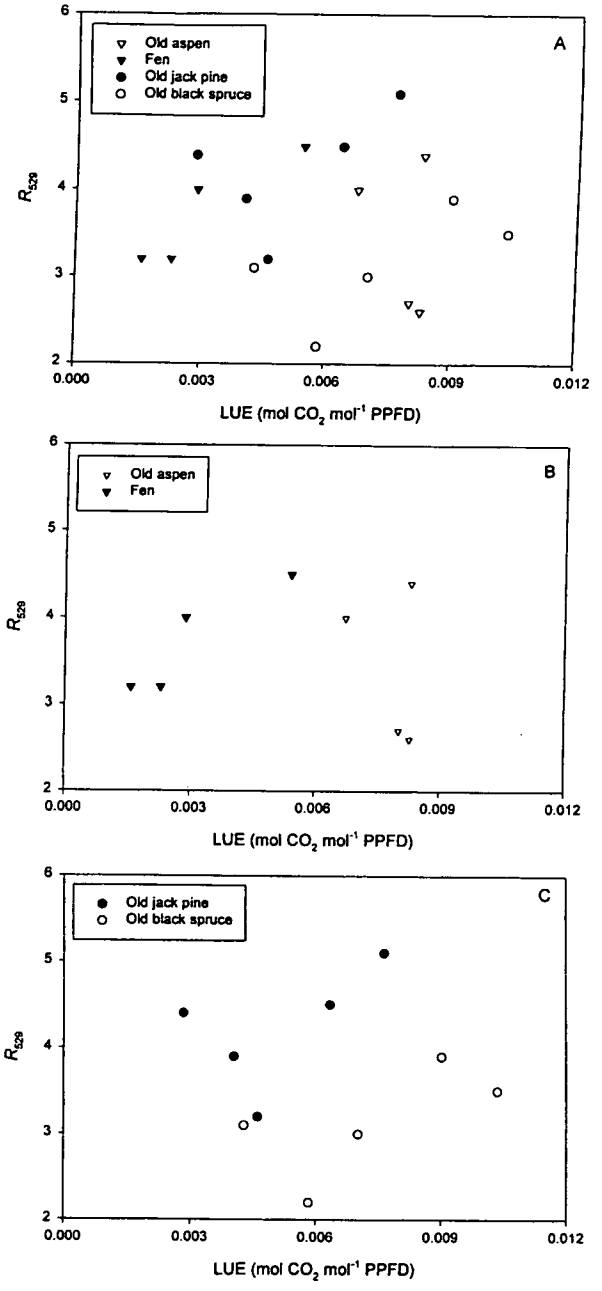


Fig. 2. Relationship between reflectance at 529 nm and canopy light-use efficiency (LUE). Each point is an average of 20–25 spectral scans and 4 h of canopy LUE data. (A) Four boreal forest species. (B) Two deciduous species. (C) Two coniferous species. Individual species are represented by the different symbols indicated.

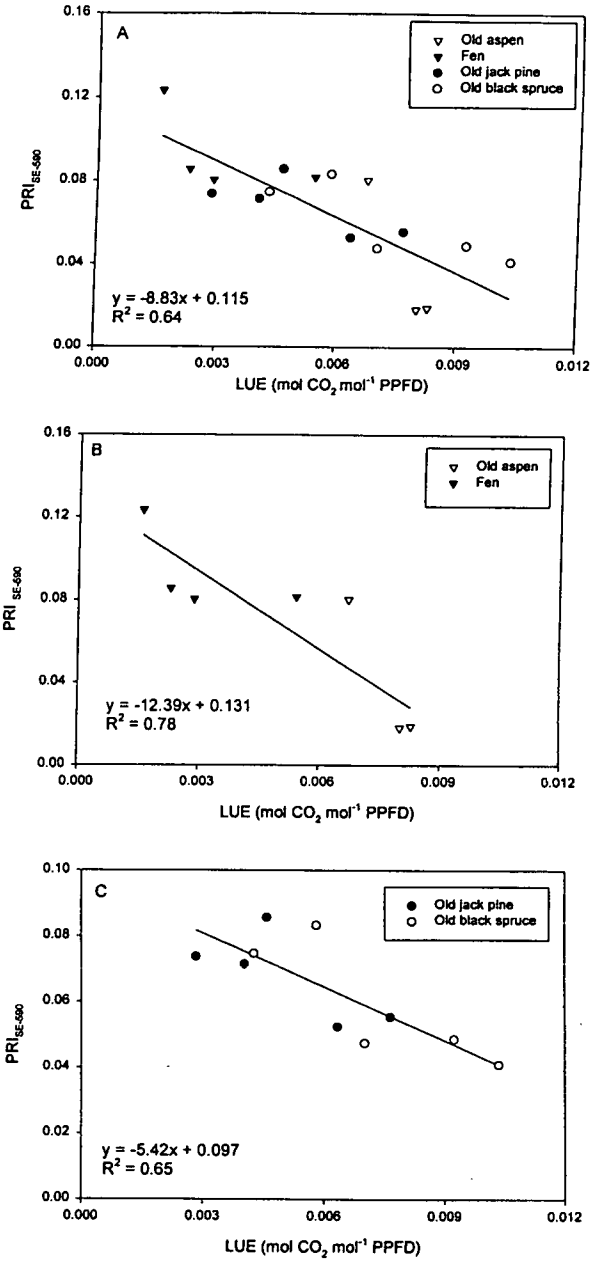


Fig. 3. Relationship between the photochemical reflectance index (PRI) and canopy light-use efficiency (LUE) for boreal forest sites sampled in full sun. Each point is an average of 20–25 spectral scans and 4 h of canopy LUE data. (A) Four boreal forest species. (B) Two deciduous species. (C) Two coniferous species. Individual species are represented by different symbols indicated.

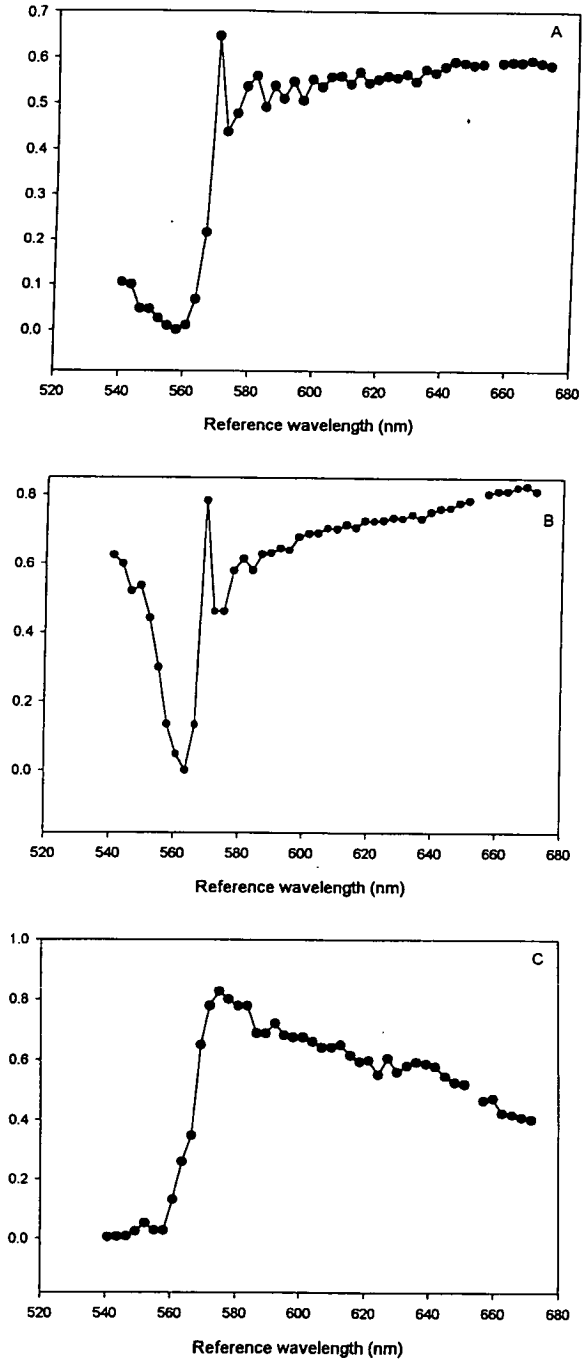


Fig. 4. A summary of the $R^2$coefficients for relationship between the photochemical reflectance index (PRI) and canopy light–use efficiency (LUE). (A) Four boreal forest species. (B) Two deciduous species. (C) Two coniferous species. PRI was calculated using $R_{529}$ as the xanthophyll waveband with reference wavelengths ranging from 540 to 670 nm, at 3 nm intervals.

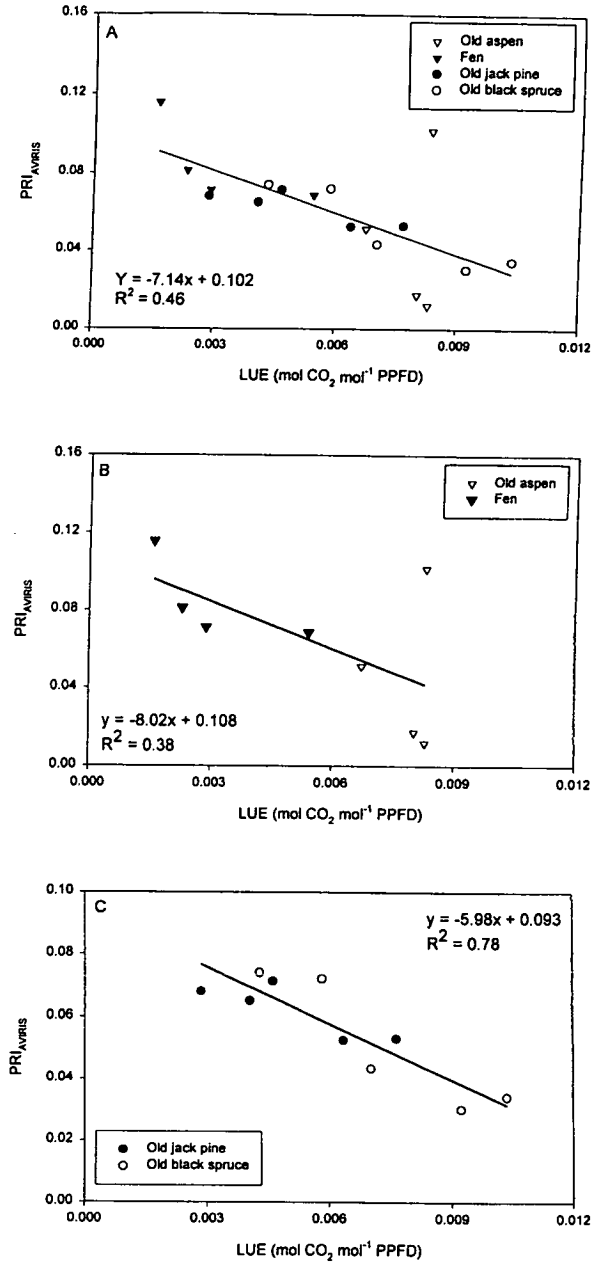


Fig. 5. Relationship between the photochemical reflectance index (PRI) and canopy light-use efficiency (LUE) where data from the SE-590 has been averaged to 10 nm to represent data generated by the AVIRIS sensor. (A) Four boreal forest species. (B) Two deciduous species. (C) Two coniferous species. Individual species are represented by different symbols indicated.

some of the scatter in the $PRI_{SE-590}$:LUE relationship could be attributed to this (Baldocchi et al., 1997).

### 5.2. Wavelength choice for the calculation of PRI

The wavelength chosen to signal activity of the xanthophyll cycle differs slightly from that used in previous studies (Gamon et al., 1990, 1992, 1997; Penuelas et al., 1995; Fillela et al., 1996). However, it has been shown that the 531 nm 'signal' consists of two spectral components (Penuelas et al., 1995; Gamon et al., 1997). Gamon et al. (1997) found the dominance of a 545 nm component in low PPFD, with an appearance of a 526 nm component at higher PPFD. The contribution of two spectral components could explain previous reports of a non-linear relationship between PRI and LUE where samples were measured over a wide range of PPFDs (Penuelas et al., 1995). Although Gamon et al. (1990) first highlighted this, a recent paper has shown that these two spectral signals are active at different PPFDs, and can be separated in laboratory conditions (Gamon et al., 1997).

The 545 nm component, which was apparent in the difference spectra, is related to chloroplast conformational changes associated with the build-up of the pH gradient, rather than to the conversion of violaxanthin to zeaxanthin. This conclusion was based on experimental work associating the generation of the thylakoid pH gradient with a change in absorbance at 540 nm (Heber, 1969, Bilger et al., 1989, Bjorkman and Demmig-Adams, 1994) and with a corresponding reflectance change near 539 nm (Gamon et al., 1990). That the 545 nm component was initiated at lower PPFDs and progressively disappeared at higher PPFDs, suggests that it is not directly a result of xanthophyll pigment interconversion or the associated heat dissipation, but is more likely a result of light scattering changes associated with the initial build-up of the thylakoid pH gradient upon the sudden transition from darkness to low PPFD (Gamon et al., 1997).

The 526 nm component, which appears at higher PPFD, is most likely caused by spectral changes associated with the conversion of violaxanthin to zeaxanthin. This conclusion can be drawn from evidence attributing a similar absorbance change near 515 nm (Bilger et al., 1989; Bjorkman and Demmig-Adams, 1994) and a related reflectance change near 525 nm (Gamon et al., 1990), to the production of zeaxanthin. Gamon et al. (1997) further showed that PRI, when calculated using the 526 nm component at high light, was more strongly correlated to LUE than PRI calculated using 531 nm. Thus, the increased activity at PPFDs above 500 $\mu mol\, m^{-2}\, s^{-1}$ of the 526 nm component is consistent with the function of xanthophyll cycle pigments as photoprotective pigments that serve to dissipate excess absorbed PPFD as heat (Demmig-Adams and Adams, 1994; Demmig-Adams et al., 1996). In the linear, quantum yield region of the photosynthetic PPFD response curve, there is no need for such energy dissipation and thus no detectable contribution of the 526 nm component in sun acclimated leaves. Given this information, we chose 529 nm to represent our xanthophyll cycle wavelength. However, because no data were acquired at low PPFD, it is not possible to confirm directly the existence of these two spectral components in this study.

We then recalculated $PRI_{SE-590}$ using a range of reference wavelengths and correlated it against LUE. Some surprising relationships emerged. When all the species were grouped together, the $R^2$ peaked at 0.645 when 569 nm was used as a reference. This was also the case for the deciduous species. However, the $PRI_{SE-590}$ data for the conifers were more strongly correlated with LUE when a slightly longer reference waveband of 575 nm was used. Gamon et al. (1992) found that any reference waveband between 539 and 570 nm would be suitable for the calculation of $PRI_{SE-590}$ and statistical correlation with LUE data. Their results however, were for a single species, rather than the four species used in this study.

### 5.3. AVIRIS data and photosynthetic light-use efficiency

The differences in the relationships between PRI and LUE from the helicopter data, as opposed to the AVIRIS simulation, suggest that the 10 nm resolution is not too broad to detect this spectral signal but does introduce scatter. This could present significant difficulty in extending the use of PRI to landscape scales as few sensors have the capability of measuring large areas at a resolution of less than 5 nm. However, when the spectra are represented as difference spectra, the width of the dip representative of the 'xanthophyll' signal appears to be wider than 10 nm (Gamon et al., 1990, 1992; Fillela et al., 1996), and this would

suggest that a 10 nm resolution should be appropriate for detecting changes in the xanthophyll cycle. Future work using AVIRIS data for PRI applications will confirm its utility for the estimation of canopy scale LUE.

### 5.4. Effects of background reflectance on PRI

The effective use of periodic remotely-sensed observations in landscape process studies depends on stable estimation of diurnally integrated conditions (Goward and Huemmrich, 1992). It has been widely documented that the reflectance measured from forest sites may vary with solar illumination angle, viewing angle, understorey or background reflectance and atmospheric effects, as well as intrinsic canopy parameters such as phytomass and leaf area index of the dominant species (Kimes, 1980; Ranson et al., 1986; Huete, 1987; Guyot, 1990; Goward and Huemmrich, 1992). Although the spectral data used in this study were acquired from a nadir orientation during conditions of highest possible solar elevation (approximately 40–60°), which would have minimised unstable calculations of PRI, a full sensitivity analysis of the PRI:LUE relationship is warranted and a companion paper will focus on these issues.

## 6. Conclusions

We have demonstrated that $PRI_{SE\text{-}590}$ can serve as an index of photosynthetic LUE over heterogeneous forest canopies. These results extend beyond earlier studies using individual leaves (Gamon et al., 1992; Penuelas et al., 1995; Fillela et al., 1996) by showing that this index is well suited to sampling areas of $\sim 70\,m^2$ in contrasting ecosystems at high PPFD. Consequently, it should be possible to derive methods of remotely estimating relative photosynthetic rates based on reflectance in the 529 nm spectral region.

Our simulation of AVIRIS data shows that the resolution of this sensor is not too coarse to detect the fine spectral signal generated by the xanthophyll cycle, although it is degraded more at this resolution. Thus we propose that the application at the landscape and larger scales will require a more rigorous test of the use of AVIRIS data as well as the use of radiative transfer and geometric models, such as SAIL (Scattering from Arbitrarily Inclined Leaves) (Verhoef, 1984) and GeoSail (Huemmrich, 1995) to scale PRI and LUE to whole landscapes.

Improvement in the accuracy of scaling processes such as photosynthetic LUE will continue to be pivotal for the development of physiological ecology and global change research. As new perspectives and methods for scaling ecological function from local to global levels continues to evolve (e.g., via micrometeorological towers, remote sensing and modeling), our understanding of how functional variables scale across ecological levels must keep pace. Without this synergy, our ability to resolve important issues such as sources and sinks of $CO_2$ will be impaired.

## Acknowledgements

This work was supported by awards to CJN from the UK's Natural Environmental Research Council and a National Aeronautics and Space Administration, Planetary Biology Internship (NASA-PBI), 1998. Eddy correlation fluxes at the old jack pine site were collected by Dennis Baldocchi, Atmospheric Turbulence and Diffusion Division, NOAA, at the fen site by Shashi Verma, University of Nebraska and at the Old Aspen site fluxes were measured by a team consisting of researchers from the Atmospheric Environment Service, Downsview, Ontario and the University of British Columbia, the latter supported by a Collaborative Special Project Grant from the Natural Science and Engineering Research Council of Canada. The 1994 AVIRIS waveband data was provided by Robert Green, NASA Jet Propulsion Lab, California.

## References

Asner, G.P., Wessman, C.A., Schimel, D.S., 1998. Heterogeneity of savanna canopy structure and function from imaging spectroscopy and inverse modelling. Ecol. Applications 8 (4), 1022–1036.

Baldocchi, D.D., Vogel, C.A., Hall, B., 1997. Seasonal variation of energy and water vapour exchange rates above and below a boreal jack pine forest canopy. J. Geophys. Res. 102 (D24), 28,939–28,951.

Bilger, W., Bjorkman, O., Thayer, S.S., 1989. Light induced spectral absorbance changes in relation to photosynthesis and

the expoxidation state of xanthophyll cycle components in cotton leaves. Plant Physiol. 91, 542–551.

Bjorkman, O., Demmig-Adams, B., 1994. Regulation of photosynthetic light energy capture, conversion and dissipation in leaves of higher plants. In: Schulze, E.-D., Caldwell, M.M. (Eds.), Ecophysiology of Photosynthesis, Ecological Studies 100. Springer, Berlin, Heidelbeig, New York, pp. 17–47.

Blanken, P.D., Black, T.A., Yang, P.C., den Hartog, G., Neumann, H.H., Nesic, M.D.,. Novak, R., Staebler, R., Lee, X., 1997. Energy balance and canopy conductance of a boreal aspen forest: partitioning overstorey and understorey components. J. Geophys. Res. 102: 28, 915–28, 927.

Bloom, A.J., Calswell, R.M., Finazzo, J., Warner, R.L., Weissbart, J., 1989. Oxygen and carbon dioxide fluxes from barley shoots depends on nitrate assimilation. Plant Physiol. 91, 352–356.

Cuenca, R.H., Stangel, D.E., Kelley, S.F., 1997. Soil water balance in a Boreal forest. J. Geophys. Res. 102 (D24), 29,935–29,365.

Demmig-Adams, B., Gilmore, A.M., Adams-III, W.W., 1996. In vivo functions of carotenoids in higher plants. FASEB J. 10, 403–412.

Demmig-Adams, B., Adams, B., 1994. The role of xanthophyll cycle carotenoids in the protection of photosynthesis. Trends in Plant Sci. 1, 21–26.

Fillela, I., Amaro, J.L., Penuelas, J., 1996. Relationship between photosynthetic radiation-use efficiency of barley canopies and the photochemical reflectance index (PRI). Physiol. Plantarum 96, 211–216.

Frank, H.A., Cua, A., Chynwat, V., Young, A., Gosztola, D., Wasielewski, M.R., 1994. Photophysics of the carotenoids associated with the xanthophyll cycle in photosynthesis. Photosynthesis Res. 41, 389–395.

Gamon, J.A., Field, C.B., Bilger, W., Bjorkman, O., Freeden, A., Penuelas, J., 1990. Remote sensing of the xanthophyll cycle and chlorophyll fluorescence in sunflower leaves and canopies. Oecologia 85, 1–7.

Gamon, J.A., Fillela, I., Penuelas, J., 1993. The dynamic 531 nanometer $\Delta$ reflectance signal: a survey of 20 angiosperm species. Current Topics in Plant Physiol. 8, 172–177.

Gamon, J.A., Penuelas, J., Field, C.B., 1992. A narrow waveband spectral index that tracks diurnal changes in photosynthetic efficiency. Remote Sensing of Environ. 41, 35–44.

Gamon, J.A., Serrano, L., Surfus, J.S., 1997. The photochemical reflectance index: an optical indicator of photosynthetic radiation use efficiency across species, functional types, and nutrient levels. Oecologia 112, 492–501.

Goulden, M.L., Daube, B.C., Fan, S.M., Sutton, A., Bazzaz, J.W., Munger, S.C. and Wofsy S.C., 1997. Physiological responses of a black spruce forest to weather (BOREAS Special Issue). J. Geophys. Res. 102 (D24), 28,987–28,966.

Goward, S.N., Huemmrich, K.F., 1992. Vegetation canopy PAR absorptance and the normalised difference vegetation index: an assessment using the SAIL model. Remote Sensing of Environ. 39, 119–140.

Green, R.O., Sarture, C.M., Chrien, T.G., Aronsson, M., Chippendale, B.J., Faust, J.A., Pavri, B.E., Chovit, C.J., Solis, M., Olah, M.R., Williams, O., 1998. Imaging Spectroscopy and the Airborne Visible/Imaging Spectroradiometer (AVIRIS). Remote Sensing of Environ. 65, 227–248.

Guyot, G., 1990. Optical properties of vegetation canopies. In: Steven, M.D,. Clark, J.A., (Eds.), Applications of Remote Sensing in Agriculture. Butterworths, London, pp. 19–44.

Harbison, J., Genty, B., Baker, N.R., 1990. The relationship between $CO_2$ assimilation and electron transport in leaves. Photosynthesis Res. 25, 213–224.

Heber, U., 1969. Conformational changes of chloroplasts induced by illumination of leaves in vivo. Biochim. Biophys. Acta. 180, 302–319.

Hogg, E.H., Black, T.A., den Hartog, G., Neumann, H.H., Zimmerman, R, Hurdle, P., Blanken, P.D., Nesic, Z., Yang, P.C., Staebler, R.M., McDonald, K.C., Oren, R., 1997. A comparison of sap flow and eddy fluxes of water vapour from a boreal deciduous forest (BOREAS Special Issue). J. Geophys. Res. 102 (D24), 28,929–28,937.

Huemmrich, K.F., 1995. An analysis of remote sensing of the fraction of absorbed photosynthetically active radiation in forest canopies. Ph.D. Thesis, University of Maryland, USA.

Huete, A.R., 1987. Soil and sun angle interactions on partial canopy spectra. Int. J. Remote Sensing 8 (9), 1307–1317.

Jarvis, P.G., Massheder, J.M., Hale, S.E., Moncrieff, J.B., Rayment, M.B., Scott, S.L., 1997. Seasonal variation of carbon dioxide, water vapour and energy exchanges of a boreal black spruce forest. J. Geophys. Res. 102 (D24), 28,953–28,966.

Kimes, D.S., 1980. Vegetation Reflectance as a function of Solar Zenith Angle. Photogrammic Eng. Remote Sensing 46 (12), 1563–1573.

Lloyd, J.L., Taylor, J.A., 1994. On the temperature dependence of soil respiration. Func. Ecol. 8, 315–323.

Owens, T.G., 1996. Processing of Excitation Energy by Antenna Pigments. In: Neil Baker (Ed.), Photosynthesis and the Environment. Kluwer Academic Publishers, NL, pp. 1–23.

Penuelas, J., Filella, I., Gamon, J.A., 1995. Assessment of the photosynthetic radiation use efficiency with spectral reflectance. New Phytol. 131, 291–296.

Penuelas, J., Llusia, J., Pinol, J., Fillela, I., 1997. Photochemical reflectance index and leaf photosynthetic radiation-use-efficiency assessment in Mediterranean trees. Int. J. Remote Sensing 18 (13), 2863–2868.

Pfundel, E., Bilger, W., 1994. Regulation and possible function of the violaxanthin cycle. Photosynthesis Res. 42, 89–109.

Ranson, K.J., Daughtry, C.S.T., Biehl, L.L., 1986. Sun angle, view angle, and background effects on spectral response of simulated balsam fir canopies. Photogrammic Eng. Remote Sensing 52 (5), 649–658.

Running, S.R., Nemani, R.R., 1988. Relating seasonal patterns of the AVHRR vegetation index to simulated photosynthesis and transpiration of forests in different climates. Remote Sensing of Environ. 24, 347–367.

Sellers, P.J., Hall, F.G., Margolis, H., Kelly, B., Baldocchi, D., den Hartog, G., Cihlar, J., Ryan, M., Goodison, B., Crill, P., Ranson, J., Lettenmaier, D., Wickland, D., 1995. The Boreal-Ecosystem-Atmosphere-Study (BOREAS): an overview and early results from the 1994 field year. Bull. Am. Meteorol. Soc. 76 (9), 1549–1577.

Sukyer, A.E., Verma, S.B., Arkebauer, T.J., 1997. Season-long measurement of carbon dioxide exchange in a boreal fen. J. Geophys. Res. 102 (D24): 29,021–29,028.

Tenhunen, J.D., Catarino, F.M., Lange, O.L., Oechel, W.C. (Eds.), 1987. Plant Responses to Stress. Functional Analysis in Mediterranean Ecosystems. Springer, Berlin.

Tucker, C.J., 1979. Red and photographic infrared linear combinations for monitoring vegetation. Remote Sensing of Environ. 8, 127–150.

Walthall, C., Williams, D.L., Markham, B., Kalshoven, J., Nelson, R., 1996. Development and present configuration of the NASA GSFC/WFF helicopter based remote sensing system. Int. Geosci. Remote Sensing Symp., Lincoln, NE.

Verhoef, W., 1984. Light scattering by leaf layers with application to canopy reflectance modelling: the SAIL model. Remote Sensing of Environ. 16, 125–141.

Yamamoto, H.Y., 1979. Biochemistry of the violaxanthin cycle in higher plants. Pure Appl. Chem. 51, 639–648.